Dual-Polarization Radar Meteorology: A Geometrical Approach

by

Richard David Scott

Submitted in partial fulfillment
of the requirements for the degree of

Doctor of Philosophy in Physics

Department of Physics
New Mexico Institute of Mining and Technology
Socorro, NM

May 5, 1999

Abstract

The polarization state of an electromagnetic wave can be described as a point on the Poincaré sphere using two spherical angles, (α, ϕ) or (δ, τ), and the degree of polarization, p. The spherical description of polarization state is used as the basis for interpreting dual-polarization radar measurements. Analysis of three classes of particles: aligned, spherical, and randomly oriented, is performed. The depolarization trajectory on the Poincaré sphere due to propagation path and backscattering effects is examined. The depolarization trajectory due to aligned particles is simplified by the introduction of a new spherical angle β. The results of the analysis are used to determine the optimal transmitted polarization state and receiver basis for meteorological studies. The optimal transmitted polarization is shown to be circular. The optimal receiver basis is shown to be horizontal and vertical (H-V). The New Mexico Tech dual-polarization radar was modified as a result of this study, to transmit circularly polarized waves and receive the backscattered wave in an H-V basis. Data of a September 15, 1998 thunderstorm are presented showing the processing performed by the radar's host computer.

Acknowledgements

I would like to express profound gratitude and sincere thanks to the many people who have helped me in this pursuit. To Dr. Paul Krehbiel for guidance and financial support of this research. And, the enthusiasm he showed for the idea of using the Poincaré sphere as a guide in polarization analyses. To Dr. William Rison for helping me resolve innumerable problems with various computers and the radar itself. To the other members of my committee, Dr. Alan Gutjahr, Dr. David Westpfahl and Dr. William Winn, for their valuable guidance and time.

Special thanks to Jeff Edmunds and Floyd Hewitt in the machine shop who provided valuable assistance in the manufacturing of parts and for their help in moving the radar to its new home at the Socorro Airport.

Special thanks also to James Edwards and Abram Baca from the Physical Plant for their able assistance with the radar.

This work is dedicated to the memory of Steve McCrary. Steve was a man with an unlimited number of ideas (some good and some wild) who ultimately was probably under appreciated by society.

My greatest appreciation, gratitude and praise is reserved for my wife Betty and my son Jesse who graciously indulged my desire to further my education. And also to Betty for listening to endless hours of my ratings and who came up with the appropriate expression: " First you take a sphere . . .".

This work has been supported by the U.S. Air Force Office of Scientific Research under Grants F49620-92-J-0320 and F49620-96-1-0304.

Contents

List of Figures

List of Tables

Notation in the Text

α	angle in the Stokes sub-space defined by $\tan^{-1}(E_V/E_H)$
A	unpolarized power in a single receiver, component of the decomposed coherency matrix **J**
A_H^2, A_V^2	specific attenuation of H and V waves (in nepers)
β	angle in the Stokes sub-space defined by $\tan^{-1}\sqrt{W_V/W_H}$
B	polarized power in receiver 1
γ	coherent depolarization rate
γ_0	free space propagation constant
C	polarized power in receiver 2
δ_ℓ	differential phase shift upon backscatter in a linear H-V basis
δ	angle in the Stokes sub-space defined by $\tan^{-1}\frac{E_L-E_R}{E_L+E_R}$ or the axial ratio of the polarization ellipse
D	complex correlation (see W)
θ	orientation angle of aligned scatterers or the rotation angle of the electric field vector
f	shape correlation coefficient of horizontally aligned particles
g	sphericity parameter of randomly oriented particles
H	horizontally polarized wave
H-V	horizontal and vertical linear polarization basis
I	total power in the two receiver channels, first Stokes parameter
Im	the imaginary part of $(\cdot)$
I_p	polarized portion of the first Stokes parameter $I = I_u + I_p$
I_u	unpolarized portion of the first Stokes parameter $I = I_u + I_p$
J	coherency, covariance or coherency density matrix
λ_1, λ_2	eigenvalues of the **J** matrix
LHC	Left Hand Circular polarization
L-R	LHC/RHC polarization basis

Notation in the Text (continued)

L-R	LHC/RHC polarization basis
LPR	linear polarization ratio, W_H/W_V
p	the degree of polarization, $0 \leq p \leq 1$
Q	difference of the power in H and V receivers, second Stokes parameter
ρ	normalized correlation coefficient $W/\sqrt{W_1 W_2}$
Re	the real part of $(\cdot)$
RHC	Right Hand Circular polarization
s_0	first Stokes parameter normalized to polarized power
s_1	second Stokes parameter normalized to polarized power
s_2	third Stokes parameter normalized to polarized power
s_3	fourth Stokes parameter normalized to polarized power
τ	angle in the Stokes sub-space defined by $\frac{1}{2}\tan^{-1}(\mathrm{ImW_{LR}/ReW_{LR}})$ or the angle up from the horizontal axis to the major axis of the polarization ellipse
U	difference of the power in + and - receivers, third Stokes parameter
ϕ	angle in the Stokes sub-space defined by $\tan^{-1}(\mathrm{ImW_{HV}/ReW_{HV}})$ or the phase difference between E_H and E_V
ϕ_{dp}	differential propagation phase shift
V	difference of the power in L and R receivers, fourth Stokes parameter or vertically polarized wave
+/-	$\pm 45^\circ$ linear polarization basis
W_{am}	arithmetic mean of the power in receiver channels 1 and 2
W_{gm}	geometric mean of the power in receiver channels 1 and 2
W_H	power in the H polarization channel defined by $\overline{\lvert E_H \rvert^2}$
W_{HV}	complex correlation between the signals in the two receiver channels in an H-V receiver basis defined by $\overline{E_H E_V^*}$

Notation in the Text (continued)

W_L	power in the LHC polarization channel defined by $\overline{\lvert E_L \rvert^2}$
W_{LR}	complex correlation between the signals in the two receiver channels in an L-R receiver basis defined by $\overline{E_L E_R^*}$
W_-	power in the -45° polarization channel defined by $\overline{\lvert E_- \rvert^2}$
W_1	power in generic receiver channel 1 defined by $\overline{\lvert E_1 \rvert^2}$
W/W_2	parameter in a circular receiver basis due to *McCormick* and *Hendry* (1979), modified cross covariance ratio
W_+	power in the +45° polarization channel defined by $\overline{\lvert E_+ \rvert^2}$
W_{+-}	complex correlation between the signals in the two receiver channels in an +/- receiver basis defined by $\overline{E_+ E_-^*}$
W_R	power in the RHC polarization channel defined by $\overline{\lvert E_R \rvert^2}$
W_2	power in generic receiver channel 2 defined by $\overline{\lvert E_2 \rvert^2}$
W_V	power in the V polarization channel defined by $\overline{\lvert E_V \rvert^2}$
ZDR	differential reflectivity, $ZDR = \langle \lvert S_{HH} \rvert^2 \rangle / \langle \lvert S_{VV} \rvert^2 \rangle$
$\widehat{(\cdot)}$	values estimated from the measurements
$\overline{(\cdot)}$	ensemble average
$\langle \cdot \rangle$	volume averaged quantity or time average

Chapter 1

Introduction

Radar serves two roles in meteorology. The first is an operational role. In an operational mode a weather radar is capable of detecting severe weather and estimating flash flood potential based on rainfall estimates for watches, warnings and emergency services planning. The other role is for the purposes of research. In this role, the microphysics and dynamics of the storm become the focus of study. Size, shape, amount, and thermodynamic phase of the hydrometeors become the items of interest (*Doviak* and *Zrnić*, 1993). Often, the goal of research is to improve the operational capabilities of weather radar.

Early radar meteorologists believed raindrops were tumbling or randomly oriented. The vertical wind tunnel studies of *Pruppacher* and *Beard* (1970) showed falling water drops were oblate spheroids with a vertical rotational axis of symmetry. Pruppacher and Beard were able to develop an empirical relationship between drop sizes and drop shapes from the wind tunnel data. Measurements made by numerous radar meteorologists in the early 1970's provided strong evidence raindrops were indeed oblate spheroids, confirming the results of the vertical wind tunnel studies (*Atlas*, 1990).

The fact that raindrops falling at their terminal velocities tend to be horizontally distorted leads naturally to the use of polarization techniques in radar meteorology. This horizontal alignment affects the propagating wave in several ways. The horizontal reflectivity (Z_H) is greater than the vertical reflectivity (Z_V) and the ratio of the reflectivity is termed the differential reflectivity ($Z_H/Z_V = ZDR$). ZDR is a measure of the size and the shape of the raindrops. Propagation through rain attenuates the horizontally (H) polarized component more than the vertically (V) polarized components of the wave. This effect is termed differential attenuation. Propagation

Band Designation	Frequency Range (GHz)	Wavelength (cm)	Total Attenuation (dB / km)	Differential Attenuation (dB / km)	Differential Phase Shift (degrees / km)
S-Band	2.60 - 3.95	11.5 - 7.6	0.003 - 0.015	< 0.01 @ 2.5 GHz	3 @ 2.5 GHz
C-Band	3.95 - 5.85	7.6 - 5.1	0.015 - 1	0.15 @ 5 GHz	8 @ 5 GHz
X-Band	8.20 - 12.40	3.7 - 2.4	3 - 8.5	1.0 @ 10 GHz	15 @ 10 GHz

Table 1.1: Frequency and Wavelength of Commonly Used Bands. Typical values of total attenuation, differential attenuation, and differential phase shift corresponding to rainfall rates of 150 mm/hr are from *Oguchi* (1983).

through rain introduces a phase shift between the H and V polarized components and is termed differential propagation phase shift (ϕ_{dp}). The differential attenuation and differential phase shift effects are cumulative in range and become progressively larger with decreasing wavelengths. Table 1.1 shows commonly used radar band designations, frequencies, and wavelengths. Typical values of total attenuation, differential attenuation and differential phase shift for rainfall rates of 150 mm/hr are also given.

Particles large enough to be in the Rayleigh-Gans or Mie scattering regime will produce a differential phase shift (δ_ℓ) between H and V components upon backscatter. Non-Rayleigh scattering can produce large changes in ZDR for relatively small changes in particle size (*Oguchi*, 1983, Figure 19). Only hail with a diameter of 5 cm or greater will produce a differential phase shift upon backscatter at S-Band wavelengths (10 cm), this has been used to infer the presence of hail using S-Band wavelengths (*Balakrishnan* and *Zrnić*, 1990). At X-Band wavelengths (3 cm), normal size raindrops are in the non-Rayleigh scattering regime. ϕ_{dp} and δ_ℓ both contribute to the phase between the H and V components and at X-Band they are comparable effects. Since differential phase shift increases monotonically with range, any sudden increases or decreases in the phase with range can be attributed to differential phase shift upon backscatter. In practice, the phase measurements tend to be rather noisy, especially at longer wavelengths, so distinguishing between ϕ_{dp} and δ_ℓ is difficult (*Hubbert* et al., 1993).

Historically, the meteorological radar community has been split into two groups: those who transmit and receive linear H-V polarizations and those who transmit and receive left (L) and right (R) circular polarizations. The H-V groups transmit

alternating pulses of H and V polarizations. The radar return corresponding to the transmitted polarization (co-polar) provide a measure of the H and V reflectivities and ZDR. The ratio of the power in the orthogonal receiver (cross-polar) to the power in the co-polar receiver is termed the linear depolarization ratio (LDR). Linear depolarization is a result of backscatter from irregularly shaped or randomly oriented hydrometeors. The correlation coefficient of the power in the co-polar receivers, $\rho_{HV}(T)$, is determined from consecutive transmission of H and V polarizations, where T is the period between transmitted pulses. The correlation coefficient at zero time lag, $\rho_{HV}(0)$, is the correlation coefficient of the signals in the two receiver channels if H and V were simultaneous transmitted. $\rho_{HV}(0)$ is a measure of the variations in the shape of drops and is estimated from $\rho_{HV}(T)$. $\rho_{HV}(T)$ is a measure of the reshuffling of scatterers occurring between the transmitted pulses (*Sachidananda* and *Zrnić*, 1985). The phase of the correlation coefficient provides a measure of the differential propagation phase shift, ϕ_{dp}, and differential phase shift upon backscatter, δ_ℓ. Phase measurements based upon the co-polar returns of consecutive transmitted pulse are noisy due to the non-simultaneous nature of the measurement and as a result of the estimation of $\rho_{HV}(0)$ from the measured $\rho_{HV}(T)$ value.

When a radar transmits alternate L and R polarizations, the radar returns corresponding to the transmitted polarization (co-polar) provide a measure of the L and R reflectivities. The ratio of the power of the radar returns in the orthogonal receiver (cross-polar) to the power in the co-polar receiver provides a measure of the circular depolarization ratio (CDR). Circular depolarization is a result of backscatter from non-spherical particles *regardless of the particle orientation* and is more sensitive to randomly oriented particles than linear polarizations (*Torlaschi* and *Holt*, 1998). Differential propagation phase shift depolarizes circular polarizations by transferring transmitted power into the cross-polar channel. As a result, the use of a single (co-polar) receiver has been shown to severely underestimate the storm reflectivity when the transmitted circular polarization is depolarized by differential propagation phase shifts (*Torlaschi* and *Pettigrew*, 1990). The phase of the correlation of the power in the co-polar and cross-polar channels, ρ_{LR}, can be used to determine particle alignment directions *Krehbiel* et al. (1996)*Chen* (1994). *McCormick* and *Hendry* (1975) pioneered much of the early work associated with the use of dual-circular polarization radars.

The focus of this study is summarized in the following questions:

1. What are the best polarizations to transmit?

2. What are the best polarizations to receive?

3. Is there any advantage to transmitting and receiving in different polarization bases?

More specific questions are:

1. When is a single transmitted polarization state adequate for determining all the parameters that radars can measure: ZDR, the differential reflectivity; δ_ℓ, the differential phase shift upon backscatter; $(A_H/A_V)^2$, the differential attenuation of the propagation path; and, K_{DP}, the specific differential phase shift of the propagation path?

2. Are there any conditions that necessitate the alternate transmission of orthogonal polarizations?

3. What other transmitted polarization state, if any, will provide additional meteorological information?

The linear (H-V) and circular (L-R) polarization methods utilize the transmission and reception of the same orthogonal polarization bases. In the case of (H-V) polarization basis, it is clear that there must be a significant amount of depolarization (LDR) due to backscatter from randomly oriented or non-horizontally aligned particles before the signal power in the cross-polar channel exceeds the noise power of the cross-polar receiver. There will be a measurable CDR before there is a measurable LDR for the same receiver noise, since randomly oriented *and* horizontally aligned precipitation particles will incoherently and coherently depolarize a circularly polarized wave. *Torlaschi* and *Holt* (1998) provide a interesting theoretical basis of this higher sensitivity. If the transmission and reception bases are allowed to differ (e.g., transmit LHC and receive H-V), the depolarization will be measurable before co-polar/cross-polar methods indicate a measurable depolarization. *Sachidananda* and *Zrnić* (1985) previously considered the transmission of alternate +45/-45 slant linear polarizations and reception of H-V polarized returns in order to reduce the data acquisition time. They did not recognize the improved sensitivity of this technique. Nor, as will be shown later, did they consider that circular polarization might have advantages for the transmitted polarization.

The geometrical interpretation of polarization state (the Poincaré sphere) is used as a guide in this study to answer the questions posed in this introduction. Chapter

2 of this dissertation summarizes different ways of representing polarization states and shows how the polarization state is determined from the measured covariances. The analysis is expanded beyond the usual treatment to include the effects of unpolarized components in the scattered wave. Chapter 3 presents an analysis of how meteorological propagation and backscattering effects change the polarization state of the transmitted polarization including determination of the unpolarized component. This analysis is done for the case of aligned, randomly oriented, and spherical particles. Chapter 4 examines the question of best polarizations to transmit and receive to provide the most meteorological information. Chapter 5 describes how the New Mexico Tech radar was modified to implement the new measurement and processing techniques of this study. The final chapter summarizes and discusses the results and discusses the questions posed in this introduction.

Appendix A contains a background discussion of polarization and the various ways to describe polarization: electric field vectors, the polarization ellipse, a planar description of polarization or polarization ratios, Stokes parameters, and a geometrical description of polarization based upon the Poincaré sphere. Appendix B shows how measurements usually made in a specific receiver basis can be determined from covariance measurements made in a different receiver basis. Appendix C shows how the Poincaré sphere can be used as a guide for radar calibrations.

Chapter 2

Radar Polarization Measurements

2.1 Introduction

In this chapter we show how the radar measurements determine the elements of the coherency matrix, or the covariances. From the radar measurements we can determine the degree of polarization which is defined as the ratio of the polarized power to the total power. The coherency matrix can be decomposed into polarized and unpolarized component matrices. Furthermore, the elements of the coherency matrix can be related to the Stokes parameters. The Stokes parameters can be used to determine spherical angles (α, ϕ) and (δ, τ) of the Poincaré sphere.

2.2 The Coherency Matrix, J

If a dual-polarization radar receives two orthogonal polarization states, the correlation between the signals in the two receivers can be determined. The coherence matrix (*Born* and *Wolf*, 1975), coherence density matrix (*Baylis* et al., 1993) or the coherency matrix is determined from the direct product of the electric field vector and its Hermitian transpose.

$$\mathbf{J} = \overline{\begin{bmatrix} E_1 \\ E_2 \end{bmatrix} \cdot \begin{bmatrix} E_1^* & E_2^* \end{bmatrix}} = \begin{bmatrix} \overline{E_1 E_1^*} & \overline{E_1 E_2^*} \\ \overline{E_1^* E_2} & \overline{E_2 E_2^*} \end{bmatrix} , \tag{2.1}$$

where the overbars represent the ensemble average. The ensemble averaged values of the matrix in (2.1) are commonly defined to be:

$$W_1 \;=\; \overline{E_1 E_1^*} = \langle |E_1|^2 \rangle$$

$$W_2 = \overline{E_2 E_2^*} = \langle |E_2|^2 \rangle \tag{2.2}$$
$$W = \overline{E_1 E_2^*} = \langle E_1 E_2^* \rangle \ ,$$

where the angle brackets represent the time average. Since radar signals are stationary and ergodic, the statistical properties of the ensemble can be deduced from time sample averages (*Doviak* and *Zrnić*, 1993). Equation (2.1) can be rewritten in the form,

$$\mathbf{J} = \begin{bmatrix} W_1 & W \\ W^* & W_2 \end{bmatrix} \ , \tag{2.3}$$

where from Equation 2.3 we can see W_1 is the power in receiver 1, W_2 is the power in receiver 2 and W is the complex cross correlation of the signals in the two receiver channels.

2.3 Partial Polarization

The polarization state of a fully polarized wave is characterized by two orthogonal electric field components and the phase relation between the components. In general, an electromagnetic wave is not fully polarized. When the wave is partially polarized the degree of polarization , the ratio of the polarized power to the total power, is required to complete the polarization state description.

Many polarization analyses require that the electromagnetic wave be decomposed into unpolarized and completely polarized components. In this section we will examine the importance of the degree of polarization. Methods to determine the degree of polarization from the measurements will be described. And a geometrical interpretation of the degree of polarization is suggested.

2.3.1 The Degree of Polarization

The coherency matrix in a general receiver basis is defined by

$$\mathbf{J} = \begin{bmatrix} W_1 & W \\ W^* & W_2 \end{bmatrix} \ . \tag{2.4}$$

Two important quantities of the coherency matrix are the trace,

$$\mathbf{Tr}[\mathbf{J}] = W_1 + W_2 \ , \tag{2.5}$$

which is a measure of the total power and the determinant,

$$\mathbf{Det}[\mathbf{J}] = W_1 W_2 - |W|^2 \ , \tag{2.6}$$

which is related to the degree of polarization. If the wave is completely polarized, $\mathbf{Det}[\mathbf{J}] = 0$. For a completely polarized wave,

$$\begin{aligned} \hat{E}_1 &= E_1 e^{j\phi_1} \\ \hat{E}_2 &= E_2 e^{j\phi_2} \ . \end{aligned}$$

The covariances can be found from

$$\begin{aligned} W_1 &= \hat{E}_1 \hat{E}_1^* = |E_1|^2 \\ W_2 &= \hat{E}_2 \hat{E}_2^* = |E_2|^2 \\ W &= \hat{E}_1 \hat{E}_2^* = E_1 E_2^* e^{j\phi} \ . \end{aligned}$$

And from 2.6,

$$\begin{aligned} \mathbf{Det}[\mathbf{J}] &= W_1 W_2 - |W|^2 \\ &= |E_1|^2 |E_2|^2 - E_1 E_2^* E_1^* E_2 \\ &= |E_1|^2 |E_2|^2 - |E_1|^2 |E_2|^2 \\ \mathbf{Det}[\mathbf{J}] &= 0 \ . \end{aligned} \tag{2.7}$$

If the wave is partially polarized, the coherency matrix can be decomposed into unpolarized and polarized matrices,

$$\mathbf{J} = \mathbf{J}_u + \mathbf{J}_p \ , \tag{2.8}$$

where $\mathbf{J}_u$ and $\mathbf{J}_p$ are unpolarized and polarized coherency matrices. This decomposition is termed a proper decomposition when $\mathbf{Det}[\mathbf{J}_p] = 0$. In the notation of *Born* and *Wolf* (1975) and *Mott* (1986), the decomposed coherency matrix can be written,

$$\mathbf{J} = \begin{bmatrix} W_1 & W \\ W^* & W_2 \end{bmatrix} = \begin{bmatrix} A & 0 \\ 0 & A \end{bmatrix} + \begin{bmatrix} B & D \\ D^* & C \end{bmatrix} \ . \tag{2.9}$$

From (2.9) we have the relationships, $W_1 = A + B$, $W_2 = A + C$, and $W = D$, where B and C are the polarized powers and A is the unpolarized power in the two receiver

channels. The polarized component must satisfy the relation $\mathbf{Det}[\mathbf{J}_p] = 0$.

$$\begin{aligned}
\mathbf{Det}[\mathbf{J}_p] &= \begin{vmatrix} B & D \\ D^* & C \end{vmatrix} \\
&= \begin{vmatrix} W_1 - A & W \\ W^* & W_2 - A \end{vmatrix} \\
&= (W_1 - A)(W_2 - A) - |W|^2 \\
&= A^2 - A(W_1 + W_2) + (W_1 W_2 - |W|^2) = 0 \ . \qquad (2.10)
\end{aligned}$$

Equation (2.10) is quadratic in A. Using the solution for a quadratic equation,

$$\begin{aligned}
2A &= (W_1 + W_2) \pm \sqrt{(W_1 + W_2)^2 - 4(W_1 W_2 - |W|^2)} \\
2A &= (W_1 + W_2) \pm \sqrt{(W_1 - W_2)^2 + 4|W|^2} \ , \qquad (2.11)
\end{aligned}$$

where we have made use of the identity $(W_1 + W_2)^2 - 4W_1 W_2 = (W_1 - W_2)^2$ in the second equation.

We can now solve for B,

$$\begin{aligned}
A + B &= W_1 \\
2A + 2B &= 2W_1 \\
2B &= 2W_1 - 2A \\
2B &= 2W_1 - (W_1 + W_2) \mp \sqrt{(W_1 - W_2)^2 + 4|W|^2} \\
2B &= (W_1 - W_2) \mp \sqrt{(W_1 - W_2)^2 + 4|W|^2} \ . \qquad (2.12)
\end{aligned}$$

Since B is the real, polarized power in receiver one, it must be a positive quantity. In (2.12) we see that the plus sign must be used for B to be positive. And therefore, the negative sign must be used in (2.11).

Solving for C,

$$\begin{aligned}
A + C &= W_2 \\
2A + 2C &= 2W_2 \\
2C &= 2W_2 - 2A \\
2C &= 2W_2 - (W_1 + W_2) \mp \sqrt{(W_1 - W_2)^2 + 4|W|^2} \\
2C &= (W_2 - W_1) + \sqrt{(W_1 - W_2)^2 + 4|W|^2} \ , \qquad (2.13)
\end{aligned}$$

where we have chosen the plus sign to make C positive.

The elements of the decomposed coherency matrix can be summarized in the equations,

$$\begin{aligned} 2A &= (W_1 + W_2) - \sqrt{(W_1 - W_2)^2 + 4|W|^2)} \\ 2B &= (W_1 - W_2) + \sqrt{(W_1 - W_2)^2 + 4|W|^2)} \\ 2C &= (W_2 - W_1) + \sqrt{(W_1 - W_2)^2 + 4|W|^2)} \\ D &= W \end{aligned} \tag{2.14}$$

In terms of the elements of the decomposed coherency matrix, the degree of polarization, the ratio of polarized to total power, can be written as

$$\begin{aligned} p &= \frac{B + C}{(B + A) + (C + A)} = \frac{B + C}{W_1 + W_2} \\ &= \frac{\sqrt{(W_1 - W_2)^2 + 4|W|^2)}}{W_1 + W_2} \\ &= \frac{\sqrt{(W_1 + W_2)^2 - 4(W_1 W_2 - 4|W|^2)}}{W_1 + W_2} \\ &= \sqrt{1 - \frac{4(W_1 W_2 - |W|^2)}{(W_1 + W_2)^2}} \\ &= \sqrt{1 - \frac{4\,\mathbf{Det}[\mathbf{J}]}{(\mathbf{Tr}[\mathbf{J}])^2}}\ , \end{aligned} \tag{2.15}$$

where $\mathbf{Det}[\mathbf{J}]$ and $\mathbf{Tr}[\mathbf{J}]$ are the determinant and trace of the coherency matrix, $\mathbf{J}$, p is the degree of polarization , B and C are the polarized power in the two receivers, and A is the unpolarized power in each receiver.

In this section we showed how the coherency matrix can be decomposed into matrices that represent the unpolarized and polarized power of the electromagnetic wave,

$$\mathbf{J} = \begin{bmatrix} A & 0 \\ 0 & A \end{bmatrix} + \begin{bmatrix} B & W \\ W^* & C \end{bmatrix}\ , \tag{2.16}$$

where A, B, C, and D are determined from Equation 2.14. If we write the radical terms in (2.14) as,

$$\begin{aligned} \sqrt{(W_1 - W_2)^2 + 4|W|^2} &= \sqrt{(W_1 + W_2)^2 - 4(W_1 W_2 - |W|^2)} \\ &= (W_1 + W_2)\sqrt{1 - \frac{4(W_1 W_2 - |W|^2)}{(W_1 + W_2)^2}} \\ &= p(W_1 + W_2) \end{aligned} \tag{2.17}$$

then we can write (2.14) in terms of p as,

$$\begin{aligned} 2A &= (W_1 + W_2)(1-p) \\ 2B &= W_1(1+p) - W_2(1-p) \\ 2C &= W_2(1+p) - W_1(1-p) \\ D &= W \ . \end{aligned} \tag{2.18}$$

2.4 The Stokes Parameters and Poincaré Sphere

In the middle of the nineteenth century, *Stokes* (1852) showed that the polarization state of light could be determined by measurements using a combination of polarizers and phase retarding plates. The first measurement involves measuring the total power incident on a detector from a particular source. This measurement determines the total intensity and the first Stokes parameter (I). A linear polarizer is then placed between the source and detector. The difference of the detected power when the polarizer is rotated to pass horizontally and vertically polarized light is the second Stokes parameter (Q). The third Stokes parameter (U) is similar to (Q) except that the power differences are taken with the linear polarizer set to +45° and -45° off horizontal (or vertical). The linear polarizer and a phase retarder (quarterwave plate) are then used to resolve the power into left and right hand circular components of the light. The difference between the power in LHC and RHC polarized components determines the fourth and final Stokes parameter (V).

The relation between the Stokes parameters is given by

$$I^2 \geq Q^2 + U^2 + V^2 \ , \tag{2.19}$$

where the equality holds only for completely polarized light. When there is partial polarization the Stokes parameter representing the total power, I, can be split into polarized

$$I_p = pI = \sqrt{Q^2 + U^2 + V^2} \tag{2.20}$$

and unpolarized

$$I_u = (1-p)I \tag{2.21}$$

power, where p is the degree of polarization defined by

$$p = \frac{\sqrt{Q^2 + U^2 + V^2}}{I} \ . \tag{2.22}$$

	RECEIVER BASIS		
	(H / V)	(+ / -)	(L / R)
I	$W_H + W_V$	$W_+ + W_-$	$W_L + W_R$
Q	$W_H - W_V$	$2\,\mathrm{Im}\,W_{+-}$	$2\,\mathrm{Re}\,W_{LR}$
U	$2\,\mathrm{Re}\,W_{HV}$	$W_+ - W_-$	$2\,\mathrm{Im}\,W_{LR}$
V	$2\,\mathrm{Im}\,W_{HV}$	$2\,\mathrm{Re}\,W_{+-}$	$W_L - W_R$

Table 2.1: The Stokes parameters in terms of the coherency matrix elements are dependent upon the polarization basis of the receivers.

Poincaré (1892) recognized the Stokes parameters could be interpreted geometrically. The triplet (Q, U, V) represents three cartesian coordinates. For the case of a completely polarized wave the Stokes parameter I represents the radius of a sphere, centered at the origin, that passes through the point (Q, U, V). In the case of a partially polarized wave, the radius of the sphere that passes through the point (Q, U, V) is pI. This sphere is commonly referred to as the Poincaré sphere.

To see how the covariances relate to the Stokes parameters and the Poincaré sphere, note from (2.16) the total polarized power is given by

$$I_p = B + C = \sqrt{(W_1 - W_2)^2 + 4|W|^2}\ . \tag{2.23}$$

If we write the cross correlation, W, in terms of its cartesian components

$$W = |W|\cos\phi + j\,|W|\sin\phi\ , \tag{2.24}$$

we recognize the total polarized power can be written in terms of three orthogonal components,

$$I_p = \sqrt{(W_1 - W_2)^2 + (2|W|\cos\phi)^2 + (2|W|\sin\phi)^2}\ . \tag{2.25}$$

This is shown graphically in Figure 2.1. The quantity $(W_1 - W_2)$ is the difference of the powers in the two receiver channels and corresponds to the Stokes parameter for that particular receiver basis.

A dual-polarization radar is normally configured to receive a specific pair of orthogonal polarizations, for example H and V polarizations. It is the choice of receiver

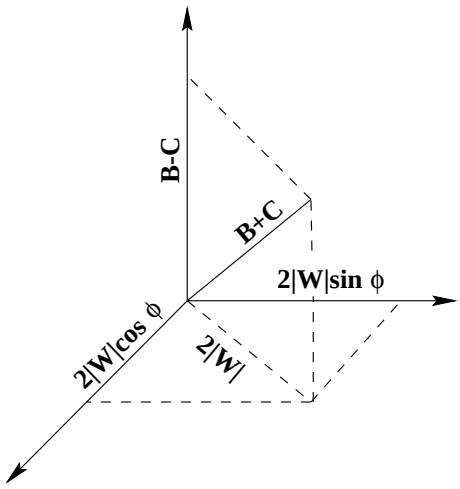

Figure 2.1: Three-dimensional representation of the covariance measurements. The vertical axis corresponds to the Stokes parameter for the basis in which the polarization measurements are made.

polarization basis that determines the relationship between the elements of the coherency matrix and Stokes parameters. Table 2.1 shows the relationship between the Stokes parameters, *which are receiver basis independent*, and the elements of the coherency matrix. In an H-V polarization basis,

$$\begin{aligned} \mathbf{J} &= \begin{bmatrix} \langle E_H E_H^* \rangle & \langle E_H E_V^* \rangle \\ \langle E_H^* E_V \rangle & \langle E_V E_V^* \rangle \end{bmatrix} \\ &= \begin{bmatrix} W_H & W_{HV} \\ W_{HV}^* & W_V \end{bmatrix} \\ \mathbf{J} &= \frac{1}{2} \begin{bmatrix} I+Q & U+jV \\ U-jV & I-Q \end{bmatrix} . \end{aligned} \tag{2.26}$$

2.4.1 The Spherical Angles of the Poincaré Sphere

Figure 2.2 illustrates the Poincaré sphere and the description of polarization state defined in terms of two sets of angles: $(2\delta, 2\tau)$ in Figure 2.2a and $(2\alpha, \phi)$ in Figure 2.2b, where 2δ and 2α are polar angles and 2τ and ϕ are azimuthal angles. The $(2\delta, 2\tau)$ description of polarization state is simply related to the covariances measured in an L-R receiver basis. From Figure 2.2a we can determine the angles $(2\delta, 2\tau)$ in terms of the Stokes parameters and from Table 2.1 we can find the Stokes parameters in

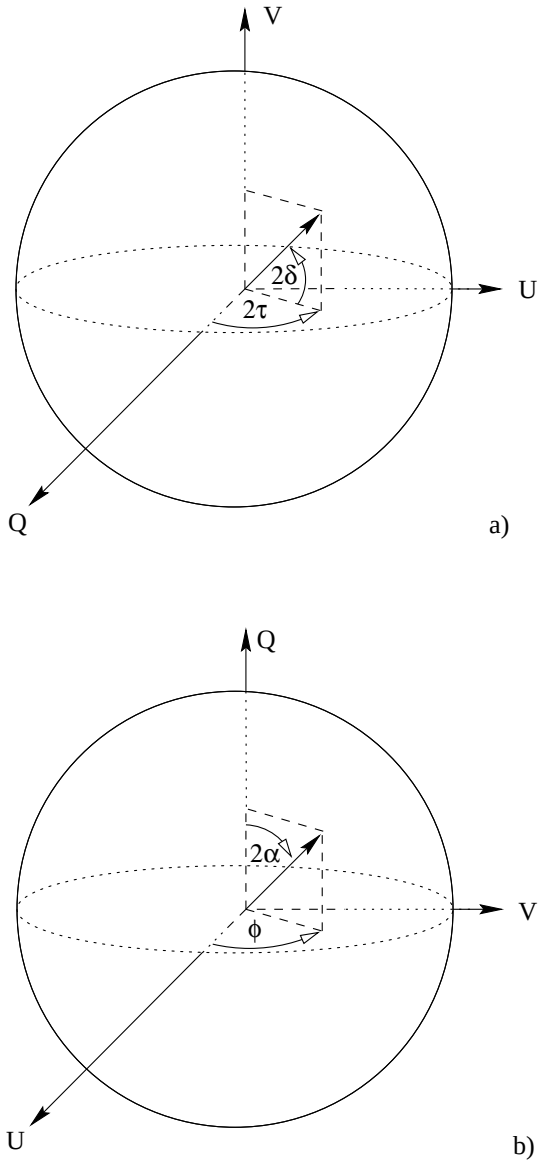

Figure 2.2: Definition of the angles of the Poincaré sphere a) (δ, τ) and b) (α, ϕ) description. Different polarizations states are depicted in the two figures.

terms of the covariances measured in an L-R receiver basis. The result is,

$$\begin{aligned} \tan 2\delta &= \frac{V}{\sqrt{Q^2+U^2}} \\ \tan 2\delta &= \frac{W_L - W_R}{2|W_{LR}|} , \end{aligned} \tag{2.27}$$

and,

$$\begin{aligned} \tan 2\tau &= \frac{U}{Q} \\ &= \frac{2\mathrm{ImW_{LR}}}{2\mathrm{ReW_{LR}}} . \end{aligned} \tag{2.28}$$

The $(2\alpha, \phi)$ description of polarization state is simply related to the covariances measured in an H-V receiver basis. From Figure 2.2b we can determine the angles $(2\alpha, \phi)$ in terms of the Stokes parameters and from Table 2.1 we can find the Stokes parameters in terms of the covariances measured in an H-V receiver basis. The result is,

$$\begin{aligned} \tan 2\alpha &= \frac{\sqrt{U^2+V^2}}{Q} \\ &= \frac{2|W_{HV}|}{W_H - W_V} , \end{aligned} \tag{2.29}$$

and,

$$\begin{aligned} \tan \phi &= \frac{V}{U} \\ &= \frac{2\mathrm{ImW_{HV}}}{2\mathrm{ReW_{HV}}} . \end{aligned} \tag{2.30}$$

The angles (α, ϕ) and (δ, τ) are the physical angles of the polarization ellipse as shown in Appendix A.

Figure 2.2b and Table 2.1 can be used to determine (δ, τ) and (α, ϕ) in terms of the covariances for different polarization receiver bases. For example, we can determine the α angle in terms of the covariances of an L-R receiver basis,

$$\begin{aligned} \tan 2\alpha &= \frac{\sqrt{U^2+V^2}}{Q} \\ &= \frac{\sqrt{(2\mathrm{ImW_{LR}})^2 + (\mathrm{W_L} - \mathrm{W_R})^2}}{2\mathrm{ReW_{LR}}} . \end{aligned} \tag{2.31}$$

The elements of the coherency matrix, the covariances, are related to the Stokes parameters. The relationship depends on the receiver basis used to make the measurement as shown in Table 2.1. The spherical angles (δ, τ) and (α, ϕ) are related to the Stokes parameters as shown in Figure 2.2. Once we choose a receiver basis, the spherical angles can be determined directly from the measurements without using the Stokes parameters. In practice, we will find it is computationally convenient to determine the Stokes parameters.

The transformation of measurements from one polarization basis to any other polarization basis is an important problem in radar meteorology. The methods of this section are well suited to that purpose. Common radar parameters measured in an *L-R* basis can be determined from *H-V* basis measurements and vice versa. Application of this technique to commonly used radar parameters can be found in the appendix.

2.4.2 Eigenvalues of J and the Degree of Polarization

The elements on the main diagonal of the coherency matrix are real and positive receiver powers. The off-diagonal elements are complex conjugates of each other. The coherency matrix is Hermitian. The degree of polarization may be described in terms of the eigenvalues of the coherency matrix. The eigenvalues of a Hermitian matrix are nonnegative, $0 \leq \lambda_2 \leq \lambda_1$. The characteristic equation for matrix $\mathbf{J}$ is,

$$\mathbf{Det}[\mathbf{J} - \lambda \mathbf{I}] = 0 \ , \tag{2.32}$$

where $\mathbf{I}$ is the identity matrix. Solving for the eigenvalues,

$$\lambda_{2,1} = \frac{W_1 + W_2 \pm \sqrt{(W_1 + W_2)^2 - 4(W_1 W_2 - |W|^2)}}{2} \ . \tag{2.33}$$

Summing the two eigenvalues we find $\lambda_1 + \lambda_2 = W_1 + W_2 = I$. The sum of the two eigenvalues is equal to the total power or the trace of the coherency matrix. The difference of the eigenvalues is,

$$\begin{aligned} \lambda_1 - \lambda_2 &= \sqrt{(W_1 + W_2)^2 - 4(W_1 W_2 - |W|^2)} \\ &= (W_1 + W_2)\sqrt{1 - \frac{4(W_1 W_2 - |W|^2)}{(W_1 + W_2)^2}} \\ &= (W_1 + W_2)p \ , \end{aligned} \tag{2.34}$$

where we recognize the last form is the same as (2.17). The ratio of the difference and the sum of the eigenvalues is,

$$\frac{\lambda_1 - \lambda_2}{\lambda_1 + \lambda_2} = p \ , \tag{2.35}$$

or, the degree of polarization.

In this section we showed how the degree of polarization is determined from the eigenvalues of the coherency matrix. The results can be summarized as,

$$\begin{aligned} \lambda_1 + \lambda_2 &= W_1 + W_2 \\ \lambda_1 - \lambda_2 &= p(W_1 + W_2) \\ \frac{\lambda_1 - \lambda_2}{\lambda_1 + \lambda_2} &= p \ . \end{aligned} \tag{2.36}$$

2.4.3 The Correlation Coefficient and the Degree of Polarization

In some radar systems, the correlation between the two receiver channel signals is expressed in terms of the correlation coefficient $|\rho| = |W|/\sqrt{W_1 W_2}$. Equation (2.16) can then be written in terms of $|\rho|$:

$$\begin{aligned} p &= \sqrt{1 - \frac{4(W_1 W_2 - |W|^2)}{(W_1 + W_2)^2}} \\ 1 - p^2 &= \frac{4 W_1 W_2}{(W_1 + W_2)^2} \cdot \left(1 - \frac{|W|^2}{W_1 W_2}\right) \\ 1 - p^2 &= \left(\frac{W_{gm}}{W_{am}}\right)^2 (1 - |\rho|^2) \ . \end{aligned} \tag{2.37}$$

where W_{gm} and W_{am} are the geometric and arithmetic mean of the signals in the two channels, respectively.

$$\begin{aligned} W_{gm} &= \sqrt{W_1 W_2} \\ W_{am} &= \frac{W_1 + W_2}{2} \ . \end{aligned} \tag{2.38}$$

Equation (2.37) provides a simple relationship between the degree of polarization and the correlation coefficient. The same result can be found in *Born* and *Wolf* (1975). The degree of polarization and the correlation coefficient are equal when $W_1 = W_2$. (When $W_1 = W_2$, $W_{gm} = W_1$, $W_{am} = W_1$, $W_{gm}/W_{am} = 1$, and $p = |\rho|$.)

To investigate the behavior of the ratio of the geometric to arithmetic mean, let $W_1 = xW_2$, where x is some positive factor. $W_{gm} = \sqrt{x}W_2$, $W_{am} = \frac{(1+x)}{2}W_2$, and

$$\begin{aligned} \frac{W_{gm}}{W_{am}} &= \frac{2\sqrt{x}}{1+x} \\ \left(\frac{W_{gm}}{W_{am}}\right)^2 &= \frac{4x}{(1+x)^2} \ . \end{aligned} \tag{2.39}$$

To find the extrema of W_{gm}/W_{am}, we take the derivative of (2.39) and set it equal to zero,

$$\frac{\partial}{\partial x}\left(\frac{W_{gm}}{W_{am}}\right)^2 = \frac{4-4x}{(1+x)^3} \ . \tag{2.40}$$

Since x is a positive factor the denominator is never zero. The ratio is maximized when $x = 1$, or $W_1 = W_2$. $W_1 = W_2$ when the power in the two receiver channels is equal. When $W_1 = 0$ or $W_2 = 0$, then $W_{gm}/W_{am} = 0$. The ratio of the geometric to arithmetic mean of the power in the two receiver channels is constrained to, $0 \leq \frac{W_{gm}}{W_{am}} \leq 1$. Since $0 \leq \frac{W_{gm}}{W_{am}} \leq 1$ it follows that

$$\begin{aligned} 1-p^2 &= \left(\frac{W_{gm}}{W_{am}}\right)^2 (1-|\rho|^2) \\ 1-p^2 &\leq 1-|\rho|^2 \\ p^2 &\geq |\rho|^2 \ . \end{aligned} \tag{2.41}$$

And, since $0 \leq |\rho| \leq 1$ and $0 \leq p \leq 1$,

$$0 \leq |\rho| \leq p \leq 1 \ . \tag{2.42}$$

Both $|\rho|$ and p can be zero or unity and $|\rho| = p$ only when $\frac{W_{gm}}{W_{am}} = 1$. The inequality (2.42) can also be found in *Born* and *Wolf* (1975).

Note that if the receiver basis is *H-V* , then the correlation ρ is $\rho_{HV}(0)$ of *Sachidananda* and *Zrnić* (1985). The zero refers to the correlation coefficient measured at zero time lag between H and V measurements. The constraint of zero lag is superfluous here since the measurement of ρ is determined simultaneously from the voltages in the two receivers. We can see that $\rho_{HV}(0)$ is closely related to the degree of polarization in (2.37). This relationship has not been recognized previously in radar meteorology literature except for a brief reference in *Torlaschi* and *Holt* (1998): "The parameter p is similar to, but not identical with, the linear correlation ρ_{HV}."

For radars that transmit and receive in the same polarization basis, $\frac{W_{gm}}{W_{am}} \approx 0$ when the means are calculated from the power in the co-polar and cross-polar channels because $W_{gm} \to 0$. Since the cross-polar channel is relatively weak, W_{gm}/W_{am} would

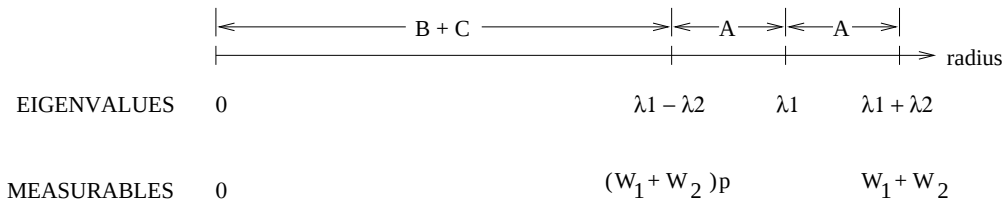

Figure 2.3: Geometrical interpretation of the degree of polarization in terms of the eigenvalues of the coherency matrix and the system measurables.

be a sensitive function of signal-to-noise ratios. $\frac{W_{gm}}{W_{am}} \approx 1$ when the means are calculated from the power in the co-polar channels for alternate orthogonal transmitted polarizations.

The parameter, $\frac{W_{gm}}{W_{am}}$, is termed the geometric-to-arithmetic mean ratio. The geometric-to-arithmetic mean ratio is useful since it is insensitive to absolute power levels (i.e., calibration) and it depends only on the ratio of the power in the two receiver channels. We can see this if we rewrite the geometric-to-arithmetic means ratio as,

$$\begin{aligned} \frac{W_{gm}}{W_{am}} &= \frac{4W_1W_2}{(W_1+W_2)^2} \\ &= \frac{4W_1W_2}{W_1^2+2W_1W_2+W_2^2} \\ &= \frac{4}{\frac{W_1}{W_2}+2+\frac{W_2}{W_1}} \ . \end{aligned} \tag{2.43}$$

The geometric-to-arithmetic means ratio depends only on the *ratio* of the power in the two channels. Equation (2.37) can be used to determine the degree of polarization directly from the measurements if the correlation coefficient is one of the radar parameters. The parameter W_{gm}/W_{am} is shown to have a geometrical interpretation in the next chapter.

2.4.4 Geometric Interpretation of the Degree of Polarization

The degree of polarization has a geometrical interpretation. Figure 2.3 shows the radial component of the Poincaré sphere in terms of the eigenvalues of the coherency matrix **J** and also in terms of the elements of the coherency matrix and the degree of polarization, p. There are three different radii shown but only two are important.

The radius of the inner sphere is $p(W_1 + W_2) = \lambda_1 - \lambda_2$. The radius of the inner sphere represents the polarized power. The radius of the outer sphere is $W_1 + W_2 = \lambda_1 + \lambda_2$. The radius of the outer sphere represents the total power (unpolarized plus polarized). The differences in the radii of the outer and inner sphere is the total unpolarized power, $I_u = 2A$. The ratio of the inner sphere radius to the outer sphere radius is the degree of polarization, p. When the outer and inner sphere have the same radius, the wave is completely polarized. When the inner sphere radius is zero, the wave is unpolarized.

The presence of an unpolarized component in the received wave does not change the polarization state of the completely polarized component (*Kostinski*, 1992). The polarization state is the same anywhere along the radius (except when $p = 0$ and the wave is unpolarized). Only the degree of polarization changes along the radius. We can still determine the spherical angles, (δ, τ) and (α, ϕ). But, we have to be careful because of the possible presence of unpolarized power. For example, $\sin 2\alpha = \frac{2|W|}{B+C}$. If we use the total power $I = (B+C+2A)$ in place of the polarized power $(B+C)$ then we introduce an error in the α angle. The differences of the power in the two receiver channels proves more useful since $W_1 - W_2 = (A + B) - (A + C) = B - C$. The unpolarized power (A), being equal in the two receiver channels, cancels. The α angle then be be correctly determined using the relationship $\tan 2\alpha = \frac{2|W|}{W_1 - W_2}$. The angle determined in this way is not corrupted by the presence of an unpolarized component. The angles (δ, τ) and (α, ϕ) can be determined from the measurements in an H-V or L-R basis regardless of the degree of polarization.

2.5 Summary

In this chapter, we showed how the measurements made using dual orthogonal receivers (coherency matrix elements) are related to the Stokes parameters and the spherical angles of the Poincaré sphere, (α, ϕ) and (δ, τ). We also showed how the measurements could be used to determine the degree of polarization of the received wave and how the eigenvalues of the coherency matrix are related to the degree of polarization and the total received power. Finally, the degree of polarization was given a geometrical interpretation of a sphere inside a sphere. The radii of the two concentric spheres are the total polarized power and total power. We will find an application of this sphere inside a sphere interpretation in the next chapter.

In the next chapter, the effect of propagation through and backscatter from me-

teorological targets on the polarization state and degree of polarization is considered in detail. In preparation for this analysis we summarize one of the results of this chapter. The spherical (α, ϕ) angles of the Poincaré sphere in terms of the elements of the coherency matrix, in an H-V basis can be written as,

$$\begin{aligned} \tan 2\alpha &= \frac{2|W_{HV}|}{W_H - W_V} \\ \tan \phi &= \frac{\mathrm{ImW_{HV}}}{\mathrm{ReW_{HV}}} \, . \end{aligned} \tag{2.44}$$

The spherical (δ, τ) angles of the Poincaré sphere in terms of the elements of the coherency matrix, in an L-R basis can be written as,

$$\begin{aligned} \tan 2\delta &= \frac{W_L - W_R}{2|W_{LR}|} \\ \tan 2\tau &= \frac{\mathrm{ImW_{LR}}}{\mathrm{ReW_{LR}}} \, . \end{aligned} \tag{2.45}$$

The spherical angles (α, ϕ) are used in the next chapter to determine the depolarization trajectory on the Poincaré sphere due to aligned non-spherical and spherical particles. The spherical angles (δ, τ) are used to determine the depolarization trajectory on the Poincaré sphere due to randomly oriented particles.

Chapter 3

Meteorological Polarimetry

3.1 Introduction

The goal of radar meteorology is to determine something about the target (e.g., rain) and the path to the target by examining the differences between the transmitted polarization state and the backscattered polarization state. A review of the published literature would find a typical approach taken by various researchers is to analyze a single, deterministic scatterer. The single scatterer analysis is then used to construct (using superposition) a cloud of spatially random scatterers. Finally, the depolarization effects due to the path to and from the cloud of scatterers is included. The approach taken here is to assume depolarization along the propagation path to a range of scatterers, depolarization upon backscatter, and depolarization along the propagation path back to the radar antenna.[1]

In this chapter we will consider three classes of scatterers: aligned scatterers, spherical scatterers, and randomly oriented scatterers. The aligned scatterer case will be further broken down into horizontally aligned and non-horizontally aligned cases. For each class of scatterers we will calculate the covariances that are the elements of the coherency matrix. From the covariances, we will examine the trajectory of the depolarization on the Poincaré sphere. For the case of horizontally aligned scatterers, the coherent depolarization trajectory is best described in terms of the spherical angles, (α, ϕ) when the wave is completely polarized or (β, ϕ) for the general case when the wave is partially polarized. The new angle β is introduced to

[1]Incoherent depolarization results in a reduction in the degree of polarization. Coherent depolarization results in a change in the polarization state. Traditionally, radar meteorologists use "depolarization" to describe both coherent and incoherent depolarization.

simplify the analysis for the case of horizontally aligned particles. For the case of randomly oriented scatterers, the depolarization trajectory is best described in terms of the spherical angles, (δ, τ). For the case of non-horizontally aligned scatterers, the coherent depolarization trajectory is best described in terms of the spherical angles, (α', ϕ') or (β', ϕ'), which are (α, ϕ) and (β, ϕ) in a rotated receiver basis.

We will adopt the convention of (*Torlaschi* and *Holt*, 1998) where the polarization state is defined by looking away from the radar. An electric field vector of constant magnitude rotating in a clockwise direction is left-hand circularly (LHC) polarized regardless of whether it is propagating towards or away from the radar.

3.2 Aligned Particle Case

For the case in which propagation is through a region of aligned particles we can assume an alignment direction for simplicity. We will assume the meteorological particles along the propagation path and the backscatters are aligned horizontally with respect to the radar beam. The equation for the H and V components of the electrical field incident upon the radar antenna due to backscatter from a given volume in range can be written,

$$\begin{bmatrix} E_H \\ E_V \end{bmatrix}^r = C \sum_{i=1}^{N} \mathbf{P}_i \mathbf{S}_i \mathbf{P}_i \begin{bmatrix} E_H \\ E_V \end{bmatrix}^t , \tag{3.1}$$

where the superscripts t and r represent the transmitted and received electric fields, c is the speed of light, C is a constant of proportionality. $\mathbf{P}_i$ is the propagation matrix to the i^{th} scatterer

$$\mathbf{P}_i = \frac{1}{r_i} \begin{bmatrix} e^{-\gamma_H r_i} & 0 \\ 0 & e^{-\gamma_V r_i} \end{bmatrix} , \tag{3.2}$$

where γ_H and γ_V are the complex horizontal and vertical propagation constants of the propagation path and r_i is the range to the i^{th} scatterer. $\mathbf{S}_i$ is the backscattering matrix of the i^{th} particle described by

$$\mathbf{S}_i = \begin{bmatrix} S_{HH_i} & 0 \\ 0 & S_{VV_i} \end{bmatrix} . \tag{3.3}$$

There are N particles within the backscattering volume. The backscattering matrix has no off diagonal elements when the particles have a rotational axis of symmetry. For the case of horizontally aligned particles, the rotational axis of symmetry is assumed to be vertical.

Multiplying out the terms on the right hand side of (3.1) we find

$$\begin{bmatrix} E_H \\ E_V \end{bmatrix}^r = \sum_{i=1}^{N} \frac{1}{r_i^2} \begin{bmatrix} E_H^t S_{HH_i} e^{-2\gamma_H r_i} & 0 \\ 0 & E_V^t S_{VV_i} e^{-2\gamma_V r_i} \end{bmatrix} \tag{3.4}$$

3.2.1 Covariance Calculations

Once we have determined the H and V components of the backscattered wave incident upon the radar antenna, we can calculate the elements of the coherency matrix (namely, the power in the two receiver channels, W_H and W_V, and the complex cross correlation, W_{HV}). The power in the horizontal receiver channel can be found from its definition, $W_H^r = \overline{(E_H E_H^*)^r}$. Using the values of E_H^r from (3.4) we find

$$\begin{aligned} W_H &= \overline{(E_H E_H^*)^t} \sum_{i=1}^{N} \sum_{j=1}^{N} \overline{\frac{1}{r_i^2 r_j^2} S_{HH_i} S_{HH_j}^* e^{-2\gamma_H r_i} e^{-2\gamma_H^* r_j}} \\ &= \langle (E_H E_H^*)^t \rangle \sum_{i=1}^{N} \sum_{j=1}^{N} \overline{\frac{1}{r_i^2 r_j^2} S_{HH_i} S_{HH_j}^* e^{-2\gamma_H r_i} e^{-2\gamma_H^* r_j}} \ . \end{aligned} \tag{3.5}$$

The double sum can be written as a sum of self ($i = j$) and mutual ($i \neq j$) terms

$$\begin{aligned} W_H^r &= \langle |E_H^t|^2 \rangle \sum_{i=1}^{N} \overline{\frac{1}{r_i^4} |S_{HH_i}|^2 e^{-4\mathrm{Re}\gamma_\mathrm{H} \mathrm{r_i}}} \\ &+ \langle |E_H^t|^2 \rangle \sum_{i=1}^{N} \sum_{j \neq i}^{N} \overline{\frac{1}{r_i^2 r_j^2} S_{HH_i} S_{HH_j}^* e^{-2\mathrm{Re}\gamma_\mathrm{H}(\mathrm{r_i}+\mathrm{r_j})} e^{-j2\mathrm{Im}\gamma_\mathrm{H}(\mathrm{r_i}-\mathrm{r_j})}} \ . \end{aligned} \tag{3.6}$$

Since the positional relationship between any two particles is uncorrelated with the position between any other two particles, the phase term in the remaining double sum (the last exponential term on the RHS) averages to zero. The self term can be volume-averaged to give

$$A_H^2 \langle |S_{HH}|^2 \rangle \equiv (1/N) \sum \overline{|S_{HH_i}|^2 \frac{e^{-4\mathrm{Re}\gamma_\mathrm{H} \mathrm{r_i}}}{r_i^4}} \ , \tag{3.7}$$

where A_H^2 represents the two way mean attenuation of the H polarized component of the wave and the angle brackets indicate volume-averaged quantities. Writing the transmitted horizontal power as

$$W_H^t = \langle |E_H^t|^2 \rangle \ , \tag{3.8}$$

the receiver power in the H channel can be written in the form

$$W_H^r = A_H^2 N \langle |S_{HH}|^2 \rangle W_H^t = A_H^2 Z_H W_H^t \ , \tag{3.9}$$

where $Z_H = N\langle|S_{HH}|^2\rangle$ is the horizontal reflectivity. By similar arguments the power in the V receiver channel is given by

$$W_V^r = A_V^2 N\langle|S_{VV}|^2\rangle W_V^t = A_V^2 Z_V W_V^t \ . \tag{3.10}$$

The ratio of the power in the two receiver channels is

$$\left(\frac{W_H}{W_V}\right)^r = ZDR\frac{A_H^2}{A_V^2}\left(\frac{W_H}{W_V}\right)^t \ , \tag{3.11}$$

where $ZDR \equiv \frac{N\langle|S_{HH}|^2\rangle}{N\langle|S_{VV}|^2\rangle} = \frac{Z_H}{Z_V}$ is the differential reflectivity and A_H^2/A_V^2 is termed the two way differential propagation attenuation or more simply as the differential attenuation.

The complex cross covariance is defined as

$$W_{HV}^r = \overline{(E_H E_V^*)^r} \ . \tag{3.12}$$

Substituting in the values of E_H and E_V^* from (3.4) we find

$$\begin{aligned} W_{HV}^r &= \overline{(E_H E_V^*)^t}\sum_{i=1}^{N}\sum_{j=1}^{N}\overline{\frac{1}{r_i^2 r_j^2}S_{HH_i}S_{VV_j}^* e^{-2\gamma_H r_i}e^{-2\gamma_V^* r_j}} \\ &= \langle(E_H E_V^*)^t\rangle\sum_{i=1}^{N}\sum_{j=1}^{N}\overline{\frac{1}{r_i^2 r_j^2}S_{HH_i}S_{VV_j}^* e^{-2\gamma_H r_i}e^{-2\gamma_V^* r_j}} \ . \end{aligned} \tag{3.13}$$

Again, we can break this sum into two parts, self and mutual terms

$$\begin{aligned} W_{HV}^r &= \langle(E_H E_V^*)^t\rangle\sum_{i=1}^{N}\overline{\frac{1}{r_i^4}S_{HH_i}S_{VV_i}^* e^{-2\mathrm{Re}(\gamma_H+\gamma_V)r_i}e^{-j2\mathrm{Im}(\gamma_H-\gamma_V)r_i}} \\ &+ \langle(E_H E_V^*)^t\rangle\sum_{i=1}^{N}\sum_{i\neq j}^{N}\overline{\frac{1}{r_i^2 r_j^2}S_{HH_i}S_{VV_j}^* e^{-2\mathrm{Re}(\gamma_H r_i+\gamma_V r_j)}e^{-j2\mathrm{Im}(\gamma_H r_i-\gamma_V r_j)}} \ . \end{aligned} \tag{3.14}$$

Due to the random position of the particles, the phase term of the double sum (the last exponential term on the RHS) again averages to zero. We can find the volume-averaged quantities

$$\sum_{i=1}^{N}\overline{\frac{1}{r_i^4}S_{HH_i}S_{VV_i}^* e^{-2\mathrm{Re}(\gamma_H+\gamma_V)r_i}e^{-j2\mathrm{Im}(\gamma_H-\gamma_V)r_i}} = N\langle S_{HH}S_{VV}^*\rangle A_H A_V e^{-j2\phi_{dp}} \ , \tag{3.15}$$

where the angle brackets on the scattering term represents volume averaged quantities and the one way differential propagation phase shift.

The correlation coefficient of the transmitted polarization state is defined as

$$\rho_{HV} = \frac{\langle E_H E_V^* \rangle}{\sqrt{\langle |E_H|^2 \rangle \langle |E_V|^2 \rangle}} \ . \tag{3.16}$$

By re-arranging this equation we find

$$\langle E_H E_V^* \rangle = \rho_{HV} \sqrt{\langle |E_H|^2 \rangle \langle |E_V|^2 \rangle} = \rho_{HV} \sqrt{W_H W_V} \ . \tag{3.17}$$

The cross correlation can be written in the form

$$W_{HV}^r = N \rho_{HV}^t A_H A_V \sqrt{W_H^t W_V^t} \langle |S_{HH} S_{VV}^*| \rangle e^{-j(2\phi_{dp} - \delta_\ell)} \ , \tag{3.18}$$

where δ_ℓ is the differential phase shift upon backscatter and is defined by

$$\delta_\ell = \mathrm{Arg} \langle S_{HH} S_{VV}^* \rangle \ . \tag{3.19}$$

The correlation coefficient of the received wave can be found

$$\begin{aligned} \rho_{HV}^r &= \frac{W_{HV}^r}{\sqrt{W_H^r W_V^r}} \\ &= \frac{N \rho_{HV}^t A_H A_V \sqrt{W_H^t W_V^t} \langle |S_{HH} S_{VV}^*| \rangle}{\sqrt{N^2 \langle |S_{HH}|^2 \rangle \langle |S_{VV}|^2 \rangle A_H^2 A_V^2 W_H^t W_V^t}} e^{-j(2\phi_{dp} - \delta_\ell)} \\ &= \rho_{HV}^t \frac{\langle |S_{HH} S_{VV}^*| \rangle}{\sqrt{\langle |S_{HH}|^2 \rangle \langle |S_{VV}|^2 \rangle}} e^{-j(2\phi_{dp} - \delta_\ell)} \ . \end{aligned} \tag{3.20}$$

The term,

$$f \equiv \frac{\langle |S_{HH} S_{VV}^*| \rangle}{\sqrt{\langle |S_{HH}|^2 \rangle \langle |S_{VV}|^2 \rangle}} \ , \tag{3.21}$$

is a measure of how well the shapes of the particles in the scattering volume are correlated with each other. We call this term the shape correlation coefficient and denote it as f. For complete correlation of the shapes, $f = 1$. If the shapes are uncorrelated, $f = 0$. The correlation coefficient of the backscattered wave is now simply related to the correlation coefficient of the transmitted wave through the shape correlation coefficient and ϕ_{dp} and δ_ℓ,

$$\rho_{HV}^r = f \rho_{HV}^t e^{-j(2\phi_{dp} - \delta_\ell)} \ . \tag{3.22}$$

The correlation coefficient is reduced upon backscatter through the shape correlation coefficient, f. By analogy, variations in the shapes of the particles in the propagation

path will also reduce the correlation coefficient. To account for this possibility, we re-write Equation 3.22 as

$$\rho_{HV}^{r} = f_{prop}^{2} \cdot f \rho_{HV}^{t} e^{-j(2\phi_{dp} - \delta_{\ell})} \ , \tag{3.23}$$

where $0 \leq f_{prop}^{2} \leq 1$ is the two way loss in the correlation coefficient due to variations in the shape of the particles in the propagation path.

In summary, the radar measurements are used to determine the covariances of the backscattered signal incident upon the radar antenna. The first two covariances are the power in the two receiver channels, W_H and W_V. The third covariance is the complex cross covariance of the signals in the two receiver channels, W_{HV}. The results are simpler when the normalized covariances are considered. The ratio of the power in the two receiver channels W_H/W_V has a simple form,

$$\frac{W_H^r}{W_V^r} = ZDR \cdot \left(\frac{A_H}{A_V}\right)^2 \left(\frac{W_H}{W_V}\right)^t \ , \tag{3.24}$$

where ZDR is the differential reflectivity, $(A_H/A_V)^2$ is the two way differential attenuation, and W_H^t/W_V^t represents the ratio of the H and V power of the transmitted polarization state. The correlation coefficient of the received H and V signals is also in a simple form

$$\rho_{HV}^{r} = f_{prop}^{2} \cdot f \rho_{HV}^{t} e^{-j(2\phi_{dp} - \delta_{\ell})} \ , \tag{3.25}$$

where $2\phi_{dp}$ is the two way differential propagation phase shift, f is the shape correlation coefficient of the scatterers in the scattering volume, f_{prop}^{2} is a measure of the variation of the propagation path, and δ_{ℓ} is the differential phase shift upon backscatter. The normalized covariances will be used in the next section to determine motion on the surface of the Poincaré sphere due to depolarization.

3.2.2 Trajectory on the Poincaré Sphere

In this section we will examine the motion of the polarization state on the Poincaré sphere due to backscatter and propagation depolarization in the presence of horizontally aligned particles.

Depolarization and Changes in the ϕ Angle

The angle, ϕ, on the Poincaré sphere is defined as the angle from the U axis to the polarization state projected onto the U-V plane. The change in the angle ϕ on the

Poincaré sphere due to coherent depolarization can be found simply from the ratio of the argument of the received ρ_{HV} to the argument of the transmitted ρ_{HV}. The result is

$$\Delta\phi = \text{Arg}\left(\frac{\rho^r_{HV}}{\rho^t_{HV}}\right) = -(2\phi_{dp} - \delta_\ell) \ , \tag{3.26}$$

where $2\phi_{dp}$ is the two way differential propagation phase shift and δ_ℓ is the differential phase upon backscatter. The phase of the correlation coefficient contains the phase information about the propagation path (ϕ_{dp}) and the backscattering process (δ_ℓ).

Depolarization and Changes in the α Angle

The spherical angle 2α is the angle between the polarization state on the surface of the Poincaré sphere and the Q axis. The angle 2α is defined by the covariances,

$$\tan 2\alpha = \frac{2|W_{HV}|}{W_H - W_V} \ . \tag{3.27}$$

If we normalize the cross correlation, W_{HV}, by the geometric mean of the power in the two receiver channels, we can determine 2α from the normalized covariances.

$$\begin{aligned} \tan 2\alpha &= \frac{2|W_{HV}|}{\sqrt{W_H W_V}} \frac{\sqrt{W_H W_V}}{W_H - W_V} \\ &= \frac{2|\rho_{HV}|}{\sqrt{\frac{W_H}{W_V}} - \sqrt{\frac{W_V}{W_H}}} \\ &= \frac{2|\rho_{HV}|\sqrt{\frac{W_V}{W_H}}}{1 - \frac{W_V}{W_H}} \\ &= \frac{2\tan\alpha}{1 - \tan^2\alpha} \end{aligned} \tag{3.28}$$

The spherical angle, α, of the transmitted polarization state is given by

$$\tan 2\alpha^t = \frac{2|\rho^t_{HV}|}{\sqrt{\frac{W^t_H}{W^t_V}} - \sqrt{\frac{W^t_V}{W^t_H}}} = \frac{2|\rho^t_{HV}|\sqrt{\frac{W^t_V}{W^t_H}}}{1 - \frac{W^t_V}{W^t_H}} \tag{3.29}$$

The α angle of the backscattered polarization state can be found in terms of the transmitted polarization state and the differential attenuation of the propagation path and the differential reflectivity of the backscatterers.

$$\tan 2\alpha^r = \frac{2f^2_{prop} \cdot f|\rho^t_{HV}|}{\sqrt{\frac{ZDR \cdot A^2_H W^t_H}{A^2_V W^t_V}} - \sqrt{\frac{A^2_V W^t_V}{ZDR \cdot A^2_H W^t_H}}} = \frac{2f^2_{prop} \cdot f|\rho^t_{HV}|\sqrt{\frac{A^2_V W^t_V}{ZDR \cdot A^2_H W^t_H}}}{1 - \frac{A^2_V W^t_V}{ZDR \cdot A^2_H W^t_H}} \tag{3.30}$$

For the special case of a fully polarized transmitted wave, $|\rho_{HV}^t| = 1$, a backscattering region where the shapes of the scatterers are all the same, $f = 1$, and no variations in the propagation path, $f_{prop}^2 = 1$, the change in the α angle is in the simple form of

$$\tan \alpha^r = \frac{1}{\sqrt{ZDR}} \frac{A_V}{A_H} \tan \alpha^t \ , \tag{3.31}$$

where we have made use of the trigonometric identity

$$\tan 2\alpha = \frac{2 \tan \alpha}{1 - \tan^2 \alpha} \ . \tag{3.32}$$

Equation 3.31 can be written in the form

$$\tan \alpha^r = G \tan \alpha^t \ , \tag{3.33}$$

where $G = (A_V/A_H)/\sqrt{ZDR}$. For the case of rain, the differential attenuation $A_H/A_V < 1$ and the differential reflectivity, $ZDR = Z_H/Z_V > 1$. Figure 3.1 shows the change in the 2α angle when the backscattering exhibits positive differential reflectivity ($ZDR > 1$) and with no depolarization from propagation ($A_V/A_H = 1$) and, therefore, $G < 1$. The plot in the figure is rotationally symmetric around the Q axis ($\alpha = 0$) since the change in 2α is independent of the phase between the H and V components of the incident wave. The backscattered polarization state moves towards the +Q pole of the sphere (H polarization state) for $ZDR > 1$.

Figure 3.2 shows the change in the 2α angle when the wave propagates through a region exhibiting positive differential attenuation ($A_V/A_H > 1$) and with no depolarization upon backscatter ($ZDR = 1$) and, therefore, $G > 1$. The plot in the figure is rotationally symmetric around the Q axis ($\alpha = 0$) since the change in 2α is independent of the phase between the H and V components of the incident wave. The backscattered polarization state moves towards the -Q pole of the sphere (V polarization state) for $A_V/A_H > 1$.

The combined effect of positive differential reflectivity and positive differential attenuation is a reduced change in the α angle compared to either effect separately. When the shapes in the backscattering region are not well correlated ($f < 1$), or the transmitted wave is not completely polarized ($|\rho_{HV}^t| < 1$), or there are variations in the propagation path ($f_{prop}^2 < 1$), the use of the trigonometric identity of (3.32) does not result in any simplification.

We would like to find a solution to the general case of Equation 3.30 that has the form of the special case solution of Equation 3.31. We can define a new angle, 2β as

$$\tan 2\beta = \frac{2}{\sqrt{\frac{W_H}{W_V}} - \sqrt{\frac{W_V}{W_H}}} = \frac{2\sqrt{\frac{W_V}{W_H}}}{1 - \frac{W_V}{W_H}} = \frac{2 \tan \beta}{1 - \tan^2 \beta} \ . \tag{3.34}$$

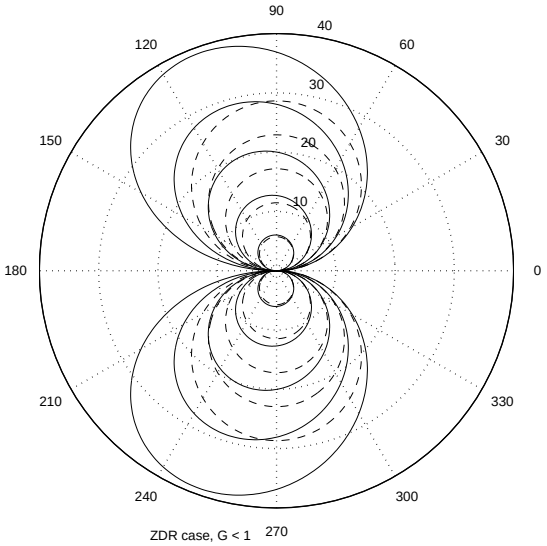

Figure 3.1: Change in the spherical angle (2α) due to scattering from aligned particles as a function of the incident value of (2α), for different values of G. The value of G varies from 0.5 to .9 in steps of 0.1 and causes 2α to move toward 0°, which is the H polarization point.

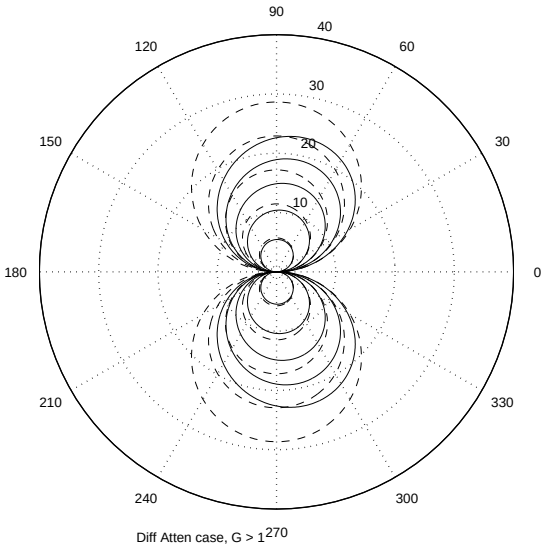

Figure 3.2: Change in the spherical angle (2α) due to propagation through aligned particles as a function of the incident value of (2α), for different values of G. The value of G varies from 1.1 to 1.5 in steps of 0.1 and causes 2α to move toward 180°, which is the V polarization point.

We can find the relation between the $\tan 2\alpha$ and $\tan 2\beta$ by taking the ratio of $\tan 2\alpha$ to $\tan 2\beta$. The result is

$$\frac{\tan 2\alpha}{\tan 2\beta} = |\rho_{HV}| \ . \tag{3.35}$$

The ratio of the tangents of the two angles is the correlation coefficient. We can use the trigonometric identity of (3.32) to find $\tan\beta$,

$$\tan\beta = \sqrt{\frac{W_V}{W_H}} \ . \tag{3.36}$$

The tangent of β is equal to the square root of the ratio of the power in the two receiver channels. The backscattered β angle can be found in terms of the incident β and the properties of the propagation path and the backscatters. The result is

$$\tan\beta^r = \frac{1}{\sqrt{ZDR}} \cdot \frac{A_V}{A_H} \tan\beta^t \ . \tag{3.37}$$

The change in the β angle is independent of the shape correlation of the backscatters, the transmitted ρ_{HV}, and the value of f_{prop} of the propagation path. The change in the 2α angle has been decomposed into changes due to differential attenuation and differential reflectivity and changes due the partial polarization of the transmitted wave and changes in the correlation coefficient. This is made clear by expressing the backscattered spherical angle 2α as

$$\begin{aligned} \tan 2\alpha^r &= f_{prop}^2 \cdot f\rho_{HV}^t \tan 2\beta^r \\ \tan 2\alpha^r &= f_{prop}^2 \cdot f\rho_{HV}^t \frac{2\sqrt{\frac{A_V^2}{ZDR \cdot A_H^2}} \tan\beta^t}{1 - \frac{A_V^2}{ZDR \cdot A_H^2} \tan^2\beta^t} \ . \end{aligned} \tag{3.38}$$

The two angles 2α and 2β are equal when $f_{prop}^2 \cdot f\rho_{HV}^t = 1$, or in other words, the two angles are equal when the transmitted wave is completely polarized, the shapes of the scatterers in the backscattering region are well correlated, and there is no reduction in the correlation coefficient due to propagation. The two angles are also equal when $2\alpha = 2\beta = \pi/2$. Figure 3.3 shows a right triangle showing the relationship between the 2β angle and sides of the triangle which are the sum of the power, the difference of the power, and the geometric mean of the power in the H and V polarizations and the 2α angle and the sides of the right triangle which are the sum of the *polarized* power, the difference of the power, and the cross correlated power in the H and V polarizations. The right triangle of Figure 3.3 can be used to

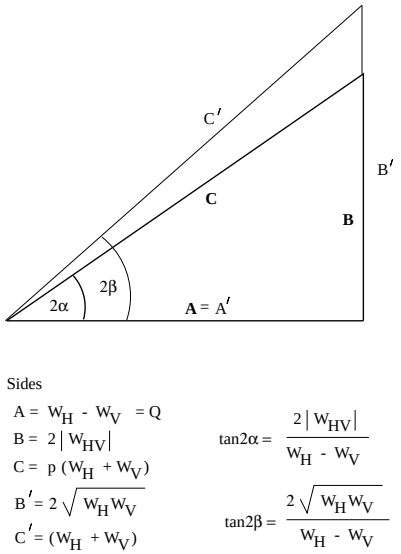

Figure 3.3: Right triangle definitions of the 2α and the 2β angle. The 2α angle depends on the cross correlation through the term W_{LR} while the 2β angle does not.

find the relationships

$$\begin{aligned} \frac{\tan 2\alpha}{\tan 2\beta} &= |\rho_{HV}| \\ \frac{\cos 2\beta}{\cos 2\alpha} &= p \\ \frac{\sin 2\alpha}{\sin 2\beta} &= \frac{|\rho_{HV}|}{p} \,. \end{aligned} \tag{3.39}$$

Figure 3.4 shows the relationship between the angles 2α and 2β in a cross sectional view of the Poincaré sphere. The angle 2β is found from a constant Q projection of the polarization state on the fully polarized inner sphere onto the outer total power sphere. The angle 2β does not depend on the degree of polarization. As the degree of polarization is reduced, the inner sphere of Figure 3.3 shrinks. The 2α angle defined by the intersection of the constant Q line with the inner sphere gets smaller for a constant 2β.

The introduction of the new angle, $\tan\beta = \sqrt{W_V/W_H}$ to decouple the degree of polarization or the correlation coefficient from the 2α angle is an original result of this work.

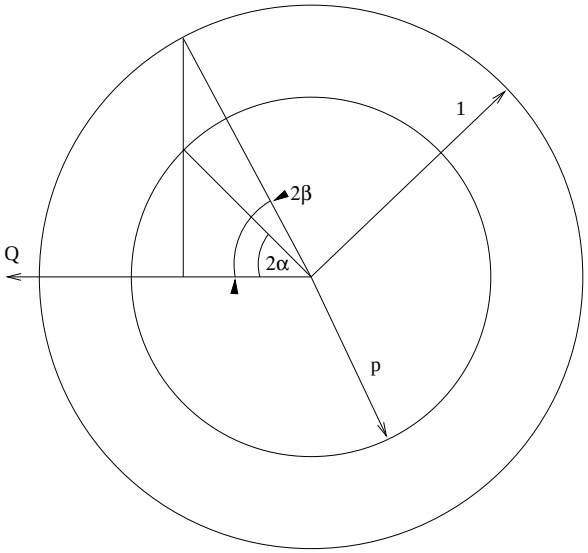

Figure 3.4: Cross sectional view of the Poincaré sphere sliced by a plane through the Q axis. The total power (outer circle) has been normalized to unity. The polarized power (inner circle) has a radius equal to the degree of polarization , p. The angle 2α is defined in terms of the polarized power while 2β is defined in terms of the total power. The point on the total power circle is a constant Q projection of the polarized power polarization state.

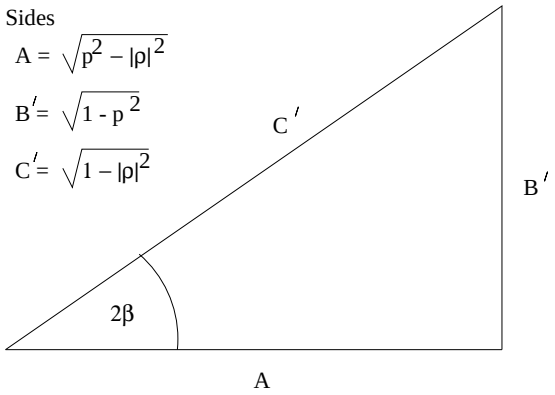

Figure 3.5: The angle 2β provides a geometrical relationship between the degree of polarization , p, and the correlation coefficient, ρ.

Depolarization and Changes in p

We will now determine how the degree of polarization, p, changes due to propagation depolarization and depolarization upon backscatter. As shown in Equation 2.37, the degree of polarization can be written as

$$\sqrt{1-p^2} = \left(\frac{W_{gm}}{W_{am}}\right)\sqrt{1-|\rho_{HV}|^2}\ , \tag{3.40}$$

where p is the degree of polarization, $W_{gm} = \sqrt{W_H W_V}$ is the geometric mean of the power in H and V polarizations, and $W_{am} = \frac{1}{2}(W_H + W_V)$ is the arithmetic mean of the power in the H and V polarizations. We can use Figure 3.3 to find a geometrical interpretation of the quantity W_{gm}/W_{am}. The result is

$$\frac{W_{gm}}{W_{am}} = \frac{2\sqrt{W_H W_V}}{W_H + W_V} = \sin 2\beta\ . \tag{3.41}$$

Substituting this result into (3.40) we find

$$\sqrt{1-p^2} = \sin 2\beta\sqrt{1-|\rho_{HV}|^2}\ . \tag{3.42}$$

This equation can be used to establish a right triangle that is similar to the right triangle of Figure 3.4 but involves the quantities, $\sqrt{1-p^2}$, $\sqrt{1-|\rho_{HV}|^2}$, and $\sqrt{p^2-|\rho_{HV}|^2}$. This geometrical relationship is shown in Figure 3.5. Although the result is interesting, the geometrical relationship of Figure 3.5 is not especially useful.

Since the relationship between $|\rho_{HV}|$ and p is not a simple relationship, the change in the backscattered degree of polarization, is not simple. Nonetheless, we can write the solution as

$$\sqrt{\frac{1-p_r^2}{1-p_t^2}} = \frac{\sin 2\beta^r}{\sin 2\beta^t}\sqrt{\frac{1-f_{prop}^4\cdot f^2|\rho_{HV}|^2}{1-|\rho_{HV}|^2}}\ , \tag{3.43}$$

where we have defined $|\rho_{HV}| = |\rho_{HV}^r| = f_{prop}^2 \cdot f|\rho_{HV}^t|$ and the superscripts used to indicate the transmitted and received quantities are shown as subscripts on the degree of polarization, p. This result is expressed more simply in terms of the correlation coefficient, ρ_{HV} as in Equation 3.25.

Summary of the Depolarization Trajectory on the Poincaré Sphere due to Horizontally Aligned Particles

To describe the coherent depolarization trajectory on the Poincaré sphere due to propagation through and backscatter from horizontally aligned particles, we will break the

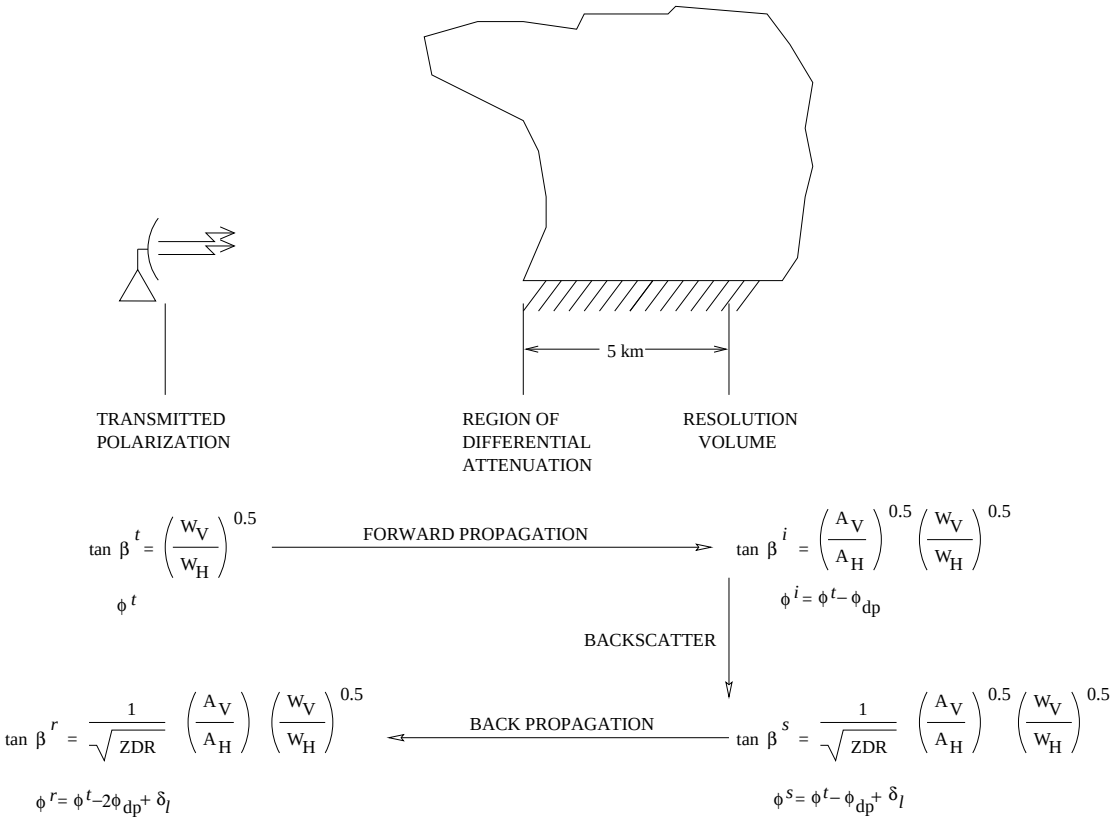

Figure 3.6: Schematic representation of the depolarization due to differential attenuation and differential phase shift of the propagation path and differential reflectivity and differential phase shift upon backscatter for the case of horizontally aligned particles. The angle β is changed only due to differential attenuation and reflectivity and the angle ϕ changes only due to differential propagation phase and phase shift upon backscatter.

problem down into four components: the transmitted polarization state, the incident polarization state, the backscattered polarization state and the received polarization state. These polarizations states will be represented by superscripts, t, i, s, r, for transmitted, incident, backscattered and received polarization states, respectively. Figure 3.6 shows a schematic representation of the affect of depolarization due to the propagation path back and forth to a region of scatterers on the angles β and ϕ for the case of horizontally aligned particles.

The trajectory of the path on the Poincaré sphere for the case of horizontally aligned particles is relatively simple. The transmitted phase between H and V components is given by ϕ^t. After propagation to the range volume of interest the incident phase between the H and V components is given by

$$\phi^i = \phi^t - \phi_{dp} \ , \tag{3.44}$$

where ϕ_{dp} is the one way differential propagation phase shift. Immediately after backscattering, the phase between the H and V components of the wave is given by

$$\phi^s = \phi^i + \delta_\ell = \phi^t - (\phi_{dp} - \delta_\ell) \ , \tag{3.45}$$

where δ_ℓ is the differential phase shift upon backscatter. After propagation back to the radar antenna, the phase between the H and V components is given by

$$\phi^r = \phi^s - \phi_{dp} = \phi^t - (2\phi_{dp} - \delta_\ell) \ , \tag{3.46}$$

where $2\phi_{dp}$ is the two way differential propagation phase shift. The correlation phase of the received wave contains information about the anisotropy of the propagation path and the size of the backscattering particles (differential phase shift upon backscatter, $\delta_\ell = 0$ for Rayleigh scattering).

The β angle of the transmitted polarization state is given by

$$\tan\beta^t = \sqrt{\frac{W_V^t}{W_H^t}} \ . \tag{3.47}$$

After propagation to the range of interest the incident β angle is given by

$$\tan\beta^i = \frac{A_V}{A_H}\tan\beta^t = \frac{A_V}{A_H}\sqrt{\frac{W_V^t}{W_H^t}} \ , \tag{3.48}$$

where A_V/A_H is the one way differential propagation attenuation. Immediately after backscatter the β angle is given by

$$\tan\beta^s = \frac{1}{\sqrt{ZDR}}\tan\beta^i = \frac{1}{\sqrt{ZDR}}\frac{A_V}{A_H}\sqrt{\frac{W_V^t}{W_H^t}} \ , \tag{3.49}$$

where ZDR is the differential reflectivity. After propagation back to the radar antenna, the β angle is given by

$$\tan\beta^r = \frac{A_V}{A_H}\tan\beta^s = \frac{1}{\sqrt{ZDR}}\frac{A_V^2}{A_H^2}\sqrt{\frac{W_V^t}{W_H^t}}\ , \tag{3.50}$$

where A_V^2/A_H^2 is the two differential propagation attenuation.

The backscattered ρ_{HV}^r is simply related to the incident ρ_{HV}^t, the correlation of the shapes within the scattering volume and the variation of the propagation path. The equation for this was found to be

$$|\rho_{HV}^r| = f_{prop}^2 \cdot f|\rho_{HV}^t|\ , \tag{3.51}$$

where ρ_{HV}^t is the correlation coefficient of the transmitted polarization state, f is the shape correlation coefficient of the scatterers in the scattering volume and f_{prop}^2 is the two way correlation coefficient of the propagation path. We could also determine the change in the α angle but in general it is a complicated result. The change in the β angle is much more useful since the result is relatively simple. The change in the angle 2α on the Poincaré sphere is more than the change in the β angle when $f_{prop}^2 \cdot f\rho_{HV}^t < 1$,

$$\tan 2\alpha^r = f_{prop}^2 \cdot f|\rho_{HV}^t|\tan 2\beta^r\ . \tag{3.52}$$

The degree of polarization , p, changes in a complicated way that is governed by Equation 3.43. The change in the correlation coefficient is much more simply expressed as in Equation 3.25.

3.3 Spherical Particle Case

Spherical particles can be considered to be a special case of the aligned particle case. The backscattering matrix for a single spherical particle is given by

$$\begin{bmatrix} S & 0 \\ 0 & S \end{bmatrix}\ , \tag{3.53}$$

where S is the backscattering cross section of the spherical particle.

Equations 3.9 and 3.10 can be used to determined the W_H and W_V covariances in the case of spherical particles. The results are

$$\begin{aligned} W_H^r &= NA_H\langle|S|^2\rangle \\ W_V^r &= NA_V\langle|S|^2\rangle\ . \end{aligned} \tag{3.54}$$

The ratio of the power in the two receiver channels is

$$\left(\frac{W_H}{W_V}\right)^r = \left(\frac{A_H}{A_V}\right)\left(\frac{W_H}{W_V}\right)^t \ . \tag{3.55}$$

The differential attenuation of the path to the spherical scatterers will depolarize the transmitted wave but there is no depolarization upon backscatter. If the path to the scatterers is full of spherical particles, then $A_H = A_V$ and the power in the two receiver channels is the same as the power in the H and V components of the transmitted wave.

The cross covariance W_{HV} of spherical particles can be found from Equation 3.18 as

$$W^r_{HV} = N|\rho^t_{HV}|\sqrt{A_H A_V W^t_H W^t_V}\langle|S|^2\rangle e^{-j\phi_{dp}} \ , \tag{3.56}$$

where the differential phase shift upon backscatter, $\delta_\ell = \mathrm{Arg}\langle|S_c|^2\rangle = 0$. The correlation coefficient of the signals in the two receiver channels can be found to be

$$\frac{W^r_{HV}}{\sqrt{W^r_H W^r_V}} = |\rho^r_{HV}| = f^2_{prop}\cdot|\rho^t_{HV}|e^{-j2\phi_{dp}} \ . \tag{3.57}$$

There is still a differential propagation phase shift to the region of spherical backscatters and a possible reduction in the correlation coefficient but there is no depolarization upon backscatter. When the propagation path consist of spherical particles, then the received ρ_{HV} is the same as the transmitted ρ_{HV}.

The degree of polarization, p, will change only as a result of the differential attenuation of the propagation path to the region of spherical scatterers. This change in the degree of polarization will have the form,

$$\frac{\sqrt{1-p^2_r}}{\sin 2\beta^r} = \frac{\sqrt{1-p^2_t}}{\sin 2\beta^t} \ , \tag{3.58}$$

where we have assumed $f^2_{prop} \approx 1$. The change in the degree of polarization due to backscatter from spherical particles has a simpler form than Equation 3.43 since $f = 1$ for spherical scatterers.

For the case of spherical backscatters, there is no depolarization upon backscatter. Only the anisotropy of the propagation path to the region of spherical backscatterers will depolarize the transmitted wave.

3.4 Randomly Oriented Particle Case

For the case of randomly oriented particles, it is possible to analyze the problem in an *H-V* basis but there is a simpler approach. To simplify the analysis for the

case of randomly oriented particles we will neglect the propagation depolarization ($\mathbf{P_i} = \frac{e^{-\gamma_0 r_i}}{r_i} \cdot \mathbf{I}$ in Equation 3.1). Any anisotropy of the propagation path to the region of randomly oriented scatterers will result in terms that represent the differential attenuation (A_H/A_V) and differential propagation phase shift (ϕ_{dp}) as in the cases of aligned and spherical particles. When we neglect depolarization of the propagation path, the polarization state incident upon the backscatterers is the same as the transmitted polarization state and the backscattered polarization state is the same as the received polarization state. The transmitted or incident polarization will be respresented with a superscript i and the backscattered or received polarization will be represented with a superscript s.

The random nature of the orientation of the particles can be exploited if we analyze the problem in a circular basis. We will use the (δ, τ) description of the polarization state, where δ is related to the ratio of the minor and major semi-axes of the polarization ellipse and τ is the ellipse orientation angle (see Figure A.5). When a linear polarization state ($2\delta = 0$ and 2τ at any angle) is incident upon a region of randomly oriented scatterers, the backscattered polarization state can be described as $(2\delta^s, 2\tau^i)$. The backscattered $2\delta^s$ is the same for any incident orientation angle, $2\tau^i$, and the backscattered angle $2\tau^s$ is the same as the incident 2τ because the scatterers are randomly oriented with no preferred orientation. When considering backscattering from randomly oriented particles the $(2\delta, 2\tau)$ description of polarization state is a better description than the $(2\alpha, \phi)$ description because only 2δ should change upon backscatter.

For the case of randomly oriented particles, the equation for the LHC and RHC components of the electric field incident upon the radar antenna due to backscatter from a given volume in range can be written

$$\begin{bmatrix} E_L \\ E_R \end{bmatrix}^s = C \sum_{i=1}^{N} \mathbf{P}_i \mathbf{S}_i \mathbf{P}_i \begin{bmatrix} E_L \\ E_R \end{bmatrix}^i , \tag{3.59}$$

where the superscripts i and s represent the incident and backscattered electric fields, c is the speed of light and , C is a constant of proportionality. $\mathbf{P}_i$ is the propagation matrix to the i^{th} scatterer

$$\mathbf{P}_i = \frac{1}{r_i} \begin{bmatrix} e^{-\gamma_0 r_i} & 0 \\ 0 & e^{-\gamma_0 r_i} \end{bmatrix} , \tag{3.60}$$

where γ_0 is the free space complex propagation constant of the propagation path. $\mathbf{S_i}$ is the backscattering matrix in a circular basis for the i^{th} scatterer described by the

matrix

$$\mathbf{S_i} = \begin{bmatrix} \Sigma_i & \Delta_i \\ \Delta_i^* & \Sigma_i \end{bmatrix} , \tag{3.61}$$

where

$$\begin{aligned} \Delta_i &= \frac{1}{2}(S_{xx_i} - S_{yy_i})e^{j\tau_i} \\ \Sigma_i &= \frac{1}{2}(S_{xx_i} + S_{yy_i}) , \end{aligned} \tag{3.62}$$

where τ_i is the alignment direction of the major axis (subscript xx) of the i^{th} particle off of the horizontal. There are N randomly oriented and positioned scatterers in the scattering volume.

Expanding Equation 3.59 we find

$$\begin{bmatrix} E_L \\ E_R \end{bmatrix}^s = \sum_{i=1}^{N} \frac{e^{-2\gamma_0 r_i}}{r_i^2} \begin{bmatrix} \Sigma_i E_L^i + \Delta_i E_R^i \\ \Delta_i^* E_L^i + \Sigma_i E_R^i \end{bmatrix} . \tag{3.63}$$

3.4.1 Covariance Calculations

Once we have determined the LHC and RHC components of the backscattered wave incident upon the radar antenna we can calculate the elements of the coherency matrix, the power in the two receiver channels W_L, and W_R, and the complex cross correlation, W_{LR}. The power in the LHC receiver channel can be found from the definition $W_L^r = \overline{(E_L E_L^*)^r}$. Using the values of E_L^r from (3.63) we find

$$W_L^r = \sum_{i=1}^{N}\sum_{j=1}^{N} \overline{\frac{e^{-2(\gamma_o r_i + \gamma_0^* r_j)}}{r_i^2 r_j^2}(\Sigma_i E_{L_i}^t + \Delta_i E_{R_i}^t)(\Sigma_i E_{L_j}^t + \Delta_i E_{R_j}^t)^*} . \tag{3.64}$$

As we have done previously for the aligned particles case, the double sum can be broken into self and mutual terms. Since the position and orientation between pairs of particles is random, the phase terms of the mutual terms ($i \neq j$) will average to zero. Only the self ($i = j$) terms will remain. The result is

$$\begin{aligned} W_L^r &= \sum_{i=1}^{N} \overline{\frac{e^{-4\mathrm{Re}\gamma_o \mathrm{r_i}}}{r_i^4}(|\Sigma_i|^2|E_{L_i}^t|^2 + (\Sigma_i^*\Delta_i E_{R_i}E_{L_i}^* + (\Sigma_i^*\Delta_i E_{R_i}E_{L_i}^*)^*)^t + |\Delta_i|^2|E_{R_i}^t|^2)} \\ &= \sum_{i=1}^{N} \overline{\frac{e^{-4\mathrm{Re}\gamma_o \mathrm{r_i}}}{r_i^4}(|\Sigma_i|^2|E_{L_i}^t|^2 + 2\mathrm{Re}(\Sigma_\mathrm{i}^*\Delta_\mathrm{i}\mathrm{E}_{\mathrm{R_i}}\mathrm{E}_{\mathrm{L_i}}^*)^\mathrm{t} + |\Delta_\mathrm{i}|^2|\mathrm{E}_{\mathrm{R_i}}^\mathrm{t}|^2)} \\ &= \sum_{i=1}^{N} \overline{\frac{e^{-4\mathrm{Re}\gamma_o \mathrm{r_i}}}{r_i^4}(|\Sigma_i|^2|E_{L_i}^t|^2 + 2\cos\tau_i|\Sigma_i^*\Delta_i|\mathrm{Re}(\mathrm{E}_{\mathrm{R_i}}\mathrm{E}_{\mathrm{L_i}}^*)^\mathrm{t} + |\Delta_\mathrm{i}|^2|\mathrm{E}_{\mathrm{R_i}}^\mathrm{t}|^2)} . \end{aligned} \tag{3.65}$$

We take the volume average of (3.65) and the result is

$$W_L^r = N\frac{e^{-4\mathrm{Re}\gamma_o \mathrm{R}}}{R^4}(\langle|\Sigma|^2\rangle W_L^t + \langle|\Delta|^2\rangle W_R^t \ , \tag{3.66}$$

where the angle brackets indicate the volume averaged quantities and the volume average of the middle term on the right hand side of (3.65) averaged to zero (over the alignment angle τ_i). Using similar arguments we can find the power, W_R^r, in the R receiver channel

$$W_R^r = N\frac{e^{-4\mathrm{Re}\gamma_o \mathrm{R}}}{R^4}(\langle|\Delta|^2\rangle W_L^t + \langle|\Sigma|^2\rangle W_R^t) \ . \tag{3.67}$$

We can find the complex cross covariance from the definition

$$W_{LR}^r = \overline{(E_L E_R^*)^r} \ . \tag{3.68}$$

Substituting in the values for E_L^r and E_R^r from (3.63) we find

$$W_{LR}^r = \sum_{i=1}^{N}\sum_{j=1}^{N}\overline{\frac{e^{-2(\gamma_0 r_i + \gamma_0^* r_j)}}{r_i^2 r_j^2}(|E_l^t|^2\Delta_i\Sigma_j + (E_L E_R^*)^t|\Sigma_i|^2 + (E_L^* E_R)^t\Delta_i\Delta_i + |E_R^t|^2\Sigma_i^*\Delta_j)} \ . \tag{3.69}$$

Since the positional relationship between particles is random, the phase term from the propagation matrix (the first term on the RHS of (3.69)) will average to zero for the mutual terms ($i \neq j$). Only the self terms ($i = j$) will remain. The remaining cross covariance terms are

$$W_{LR}^r = \sum_{i=1}^{N}\overline{\frac{e^{-4\mathrm{Re}\gamma_0 \mathrm{r_i}}}{r_i^4}|E_l^t|^2\Delta_i\Sigma_i^* + (E_L^* E_R)^t\Delta_i\Delta_i + (E_L E_R^*)^t|\Sigma_i|^2 + |E_R^t|^2\Sigma_i\Delta_i^*} \ . \tag{3.70}$$

When we take the volume average of (3.70) only one term survives

$$W_{LR}^r = N\frac{e^{-4\mathrm{Re}\gamma_0 \mathrm{R}}}{R^4}\langle E_L E_R^*\rangle^t\langle|\Sigma|^2\rangle = N\frac{e^{-4\mathrm{Re}\gamma_0 \mathrm{R}}}{R^4}|W_{LR}^t|e^{j2\tau^t}\langle|\Sigma|^2\rangle \ . \tag{3.71}$$

In this section we were able to determine the covariances due to backscatter from randomly oriented particles at a given volume in range. In the next section we will use the covariances to determine the trajectory of the polarization state on the Poincaré sphere due to randomly oriented particles.

3.4.2 Trajectory on the Poincaré sphere

In this section we will use the covariances that were determined in the last section to determine the trajectory on the Poincaré sphere due to backscatter from randomly oriented particles at a given volume in range. We will determine the trajectory on the Poincaré sphere in terms of the spherical angles 2δ and 2τ and the degree of polarization , p.

Depolarization and Changes in τ

The simplest result for the trajectory on the Poincaré sphere is found in the angle 2τ. From 2.45, the angle 2τ is defined to be $\mathrm{Arg}(W_{LR})$ and from Equation 3.71 we find

$$\mathrm{Arg}(W^r_{LR}) = \mathrm{Arg}(W^t_{LR}) \ . \tag{3.72}$$

Or,

$$2\tau^r = 2\tau^t \ . \tag{3.73}$$

The angle 2τ of the backscattered polarization state is the same as the 2τ of the incident polarization state. The orientation angle of the polarization ellipse does not change due to backscatter from randomly oriented backscatterers.

Depolarization and Changes in δ

The angle 2δ on the Poincaré sphere is defined in terms of the backscattered covariances,

$$\tan 2\delta^r = \frac{W^r_L - W^r_R}{2|W^r_{LR}|} \ . \tag{3.74}$$

When we substitute the backscattered values of W_L, W_R and W_{LR} from equations 3.66, 3.67 and 3.71 into (3.74) the result is

$$\begin{aligned} \tan 2\delta^r &= \frac{W^t_L - W^t_R}{2W^t_{LR}} \frac{(\langle|\Sigma|^2\rangle - \langle|\Delta|^2\rangle)}{\langle|\Sigma|^2\rangle} \\ &= \tan 2\delta^t \frac{(\langle|\Sigma|^2\rangle - \langle|\Delta|^2\rangle)}{\langle|\Sigma|^2\rangle} \ , \end{aligned} \tag{3.75}$$

where we have made the substitutions, $\langle|E^t_L|^2\rangle = W_L$, $\langle|E^t_R|^2\rangle = W_R$, and $\langle E_L E^*_R\rangle^t = W^t_{LR}$. Equation 3.75 can be further simplified by finding

$$\begin{aligned} \langle|\Sigma|^2\rangle - \langle|\Delta|^2\rangle &= \langle|S_{xx}|^2\rangle + 2\mathrm{Re}(\langle \mathrm{S_{xx}S^*_{yy}}\rangle) + \langle|\mathrm{S_{yy}}|^2\rangle \\ &- \langle|S_{xx}|^2\rangle + 2\mathrm{Re}\langle \mathrm{S_{xx}S^*_{yy}}\rangle - \langle|\mathrm{S_{yy}}|^2\rangle \\ &= 4\mathrm{Re}(\mathrm{S_{xx}S^*_{yy}}) \ . \end{aligned} \tag{3.76}$$

Equation 3.75 can now be written as

$$\tan 2\delta^r = g \tan 2\delta^t \ , \tag{3.77}$$

where we have defined

$$g = \frac{4\mathrm{Re}(\mathrm{S_{xx}S^*_{yy}})}{\langle|S_{xx} + S_{yy}|^2\rangle} \ . \tag{3.78}$$

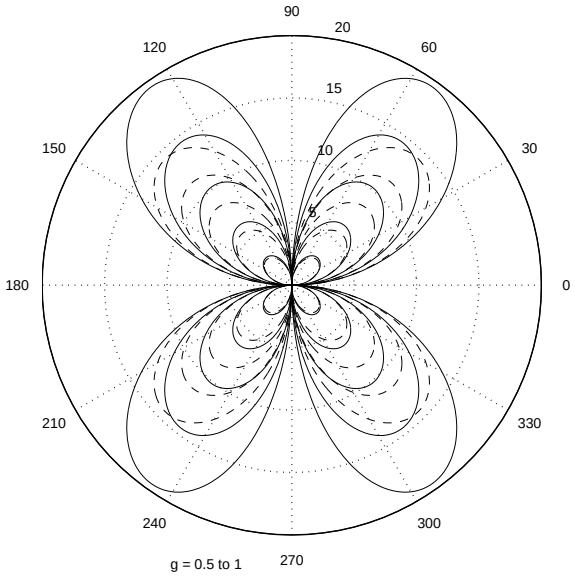

Figure 3.7: Change in the polarization parameter ($2\delta^s$) due to scattering by randomly oriented particles as function of the incident value of ($2\delta^i$), for different values of the scattering parameter g. The change is evaluated in degrees and always moves the polarization state toward the equator of the Poincaré sphere ($2\delta = 0$). g changes from 0.9 to 0.5 in steps of 0.1.

The parameter $0 \leq |g| \leq 1$ is termed the sphericity parameter and is a measure of how the average particle within the scattering volume differs from spherical.

Figure 3.7 shows a plot of (3.77). The solid line shows the actual change in the 2δ angle,

$$\begin{aligned} \Delta(2\delta) &= 2\delta^r - 2\delta^t \\ &= \tan^{-1}[g \tan 2\delta^t] - 2\delta^t \,, \end{aligned} \tag{3.79}$$

while the dashed line shows the small signal approximation to the change,

$$\Delta(2\delta) = (g-1)\left\{\frac{\sin[2(2\delta^t)]}{2}\right\} . \tag{3.80}$$

For g close to unity, the change in 2δ is a maximum halfway between the linear and circular polarization states (e.g., $2\delta = \pi/4$). The point of maximum change is skewed slightly toward circular if g departs significantly from unity. The backscattered 2δ is the same of as the incident value of 2δ when $2\delta = \pm 45^\circ$ or $2\delta = 0$ regardless of the value of g. For other values of incident 2δ, the polarization state backscattered from

randomly oriented particles is always more linear (less circular) than the incident polarization.

Depolarization and Changes in p

The change in the degree of polarization, due to backscattering from randomly oriented particles can be found in terms of the covariances. From Equation 2.45 we have the definition

$$\cos 2\delta = \frac{2|W_{LR}|}{p(W_L + W_R)} \ . \tag{3.81}$$

Or,

$$p \cos 2\delta = \frac{2|W_{LR}|}{W_L + W_R} \ . \tag{3.82}$$

We can write (3.82) is terms of transmitted and received quantities, take the ratio and substitute in the previously determined covariances. The result is

$$\frac{p^t \cos 2\delta^t}{p^r \cos 2\delta^r} = \frac{\langle|\Sigma|^2\rangle + \langle|\Delta|^2\rangle}{\langle|\Sigma|^2\rangle} \ . \tag{3.83}$$

The sphericity parameter, g, as defined in terms of the volume averaged backscattering matrix elements (Equation 3.75) is

$$\begin{aligned} g &= \frac{\langle|\Sigma|^2\rangle - \langle|\Delta|^2\rangle}{\langle|\Sigma|^2\rangle} \\ &= 1 - \frac{\langle|\Delta|^2\rangle}{\langle|\Sigma|^2\rangle} \ . \end{aligned} \tag{3.84}$$

Or,

$$1 - g = \frac{\langle|\Delta|^2\rangle}{\langle|\Sigma|^2\rangle} \ . \tag{3.85}$$

We can simplify the volume average backscattering term in (3.83) as

$$\begin{aligned} \frac{\langle|\Sigma|^2\rangle + \langle|\Delta|^2\rangle}{\langle|\Sigma|^2\rangle} &= 1 + \frac{\langle|\Delta|^2\rangle}{\langle|\Sigma|^2\rangle} \\ &= 1 + 1 - g \\ &= (2 - g) \ . \end{aligned} \tag{3.86}$$

Equation 3.83 can be written as

$$\frac{p^t \cos 2\delta^t}{p^r \cos 2\delta^r} = (2 - g) \ . \tag{3.87}$$

The ratio of the transmitted and received quantity, $p\cos 2\delta$, is equal to $(2-g)$, where g is the sphericity parameter of the randomly oriented particles in the scattering volume. The quantity $p\cos 2\delta$ is a measure of the polarized linear component of the wave. Equation 3.87 shows the polarized linear component of the received wave is always less than or equal to the polarized linear component of the transmitted wave after backscatter from randomly oriented particles. For incident linear polarizations the backscattered degree of polarization is given by

$$p^r = \frac{p^t}{(2-g)} \ . \tag{3.88}$$

Figure 3.8 shows a plot of (3.87) for various values of the sphericity parameter, g. Since the depolarization is independent of the value of τ the plot is rotationally symmetric about the V axis of the Poincaré sphere (see Figure A.9). For any particular value of the sphericity parameter, g, the ratio of the received degree of polarization to the transmitted degree of polarization is smallest when the transmitted polarization state is described by $2\delta = \pm\pi/2$ which is LHC or RHC. The ratio of the received degree of polarization to the transmitted degree of polarization is largest when the incident polarization state is described by $2\delta = 0$ or $2\delta = \pi$ which are linear polarizations at an arbitrary orientation angle, τ.

Summary of the Depolarization Trajectory on the Poincaré Sphere due to Randomly Oriented Particles

The depolarizing effects from randomly oriented particles can be summarized as follows. If the polarization state is defined in terms of the spherical angles (δ, τ) on the Poincaré sphere, the τ angle is seen to remain unchanged after backscattering. The δ angle and the degree of polarization both can change based upon the particle sphericity parameter, g, and the δ of the transmitted polarization state. Since $0 \leq |g| \leq 1$, the received δ angle is always less than the transmitted δ angle, from Equation 3.77

$$\delta^r \leq \delta^t \ . \tag{3.89}$$

The degree of polarization can never increase due to backscatter from randomly oriented particles. From Equation 3.87,

$$p^r(2-g) = \frac{p^t \cos 2\delta^t}{\cos 2\delta^r} \leq p^t \ . \tag{3.90}$$

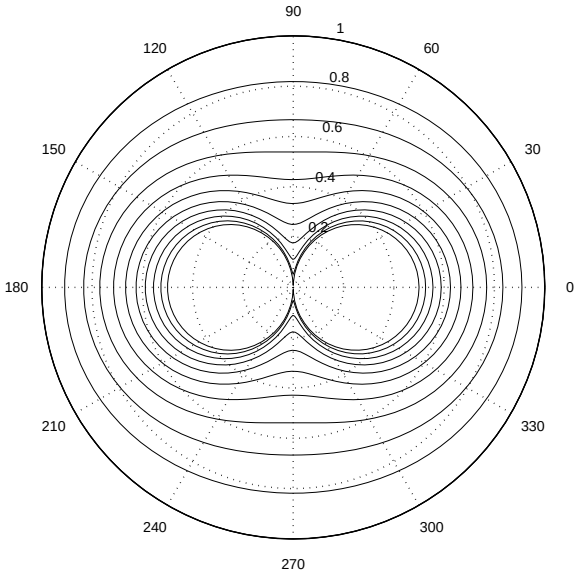

Figure 3.8: Fractional change in the degree of polarization p caused by randomly oriented non-spherical particles. The results are shown in a vertical plane through the polar axis of the Poincaré sphere, with the different curves representing different values of the sphericity parameter g. g varies from 1.0 to 0.0 in 0.1 steps from the outer to the inner curves, respectively.

The inequality comes from $\delta^r \leq \delta^t$, and $\cos 2\delta^t / \cos 2\delta^r \leq 1$. The result is,

$$p^r \leq \frac{p^t}{2-g} \; . \tag{3.91}$$

The backscattered degree of polarization from randomly oriented particles is always less than or equal to the transmitted degree of polarization.

The change in the α and ϕ angles can be found from Equation (A.58). In general both α and ϕ change when δ alone changes. The (δ, τ) description of polarization state is the better description basis since τ is invariant and only δ and p change due to backscatter from randomly oriented particles.

3.5 Non-Horizontally Aligned Particles

Previously we considered the case of horizontally aligned particles. It may be possible for precipitation particles to be aligned other than horizontally. If we assume horizontal alignment, then the interpretation of the depolarization trajectory on the

Poincaré sphere will be erroneous. The further the alignment is from horizontal the more erroneous the interpretation. In this chapter we describe a technique for determining alignment direction of precipitation particles involving the transmission of alternate orthogonal polarizations. In a later chapter, we will present a technique for determining the alignment direction of ice crystals in the upper parts of storms involving only a single transmitted polarization. Alignment direction measurements using a single transmitted polarization are possible only when there is a dominant coherent depolarization effect. In the case of ice crystals, the dominant depolarization effect is differential propagation phase. For the case of liquid precipitation, there is no dominant depolarization effect and the technique of this chapter must be used.

Assume the radar is capable of transmitting alternate orthogonal polarizations (i.e., LHC and RHC). This situation is illustrated in Figure 3.9a. When the particles are horizontally aligned, incident H and V polarizations will not be depolarized upon backscatter. H and V are therefore the characteristic polarizations for horizontally aligned particles. When the particles are oriented at an angle τ off of the horizontal the characteristic polarizations are $(2\delta = 0, 2\tau)$ and $(2\delta = 0, 2\tau + \pi/2)$. The ZDR of the particles transforms the incident LHC $(Q = U = 0, V = 1)$ and RHC polarization $(Q = U = 0, V = -1)$ towards the characteristic polarization state on the Poincaré sphere. When the particles are large enough to have a differential phase shift upon backscatter, the polarization states rotate around the characteristic polarization state.

For transmitted LHC and RHC pulses, the radar measurements can be used to determine the Stokes parameters, (Q_L, U_L, V_L) and (Q_R, U_R, V_R) where the subscripts refer to the transmitted polarization, LHC or RHC. We wish to determine the alignment direction of the particles from the known (Q_L, U_L, V_L) and (Q_R, U_R, V_R) values.

In Figure 3.9b, we can see that there is a rotated receiver basis where,

$$Q_L{}' = Q_R{}' \tag{3.92}$$

$$U_L{}' = -U_R{}' \,, \tag{3.93}$$

where the primes indicate the Stokes parameters in the rotated basis. The receiver basis is rotated through angle 2τ around the V axis. The rotation can be described mathematically as,

$$\begin{aligned} Q' &= Q\cos 2\tau - U\sin 2\tau \\ U' &= U\cos 2\tau + Q\sin 2\tau \,. \end{aligned} \tag{3.94}$$

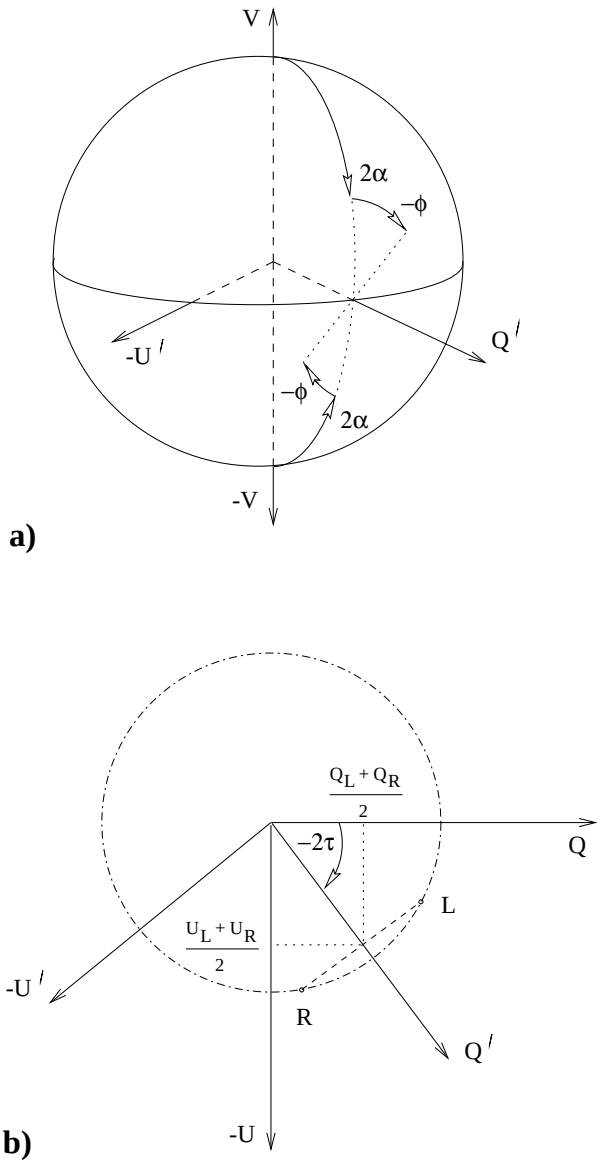

Figure 3.9: Backscatter from non-Rayleigh particles aligned at angle τ from the horizontal when LHC and RHC are transmitted on a) the Poincaré sphere and b) in the $Q - U$ plane.

Combining (3.92), (3.93), and (3.94) we can find the alignment angle 2τ,

$$\begin{aligned} \tan 2\tau &= \frac{Q_L - Q_R}{U_L - U_R} \\ &= -\frac{U_L + U_R}{Q_L + Q_R} \, . \end{aligned} \tag{3.95}$$

We can use either form of (3.95) to determine 2τ. We can also use the two forms of (3.95) to find the relationship,

$$\begin{aligned} \frac{Q_L - Q_R}{U_L - U_R} &= -\frac{U_L + U_R}{Q_L + Q_R} \\ Q_L^2 - Q_R^2 &= U_L^2 - U_R^2 \\ Q_L^2 + U_L^2 &= Q_R^2 + U_R^2 \, . \end{aligned} \tag{3.96}$$

This is the equation of a circle. The two points (Q_L, U_L) and (Q_R, U_R) lie on a circle in the Q/U plane as shown in Figure 3.9b.

In summary, α type changes always occur in a plane containing the two characteristic polarizations. By rotating the receiver basis, we are matching the receiver basis to the characteristic polarizations. ϕ changes, on the other hand, are rotations around the line connecting the two characteristic polarizations.

It is the assumption that rain is aligned horizontally that allows us to obtain all the polarization information while only transmitting a single polarization state. The fact that all the polarization information is available from a single transmitted polarization state if the particles are aligned along H and V has been previously noted in *Torlaschi* and *Holt* (1998). As has the fact that if one transmits a characteristic polarization, the orthogonal polarization must also be transmitted to determine the polarization response. Transmission of characteristic polarizations should be avoided since the orthogonal polarization must also be transmitted. The only additional information available from alternately transmitted orthogonal polarizations is the alignment direction of the backscatterers. When the backscatters are aligned horizontally there is no additional information contained in the radar returns from the transmitted orthogonal polarization.

3.6 Qualitative Description

In this section we provide a qualitative description of depolarization due to horizontally aligned and randomly oriented particles.

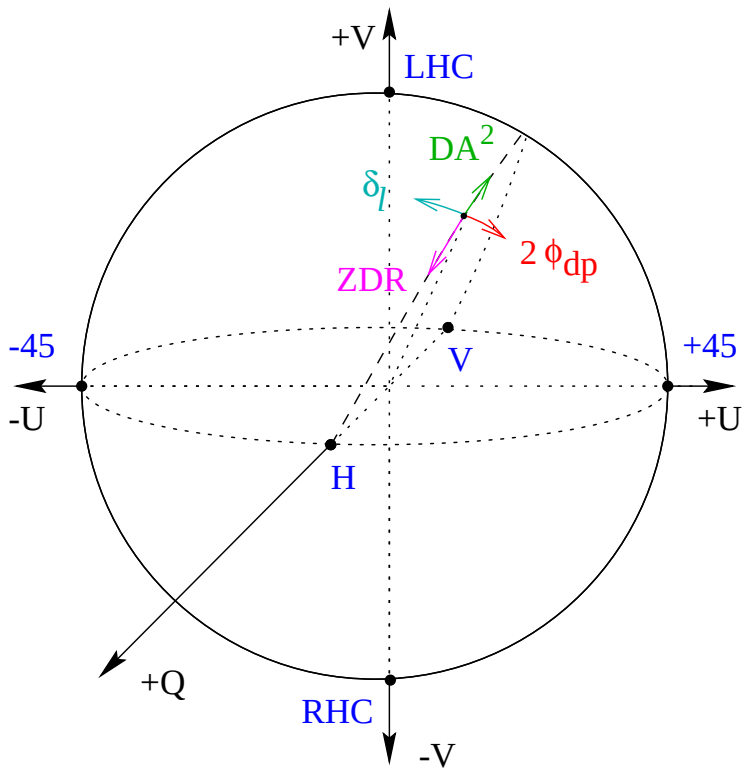

Figure 3.10: The effect of differential reflectivity (ZDR), differential attenuation ($DA^2 = A_H^2/A_V^2$), differential propagation phase (ϕ_{dp}), and differential phase shift upon backscatter (δ_ℓ) on the polarization state.

3.6.1 Horizontally Aligned Particles

Backscatter from horizontally aligned rain drops will result in an increase of the power in the H receiver channel relative to the V receiver channel. This is shown schematically in Figure 3.10 for differential reflectivity, $ZDR \equiv Z_H/Z_V > 1$. The polarization state moves towards the H polarization point along a great circle defined by the incident polarization state and the H and V polarization points on the Poincaré sphere. The great circle is oriented at an angle ϕ from the U axis. The phase between the H and V polarized components ($\phi = \phi_H - \phi_V$) is assumed to be unaffected by horizontally aligned particles within the resolution volume. For non-Rayleigh scattering, there is a differential phase shift upon backscatter resulting in a rotation of the great circle through the angle δ_ℓ around the Q-axis (counterclockwise).

Roundtrip propagation through a region of horizontally aligned drops will result in an increase in the V receiver channel power relative to the H receiver channel due

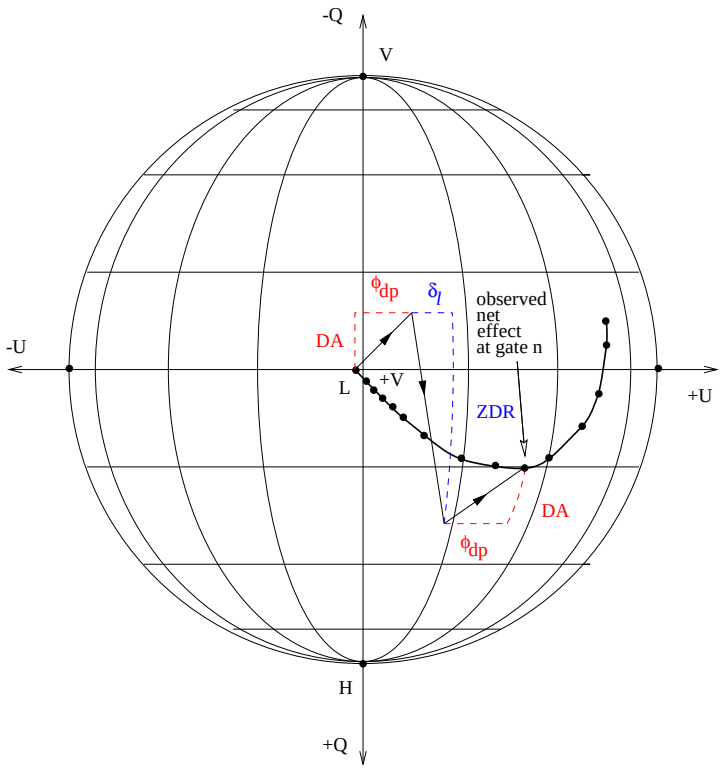

Figure 3.11: Schematic representation of the combined depolarization due propagation away from the radar, backscatter, and propagation back to the radar.

to differential attenuation $(A_H/A_V)^2 < 1$, where A_H and A_V are attenuation factors as defined in Equation 3.7. The polarization state moves towards the V polarization point along a great circle defined by the transmitted polarization state and the H and V polarization points on the Poincaré sphere. The great circle is oriented at an angle ϕ from the U axis. Forward scattering from the aligned particles retards the phase of the H component relative to the V component resulting in a rotation of the great circle through the angle $-2\phi_{dp}$ around the Q-axis (clockwise).

Figure 3.11 shows the combination of the propagation and backscattering effects. In this figure, the Poincaré sphere is oriented so the LHC pole is the nearest point to the viewer. The H polarization point is towards the bottom of the page and the +45 polarization point is to the right. The transmitted polarization state is close to LHC. The differential attenuation and differential phase of the propagation path to the range of interest moves the polarization state towards the V and +45 polarization points, respectively. Upon backscatter, the polarization state moves towards the

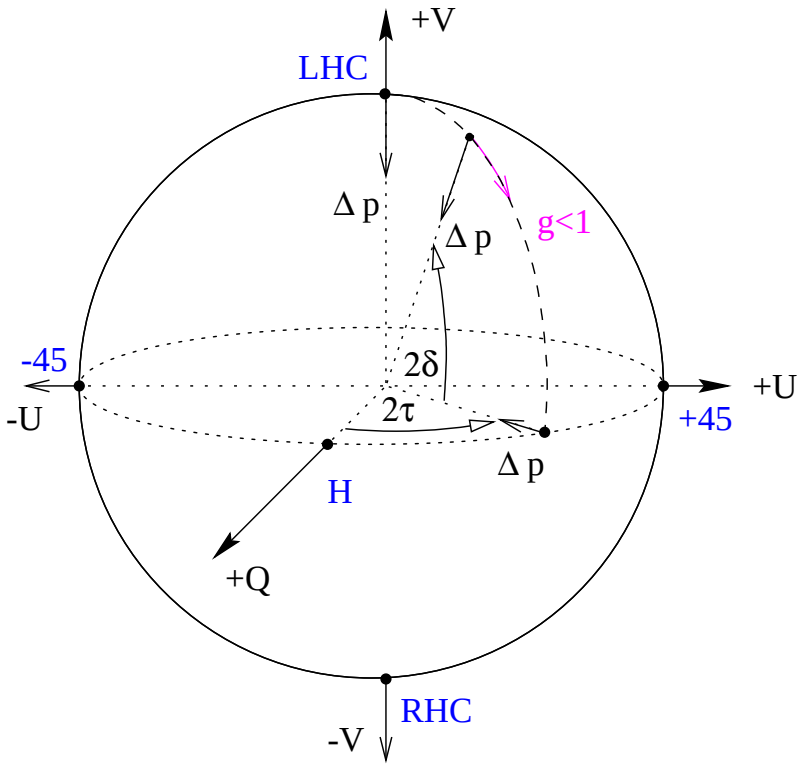

Figure 3.12: Depolarization due to backscatter from randomly oriented particles.

H polarization point. Additionally, for differential phase shift upon backscatter, the polarization state moves towards the +45 polarization point (δ_ℓ is typically negative). The backscattered wave is depolarized further by the differential attenuation and differential phase shift of the path as it propagates back to the radar. Only the net depolarization is visible at any particular range. Changes in the polarization state from one range to the next are a result of the incremental differential attenuation and differential phase of the intervening path and the changes in the differential reflectivity and differential phase upon backscatter from one range gate to the next. The total change in the polarization state from the near side to the far side of a storm through the rain region can be used to determine the average rainfall rate from the total differential attenuation or the total differential phase shift.

3.6.2 Randomly Oriented Particles

The depolarization due to backscatter from randomly oriented particles is a function of the incident polarization state and the average sphericity of the particles, g, as

shown schematically in Figure 3.12. The sphericity parameter, $g = 1$ for spherical particles and $g = 0$ for highly elongated particles (g is defined in Equation 3.78). For incident circular or linear polarizations, the depolarization is described by a reduction in the degree of polarization (see Figure 3.8 and Equation 3.77 for $2\delta^t = 0, \pm\pi/2$). The reduction in the degree of polarization for incident circular polarizations is a factor of g greater than the reduction in the degree of polarization for incident linear polarizations (from Equations 3.77 and 3.87). For incident elliptical polarizations, the polarization state moves along a great circle containing the incident polarization state and the L and R polarization points on the Poincaré sphere since the depolarization involves only a change in the polar angle 2δ (Equation 3.77) and not a change in the angle 2τ (Equation 3.73). The great circle is oriented at an angle 2τ from the Q-axis. The spherical angle 2δ is reduced and the degree of polarization is reduced by an amount greater than incident linear polarizations and less than incident circular polarization (see Figure 3.8). With incident elliptical polarizations, the backscattered polarization state will contain a larger linear component (from Equation 3.77, smaller 2δ is more linear) and larger unpolarized component than the incident polarization state (from Equation 3.91). The reduction in the spherical angle 2δ is greatest when the incident polarization is about halfway between linear and circular polarizations (see Figure 3.7).

Chapter 4

Optimal Polarization States

4.1 Introduction

In this chapter we examine the questions: what is the best polarization to transmit? And what is the best receiver basis? We will answer the second question first in this section. The remainder of this chapter is devoted to answering the first question.

The analysis of the previous chapter assumed an *H-V* receiver basis for horizontally aligned particles. The characteristic polarizations of a region of horizontally aligned raindrops are H and V. Characteristic polarizations are defined by the incident polarizations that produce minimum depolarization upon backscatter. An *H-V* receiver basis matches the characteristic polarizations of rain. The phase of the cross correlation, ϕ_{HV}, in an *H-V* receiver basis provides a direct measure of the combined effects of differential propagation phase shift (ϕ_{dp}) and differential phase shift upon backscatter (δ_ℓ). From (3.26), $\Delta\phi = -(2\phi_{dp} + \delta_\ell)$. The angle 2β provides a measure of the combined effects of differential reflectivity, ZDR, and differential attenuation in an *H-V* receiver basis in (3.37).

When H and V polarizations are separately transmitted on alternate pulses and simultaneously received, the co-polar signal (e.g., transmit H, receive H) is relatively strong while the cross-polar signal (e.g., transmit H, receive V) may not exceed the noise power level of the receivers. On the other hand, when equal amounts of H and V are transmitted simultaneously and there is sufficient backscattering, the signals in the two receiver channels will rise above the receiver noise power level almost simultaneously. To minimize the signal to noise effects in the receivers, we chose to transmit equal amount of H and V polarized power. In order to match the receiver basis to the characteristic polarizations of rain, we chose to receive in an *H-V* basis.

The proposed technique is transmission of equal amounts of H and V polarized power and reception of the backscattered signals in an *H-V* basis. The only free variable is the choice of the phase between the transmitted H and V components. When the phase difference between the transmitted H and V components is $\phi = \pm\pi/2$, the wave is circularly polarized. When the phase difference is $\phi = 0$ or $\phi = \pi$, the transmitted wave is slant linearly polarized.

It was shown in the previous chapter that there is no depolarization due to backscattering from spherical particles. Spherical particles backscatter the incident polarization state without depolarization. The backscatter from aligned and randomly oriented scatterers is examined in this chapter to determine the effect of different phases between the transmitted H and V components. To simplify the analysis, the depolarization of the path between the radar and the region of backscatter will be neglected.

4.2 Aligned Particles

The analysis of backscattering from aligned particles was performed in the last chapter and the depolarization effects on the degree of polarization and the spherical angles α and ϕ was determined. We can also find the effect of backscattering from aligned particles in terms of the measurables, the ratio of the power in the two receiver channels W_H and W_V, the correlation coefficient of the signal in the two receiver channels ρ_{HV}, and the phase of the correlation ϕ. Neglecting propagation effects, the backscattered measurable quantities are related to the incident (transmitted) polarization state and the ensemble of particles within the scattering volume by the equations,

$$\begin{aligned} \left(\frac{W_H}{W_V}\right)^s &= ZDR \cdot \left(\frac{W_H}{W_V}\right)^i \\ \phi^s &= \phi^i - \delta_\ell \\ \rho^s_{HV} &= f \cdot \rho^i_{HV} \ , \end{aligned} \tag{4.1}$$

where the superscripts i and s represent the incident and scattered values, ZDR is differential reflectivity, δ_ℓ is the differential phase shift upon backscattering and f is the shape correlation coefficient which is a measure of shape variation of the particles in the scattering volume. We can solve (4.1) to find the meteorological quantities, differential reflectivity, differential phase shift upon backscatter and the

shape correlation coefficient,

$$ZDR = \left(\frac{W_H}{W_V}\right)^s / \left(\frac{W_H}{W_V}\right)^i \tag{4.2}$$

$$\delta_\ell = \phi^i - \phi^s \tag{4.3}$$

$$f = |\rho^s_{HV}|/|\rho^i_{HV}| \ . \tag{4.4}$$

For the special case of equal amounts of fully polarized H and V transmitted power, only the differential phase shift upon backscatter δ_ℓ depends on the phase difference of the H and V components of the transmitted polarization state. ZDR is measured directly by the ratio of the power in the two receiver channels and f is measured directly by $|\rho^s_{HV}|$.

The phase of the correlation between the signals in the two receiver channels would be a direct measure of δ_ℓ if the transmitted phase $\phi = 0$. This suggests the transmitted polarization state should be slant linearly polarized ($W_H = W_V, \phi = 0$). The development in the next section provides a stronger argument not to transmit slant linear polarizations.

4.3 Randomly Oriented Particles

The analysis of backscattering from randomly oriented particles was performed in the last chapter. Since the particles are randomly oriented there is no preferred orientation, τ, of the polarization ellipse. The depolarization due to randomly oriented particles is azimuthally symmetric around the LHC and RHC poles of the Poincaré sphere (see Figure A.9). Because of this symmetry the depolarization is best described in terms of the spherical angles (δ, τ), where δ is a measure of the ellipticity of the polarization ellipse and τ is the orientation angle off of horizontal. The depolarization due to backscattering from randomly oriented particles in terms of the angles δ and τ and the degree of polarization , p is described by the equations,

$$\tan 2\delta^s = g \cdot \tan 2\delta^i \tag{4.5}$$

$$\tau^s = \tau^i \tag{4.6}$$

$$p^s \cos 2\delta^s = \frac{p^i \cos 2\delta^i}{(2-g)} \ , \tag{4.7}$$

where the superscripts i and s represent the incident and scattered values, and g is a measure of the ensemble average of the sphericity of the randomly oriented particles.

Figure 3.7 shows a plot of (4.6) for various values of $0 < g < 1$ and incident polarization states described by the spherical angle, $2\delta^i$. $\tan 2\delta^s = \tan 2\delta^i$ when $2\delta^i = 0$ (linear polarizations) or when $2\delta^i = \pm\pi/2$ (circular polarizations) regardless of the value of the sphericity parameter, g. The spherical angle δ does not change due to backscatter from randomly oriented particles when the incident polarization state is circular or linear. The backscattered spherical angle $2\delta^s$ shows the greatest coherent depolarization when the incident polarization state is $2\delta^i = \pi/4$ when the randomly oriented particles are not spherical, $g < 1$.

Figure 3.8 shows a plot of (4.7) for various values of g and incident polarization states described by the spherical angle, $2\delta^i$. The backscattered degree of polarization, p^s, shows the largest fractional change from the incident degree of polarization, p^i, when $2\delta^i = \pm\pi/2$ (circular polarizations). The degree of polarization used as a measure of randomly oriented particles, is the most sensitive when the incident wave is circularly polarized. The fractional change in the backscattered degree of polarization is minimized when the incident polarization state is linearly polarized ($2\delta^i = 0$).

We can maximize or minimize the coherent depolarization upon backscatter from randomly oriented particles. To minimize the signal to noise effects we have already determined the H and V components of the transmitted wave should have equal power. From the definition of the Stokes parameter, $Q = W_H - W_V$, when $W_H = W_V$, $Q = 0$. The transmitted polarization state lies in the $U - V$ plane of the Poincaré sphere of Figure A.9b. In terms of the spherical angles (α, ϕ) the transmitted polarization state is described by $(2\alpha = \pi/2, \phi)$. The $U - V$ plane of Figure A.9a can also be described in terms of the spherical angles, $(2\delta, 2\tau = \pm\pi/2)$. In the case of equal transmitted power in the H and V components, 2δ and ϕ are both angles from the U axis with positive rotation towards the V axis. Changes in the spherical angle δ due to backscatter from randomly oriented particles is indistinguishable from differential phase shift upon backscatter from horizontally aligned particles. To avoid misinterpreting backscatter from randomly oriented scatterers as large (non-Rayleigh) horizontally aligned backscatters we choose to minimize the change in the 2δ angle upon backscatter from randomly oriented particles by transmitting circular polarization. Furthermore, the fractional change in the backscattered degree of polarization is maximized for incident circular polarizations.

4.4 Summary

The change of the degree of polarization upon backscatter is a function of the variation of the shapes of the particles within the scattering volume through the shape correlation coefficient, f, and the average sphericity of randomly oriented particles, g in the same scattering volume. The depolarization due to backscatter from horizontally aligned particles is insensitive to the phase of the transmitted polarization state. The change in the degree of polarization due to backscattering from randomly oriented particles is a function of the phase of the incident polarization state. The change in the degree of polarization is maximized when the incident polarization state is circular. The change in the spherical angle 2δ is a function of the phase of the incident polarization state. The change in 2δ is minimized when the incident polarization state is circular or linear. Incident circular polarization minimizes the change in the spherical angle 2δ due to backscatter from randomly oriented particles and changes in 2δ are less likely to be confused with differential phase shift upon backscatter from horizontally aligned particles.

For regions where both randomly oriented and aligned particles are present, it may be possible to sort out the effects due to variations in the shape of aligned particles in the scattering volume and the effects due to randomly aligned particles or to determine the reflectivity weighted proportions of aligned and randomly oriented particles by alternately transmitting circular and slant linear polarizations and receiving in an H-V basis. Unfortunately, this is beyond the present capabilities of the radar used in this study and is left as an area of future research.

Chapter 5

System Description and Practical Techniques

5.1 Introduction

The purpose of this chapter is to describe the radar system as it was configured based upon the analyses in the previous chapters. An in-depth description of the system hardware (prior to the modifications of this study) can be found in *Chen* (1994). We focus here on the basic system definition and the modifications to the radar that were made for this study. A cursory look at the techniques used to deal with system non-idealities, such as receiver channel gain differences and system noise, is given.

5.2 System Description

Table 5.1 presents the important operating parameters and Figure 5.1 shows a simplified schematic of the New Mexico Tech dual-polarization radar. The radar itself is much more versatile than indicated in the table. For example, the radar has the capability to transmit pulse widths from 0.25 μs to 3 μs. The radar can also transmit noise of 300 MHz bandwidth.

The parameters listed most closely represent the system as it was used to gather the data of this and the next chapter. A more detailed description of the complete capabilities of the radar is found in *Chen* (1994) and in *Krehbiel* et al. (1996).

The radar operation is as follows. A 1 μs pulse is transmitted. The power at the transmitter is about 16 kW. Some power is lost in the path between the transmitter and the antenna. The path losses result from long runs of waveguide, rotary joints,

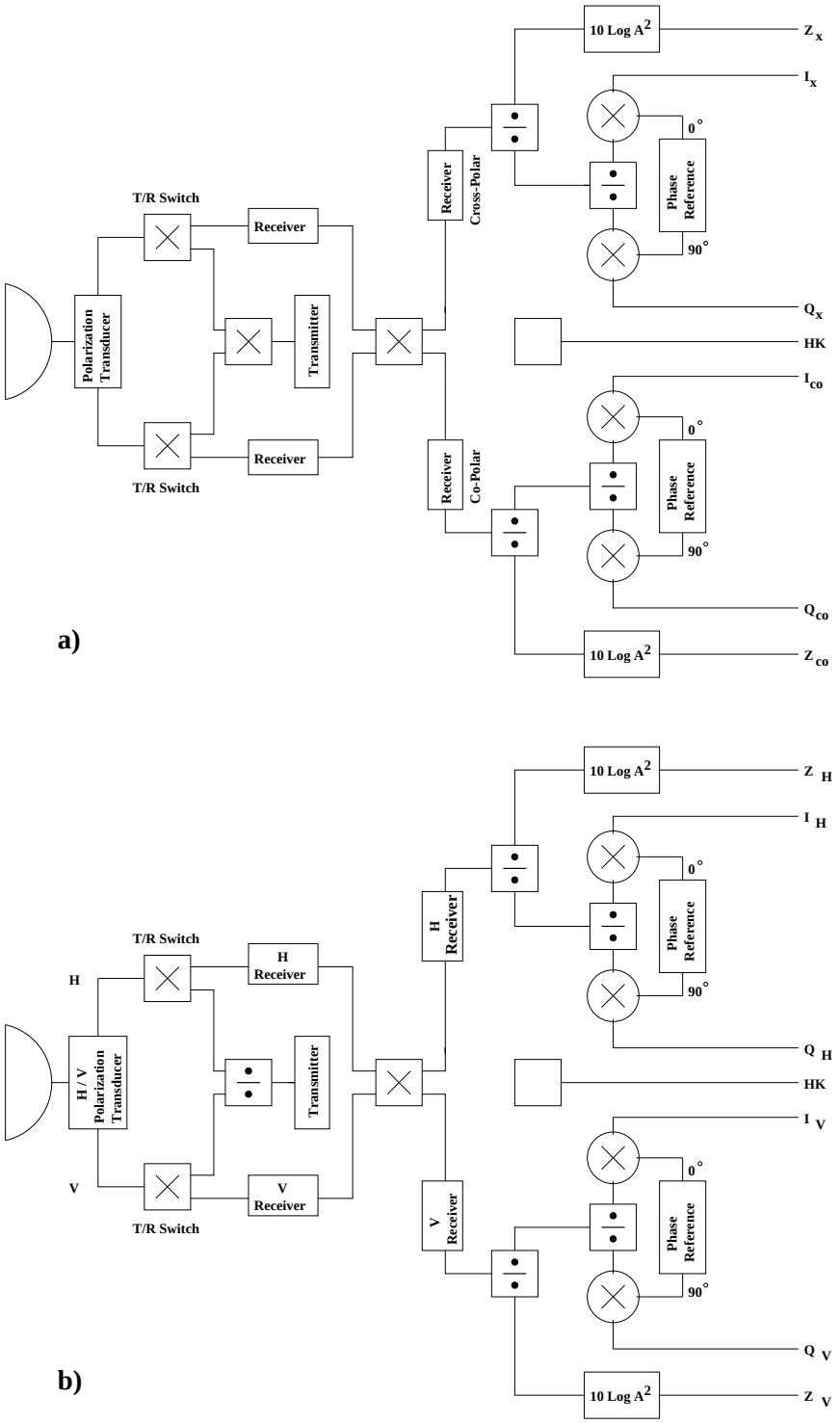

Figure 5.1: Schematic representation of the radar: a) the original configuration and b) as modified to transmit and receive different polarization bases.

Antenna:	
Type:	Cassegrain
Size:	3.7 meters in diameter
3 dB Beamwidth:	0.6°
Gain:	48 dBi
First Sidelobe:	-16 to -20 dB
Feed Type:	Corrugated horn
Transmitter:	
Frequency:	9.8 GHz
Polarization:	close to RHC
Peak Power:	20 kW
Pulse width:	1 micro-sec
PRF:	4 kHz
Receiver:	
IF:	60 MHz
Polarization:	H and V
Incoherent channels:	
IF amplification:	Logarithmic
Dynamic Range:	80 dB
Coherent channels:	
IF amplification:	Constant-phase, amplitude limiting
Dynamic Range:	60 dB

Table 5.1: System parameters of the New Mexico Tech dual-polarization radar

switches and T/R tubes. The effective radiated power is about 5 kW. The signals in the receivers, due to radar returns, are sampled and digitized at a rate of 1 MHz. This yields a range gate resolution of 150 meters ($\frac{1}{2} \cdot c \cdot \tau_p$) and range gate separation of 150 meters ($\frac{1}{2} \cdot c \cdot \tau_s$) , where c is the speed of light, τ_p is the transmitted pulse width and τ_s is the sampling period. The range samples are, therefore, contiguous and independent. The digitized samples are temporarily stored in a First-In First-Out (FIFO) buffer and are routed to Digital Signal Processors (DSPs) for further processing.

5.2.1 Transmitter and Receiver Configuration

Figure 5.1a shows the original configuration of the radar used by *Chen* (1994). The radar transmitted alternate pulses of LHC and RHC polarizations. The radar returns were resolved into LHC and RHC components and simultaneously received in parallel receiver channels. In the case of circular transmitted polarizations there is

a change in rotation sense of the radar return upon backscatter. For example, when LHC polarization is transmitted, most of the radar return power will be in the RHC polarization channel.

When orthogonal polarizations are alternately transmitted and simultaneously received, there must be a significant amount of depolarization before the power in the cross-polar channel rises above the cross-polar receiver noise power level. The receiver channel that corresponds to the transmitted polarization is termed the co-polar channel. The orthogonal channel is referred to as the cross-polarized channel. Propagation and/or backscattering effects that transfer power between polarization channels are termed depolarizing effects.

Figure 5.1b shows how the radar was reconfigured as a result of this study. The radar transmits circular polarization. The radar returns are resolved into H and V components and simultaneously received in parallel receiver channels. The two receiver powers are equal when circular polarization is resolved into H and V components. No depolarization of the transmitted wave is required to produce a strong signal in both receivers. There are no cross-polar or co-polar channels when the transmitted polarization does not correspond to either of the receiver channels.

The polarization transducer is manually changeable to be either circular or linear type. Polarization transducers are commonly referred to as Ortho-Mode Transducers (OMT). In Chen's case, the OMT was the circular type. A polarization switch routed the transmitter pulse to one side or the other of the OMT (i.e., the transmitted pulse was either RHC or LHC).

For this study, the polarization switch was replaced with a power divider. The power is split with a high power -3 dB coupler and a linear OMT is used. The transmitter pulse is split into (nearly) equal power levels and routed to the two sides of the linear OMT. The transmitted wave, therefore, contains nearly equal amounts of power in the horizontally and vertically polarized components. Since the Stokes parameter, Q, represents the difference in the H and V power, from (A.35), the transmitted polarization state will lie in the $U - V$ plane of Figure A.9b ($2\alpha = \pi/2$).

Laboratory measurement of the -3 dB coupler showed the difference between the power in the two paths was 0.7 dB, with greater loss in the H path than the V path. The result is the vertically polarized component of the transmitted signal is slightly greater than the horizontally polarized component.

The phase difference between the transmitted H and V components was manually adjusted by adding delay (with spacers) into either the H or V path after the power

split. The goal, as described in the previous chapter, was a circularly polarized transmitted polarization state with equal amounts of H and V power and a $+\pi/2$ or $-\pi/2$ phase difference between E_H and E_V. The H polarization side of the OMT required one spacer to adjust the phase to approximately $-\pi/2$. The transmitted polarization is close to RHC.

5.2.2 DSP Processing

The coherently received radar returns are down converted for further processing. The complex voltages (V_x) in the receivers can be represented by its in-phase (I_x) and quadrature (Q_x) components,

$$\begin{aligned} V_H &= I_H + j\, Q_H \\ V_V &= I_V + j\, Q_V \ , \end{aligned} \tag{5.1}$$

where the subscripts represents the H or V receiver channel. The I_H, Q_H, and V_H values with subscripts, should not be confused with the Stokes parameters, I, Q, U and V.

The coherently received I_x and Q_x signals were digitized and routed to the DSPs. The DSPs performed the calculations to determine the complex cross correlation of the signals in the two receiver channels,

$$W_{HV} = V_H V_V^* = (I_H I_V + Q_H Q_V) + j(I_V\, Q_H - I_H\, Q_V) \ . \tag{5.2}$$

The phase of the cross correlation was calculated from,

$$\tan\phi_{HV} = \frac{\mathrm{ImW_{HV}}}{\mathrm{ReW_{HV}}} = \frac{I_V Q_H - I_H Q_V}{I_H I_V + Q_H Q_V} \ . \tag{5.3}$$

The DSPs also calculated the square magnitude of the correlation coefficient,

$$|\rho_{HV}|^2 = \frac{|W_{HV}|^2}{W_H W_V} = \frac{(I_H I_V + Q_H Q_V)^2 + (I_V Q_H - I_H Q_V)^2}{(I_H^2 + Q_H^2)(I_V^2 + Q_V^2)} \ , \tag{5.4}$$

where,

$$\begin{aligned} W_H &= V_H V_H^* = I_H^2 + Q_H^2 \\ W_V &= V_V V_V^* = I_V^2 + Q_V^2 \ , \end{aligned} \tag{5.5}$$

are the power in the H and V channels. Due to the large dynamic range of the radar returns, the power in the receiver channels is determined by the incoherent equivalent

of the coherent quantities of (5.5) and were measured using a logarithmic amplifier. The coherent quantities of (5.1) were measured using constant phase limiters to preserve the phase information of (5.3).

The radar transmitted pulses at a pulse repetition frequency (PRF) of 4 kHz. Due to processing speed and memory limitations of the DSPs, returns were processed only for every other transmitted pulse. In the original configuration, when LHC and RHC were alternately transmitted, the processed returns always corresponded to the same transmitted polarization. In the reconfigured system, RHC is transmitted on every pulse and the speed and memory limitation of the DSPs result in a loss of half the available return data.

The DSPs accumulated return samples from 32 of every 64 transmitted pulses (16 ms) and passed the averaged data to the host computer. The average of the returns from 32 transmitted pulses is termed a *ray*.

In the original configuration, the radar DSPs were used to determine the four quantities,

$$\begin{aligned} W_L &= W_{co}\,[\,dB\,] \\ W_R &= W_x\,[\,dB\,] \\ |\rho_{LR}|^2 &= \frac{|W_{LR}|^2}{W_L W_R} \\ \tan\phi_{LR} &= \tan 2\tau\ . \end{aligned} \tag{5.6}$$

The phase of the cross correlation, ϕ_{LR} was a measure of the angle, 2τ in Figure A.9. The angle τ indicates the alignment angle of aligned particles. ϕ_{LR} was found using an 8x8 bit inverse tangent lookup table. The values calculated in the DSPs are passed to the host computer as eight bit numbers. The phase of the correlation was passed to the host computer with a resolution of $360 \cdot 2^{-8} = 1.4^\circ$ per bit so the alignment direction has a resolution of 0.7° per bit ($\tau = \phi_{LR}/2$).

In the reconfigured radar, the radar DSPs were used to determine the four quantities,

$$\begin{aligned} W_H &\ [\,dB\,] \\ W_V &\ [\,dB\,] \\ |\rho_{HV}|^2 &= \frac{|W_{HV}|^2}{W_H W_V} \\ \tan\phi_{HV} &= -\tan(2\phi_{dp} + \delta_\ell)\ . \end{aligned} \tag{5.7}$$

The phase of the cross correlation corresponds to the angle ϕ of figure A.9. The

ϕ angle measures the differential propagation phase, ϕ_{dp}, of the scatterers and the differential phase upon backscatter, δ_ℓ. A typical value of ϕ_{dp} is on the order of one degree per kilometer or 0.15 degree per gate. Therefore, better phase resolution was required in the modified configuration to achieve the needed accuracy.

The same DSP memory limitation would not permit a higher resolution inverse tangent lookup table. In order to obtain the better phase resolution, the real and imaginary parts of the cross correlation (5.2) were passed to the host computer as the most significant 16 bits of 24-bit numbers. The host computer then calculated the phase from $\phi_{HV} = \arctan(\mathrm{ImW}/\mathrm{ReW})$ with a resolution of $360 \cdot 2^{-(16-1)} = .011^\circ$ per bit. An additional bit was needed in the host program to indicate a bad data value.

5.2.3 Display Processing

The host computer has an Intel Pentium processor with a 133 MHz clock. A program in the host computer allows for writing raw data to disk and supports a realtime display. The program in the host computer is used to:

1. Correct the raw data based upon radar calibration data.
2. Determine the ratio of the power in the two receiver channels.
3. Correct the data for receiver noise.
4. Perform further averaging of the data.
5. Convert the data to quantities with clearer meteorological interpretations.

Calibration Corrections

In the reconfigured system, the host computer has range gated samples of the power in the two receiver channels (W_H and W_V in dB), the correlation coefficient squared ($|\rho_{HV}|^2$) and the correlation phase (ϕ) in memory available for further processing. These are the four measured quantities.

In processing, the raw W_H and W_V values were corrected for small gain differences in the two receiver channels. The gain difference of the H and V receiver channel was found to be less than about 0.25 dB during calibration.

There were phase differences in the two receiver channels that caused an offset in the phase angle $\phi \equiv \phi_H - \phi_V$. The phase offset was determined during system

calibration and found to be $-53\,^\circ$ between the channels. The measured ϕ values were corrected for the phase offset of the two receiver channels.

The host program was used to calculate the magnitude of the correlation coefficient from, $|\rho_{HV}| = \sqrt{|\rho_{HV}|^2}$.

Signal to Noise Corrections

The parameters W_H, W_V, ρ_{HV} and ϕ have been corrected for gain and phase offsets of the H and V receiver channels. W_H, W_V, and ρ_{HV} are noise contaminated values, denoted by $\hat{W}_H$, $\hat{W}_V$, and $\hat{\rho}_{HV}$. The noise contaminated ratio of the power in the two receiver channels was calculated from,

$$\widehat{LPR} = \frac{\hat{W}_H}{\hat{W}_V} \ , \tag{5.8}$$

where LPR is the linear polarization ratio.

As shown in *Chen* (1994), we can correct for the signal to noise effects in $\widehat{LPR}$ and $\hat{\rho}_{HV}$ using the expressions,

$$LPR = \widehat{LPR} \cdot \frac{1 + 1/SNR_V}{1 + 1/SNR_H} \tag{5.9}$$

$$\rho_{HV} = \hat{\rho}_{HV} \sqrt{(1 + 1/SNR_H)(1 + 1/SNR_V)} \ , \tag{5.10}$$

where SNR_H and SNR_V are the signal to noise ratios in the H and V receiver channels. The receiver noise was determined by averaging the noise power over an eight-gate echo free region. The signal-to-noise ratios (SNR) in (5.9) and (5.10) were estimated from $SNR = \frac{\hat{S}}{N} - 1$, where $\hat{S}$ was the noise contaminated estimate of the signal power level and N was the echo free receiver noise power level. The correction of (5.9) applies to linear (non-logarithmic) LPR values. The signal-to-noise correction performed by the host computer utilized a logarithmic version of (5.9) in dB. The LPR values were converted into linear values and stored for later use.

To illustrate the calibration and S/N corrections, Figure 5.2 shows the power in the two receiver channels, W_H and W_V, the magnitude of the correlation coefficient, $|\rho_{HV}|$, the phase of the correlation, ϕ and the linear polarization ratio, LPR, due to radar returns from a vertical scan through a storm.

W_H and W_V were corrected for gain differences of the two receiver channels and were converted into logarithmic reflectivity units, dBZ, where Z_H and Z_V are in standard meteorological units of $mm^6 \cdot m^{-3}$. $|\rho_{HV}|$ was corrected for receiver noise in

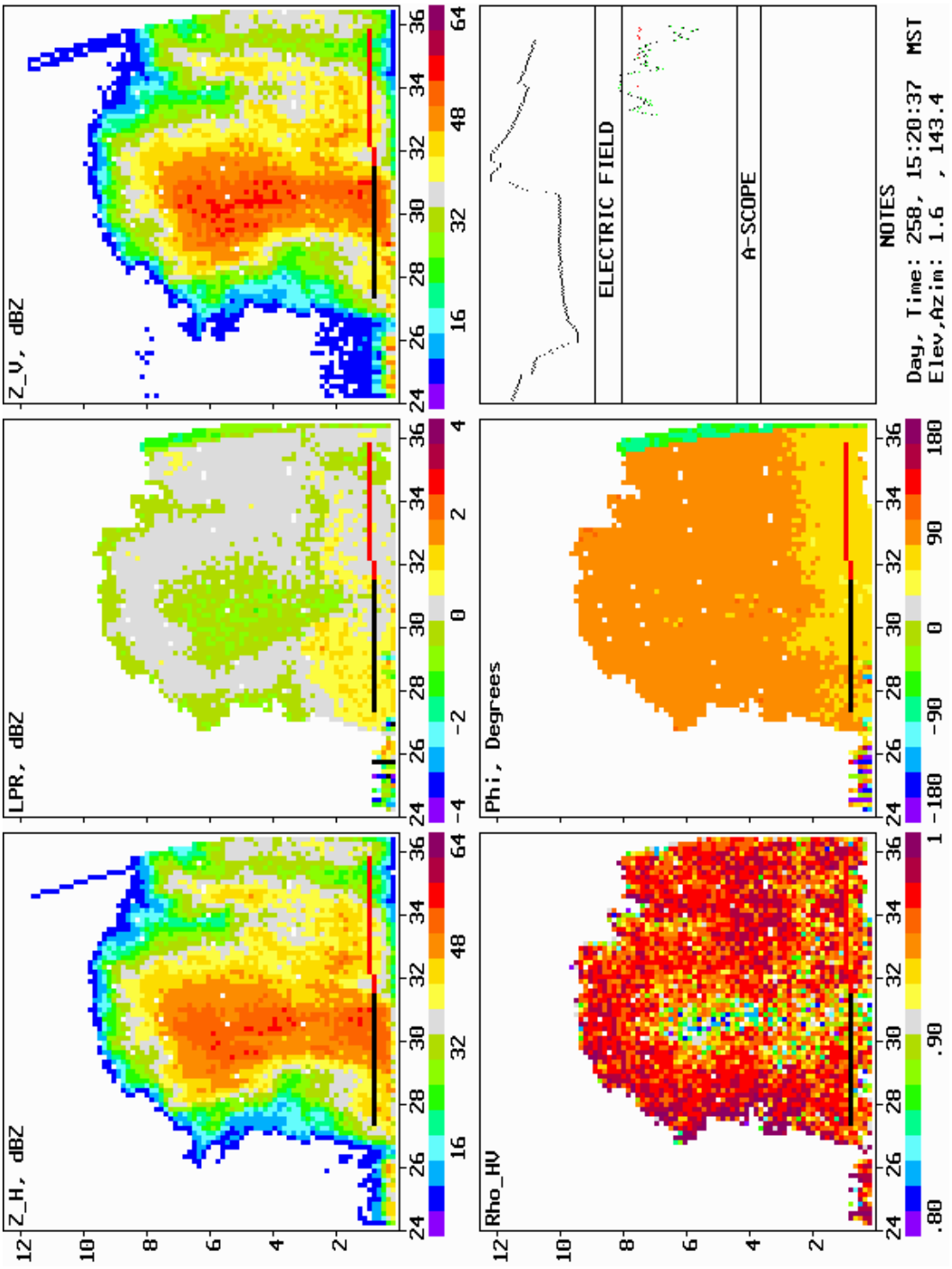

Figure 5.2: The four measurables: W_H, W_V, ρ_{HV} and ϕ, and the derived parameter, $LPR = W_H/W_V$.

the two channels. ϕ was corrected for the phase offset of the two receiver channels. And, the linear polarization ratio, LPR, was calculated from the calibration corrected power in the receivers and was corrected for receiver noise. The only averaging was the 32 beam average performed in the DSPs (one ray = 32 beams).

The figure was generated by the host program. The display shown is referred to as a six-panel display. The upper left panel is considered to be panel one. Panel one through three run from left to right in the top row. In the bottom row are panels four through six. The numbers along the bottom of each panel are the range distances from the radar in kilometers. The numbers along the left edge of panels one and four are the altitude in kilometers above the radar.

Panels one and three show the power in the H and V receiver channels, respectively. Panel two shows the ratio of power in the two receiver channels, $LPR \equiv W_H/W_V = Z_H/Z_V$, where LPR is the linear polarization ratio. Above 3 km, $W_H \leq W_V$ indicating that the transmitted polarization state had a greater V component than H component (green and gray regions). Below about 3 km altitude, $W_H \geq W_V$ indicating that power was being preferentially backscattered into the H receiver (yellow and gray regions). This preferential backscattering into the H channel was due to precipitation particles with positive differential reflectivity ($ZDR \equiv Z_H/Z_V > 1, ZDR_{dB} > 0$).

The cross correlation coefficient ($|\rho_{HV}|$) of the signal in the two receivers is shown in panel four. Reduced values of ρ_{HV} ($\rho_{HV} < 1$) are visible in regions that correspond to high reflectivity (vertical) regions in panels one and three and along a horizontal line directly below 3 km altitude (indicative of the melting of frozen precipitation).

Panel five shows the phase of the correlation phase, ϕ, of the received signal. $\phi \approx 90°$ indicates the received wave is close to left hand circular (LHC) over most of the storm. This corresponds to a transmitted RHC polarization state. The reduced values of ϕ below about 3 km indicates positive differential propagation phase, ϕ_{dp}. Positive differential propagation phase shift, ϕ_{dp}, reduces ϕ from (3.26).

Data Averaging

Further averaging of the data was accomplished by performing the following steps:

1. Determine the spherical angles of the Poincaré sphere, α and ϕ, and the degree of polarization, p.

2. Convert the α, ϕ and p values into the Stokes parameters.

3. Average the Stokes parameters with a five gate and five ray running average.

4. Convert the Stokes parameters back into averaged α, ϕ and p values.

Once the magnitude of the correlation coefficient, $|\rho_{HV}|$, and the linear polarization ratio, LPR have been corrected for signal-to-noise and the linear value of LPR has been determined, we determined the polarization state in terms of the spherical angles on the Poincaré sphere (α, ϕ) and the degree of polarization , p. We used (2.29) and found α in terms of ρ_{HV} and LPR,

$$\begin{aligned} \tan 2\alpha &= \frac{2|W|}{W_H - W_V} \\ &= \frac{2|W_{HV}|}{\sqrt{W_H W_V}} \left[\frac{\sqrt{W_H W_V}}{W_H - W_V} \right] \\ \tan 2\alpha &= \frac{2|\rho_{HV}|}{\sqrt{LPR} - 1/\sqrt{LPR}} \; . \end{aligned} \tag{5.11}$$

The α angle is a function of the magnitude of the correlation coefficient and the linear polarization ratio, LPR.

We used the first equation in (2.16) and found the degree of polarization ,

$$\begin{aligned} p &= \sqrt{1 - \frac{4(W_H W_V - |W|^2)}{(W_H + W_V)^2}} \\ &= \sqrt{1 - \frac{4W_V W_V (1 - |\rho_{HV}|^2)}{(W_H + W_V)^2}} \\ &= \sqrt{1 - \frac{4(1 - |\rho_{HV}|^2)}{\frac{(W_H + W_V)^2}{W_H W_V}}} \\ p &= \sqrt{1 - \frac{4(1 - |\rho_{HV}|^2)}{LPR + 2 + 1/LPR}} \; . \end{aligned} \tag{5.12}$$

The degree of polarization , p, is also a function of the magnitude of the correlation coefficient and the linear polarization ratio, LPR.

The spherical ϕ angle on the Poincaré sphere is the phase of the cross correlation in an H-V receiver basis, $\phi = \phi_{HV}$. Recognizing this, we designated the phase of the cross correlation as ϕ.

To illustrate the conversion between the measured values and the spherical angles of the Poincaré sphere and the degree of polarization , Figure 5.3 shows the total polarized power, $I_p = p(W_H + W_V)$, the degree of polarization , p, found from (5.12), the spherical angle, 2α, found from (5.11), the spherical angle, ϕ, which is the same as the phase of the correlation coefficient, ρ_{HV}. The polarization state on the Poincaré

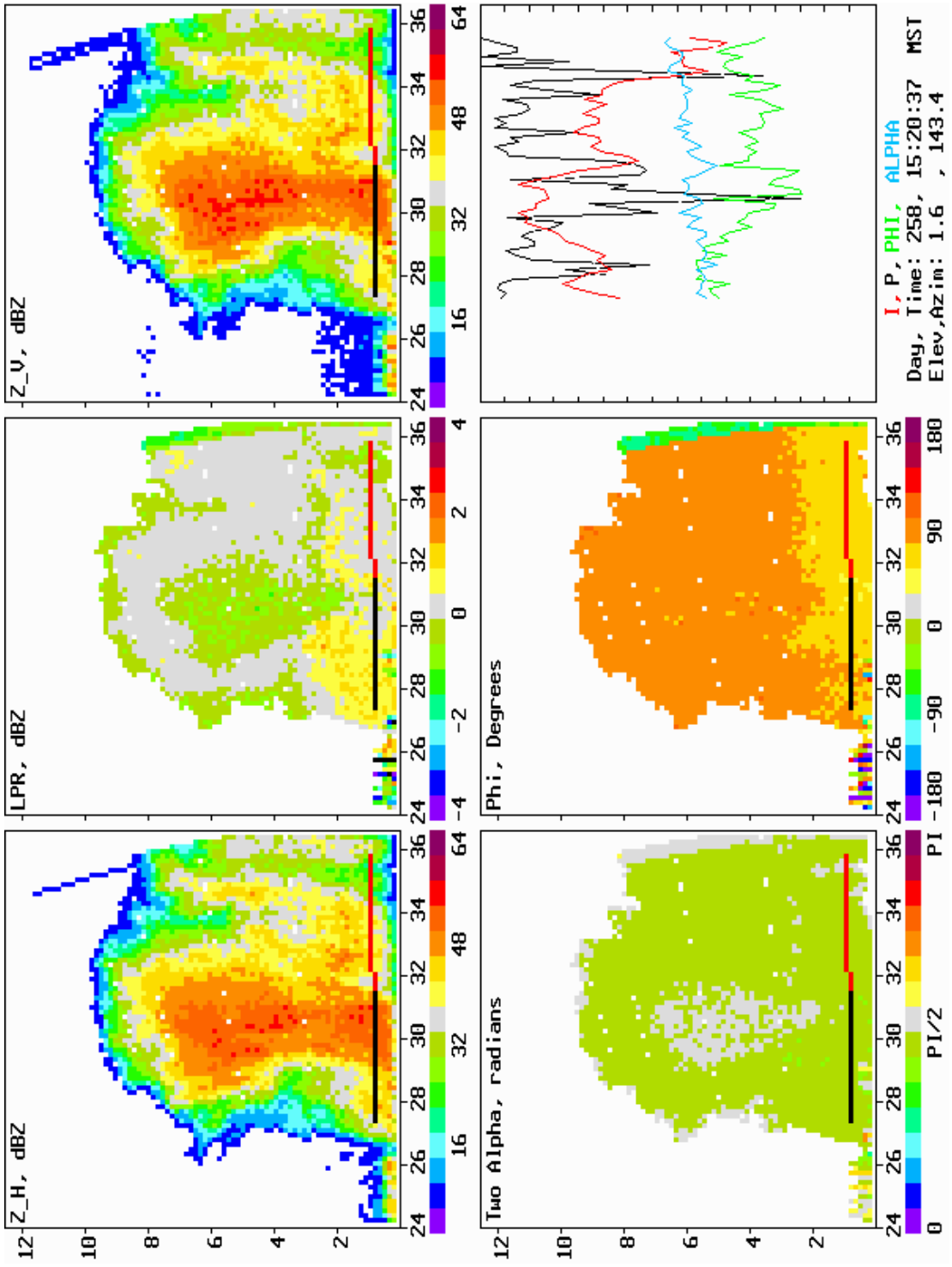

Figure 5.3: Same data as Figure 5.2 showing: Stokes parameter, I, degree of polarization, unpolarized power, and the angles, α and ϕ.

sphere and the value of I_p, p, 2α, and ϕ at each gate along the ray cursor (black and red line), referred to as range plots, are also shown.

Panel one shows the total polarized power, $I_p = p(W_H + W_V)$, where W_H and W_V was the power in the H and V channels. To determine I_p, the magnitude of the logarithmic power was converted into linear values, added, multiplied by the value of the degree of polarization , p, and converted back into logarithmic units (dBZ).

Panel two shows the degree of polarization. The degree of polarization looks similar to ρ_{HV} of the previous figure. This is due to near equal amounts of power in the two channels. When $W_H \approx W_V$, the degree of polarization $p \approx \rho_{HV}$ from (2.37) and (2.38).

Panel four shows the spherical angle 2α calculated from (5.11). The value $2\alpha \approx \pi/2$ (light green and gray) indicates near equal amount of power in the H and V receivers.

Panel five shows the spherical angle, ϕ, and is identical to panel five of Figure 5.2.

Panel three shows the polarization state on the Poincaré sphere along the ray cursor. Values on the Poincaré sphere above the green line are closer to the V polarized pole of the sphere and correspond to the red/yellow colors of panel four (2α). Values below the green line are closer to the H polarized pole and correspond to the blue/green colors of panel four. Values on the Poincaré sphere near the slant linear (+U) point, to the right of the red line, correspond to the gray color of panel five (ϕ) while values close to (-U), to the left of the red line correspond to the brightest red values of panel five. Values on the Poincaré sphere close to the intersection of the red and green line will be close to the green/gray transition of panel four and the orange/red transition of panel five.

Panel six shows the data values (range plots) along the cursor of panels one, two, four and five. The gate to gate polarization plots of panel three and the range plots of panel six are noisy and show the need for further averaging.

From the degree of polarization , p, and the spherical angles α and ϕ we calculated the normalized Stokes parameters from (A.56),

$$\begin{aligned} s_0 &= I/I_p = \frac{1}{p} \\ s_1 &= Q/I_p = \cos 2\alpha \\ s_2 &= U/I_p = \sin 2\alpha \cos\phi \\ s_3 &= V/I_p = \sin 2\alpha \sin\phi \ . \end{aligned} \tag{5.13}$$

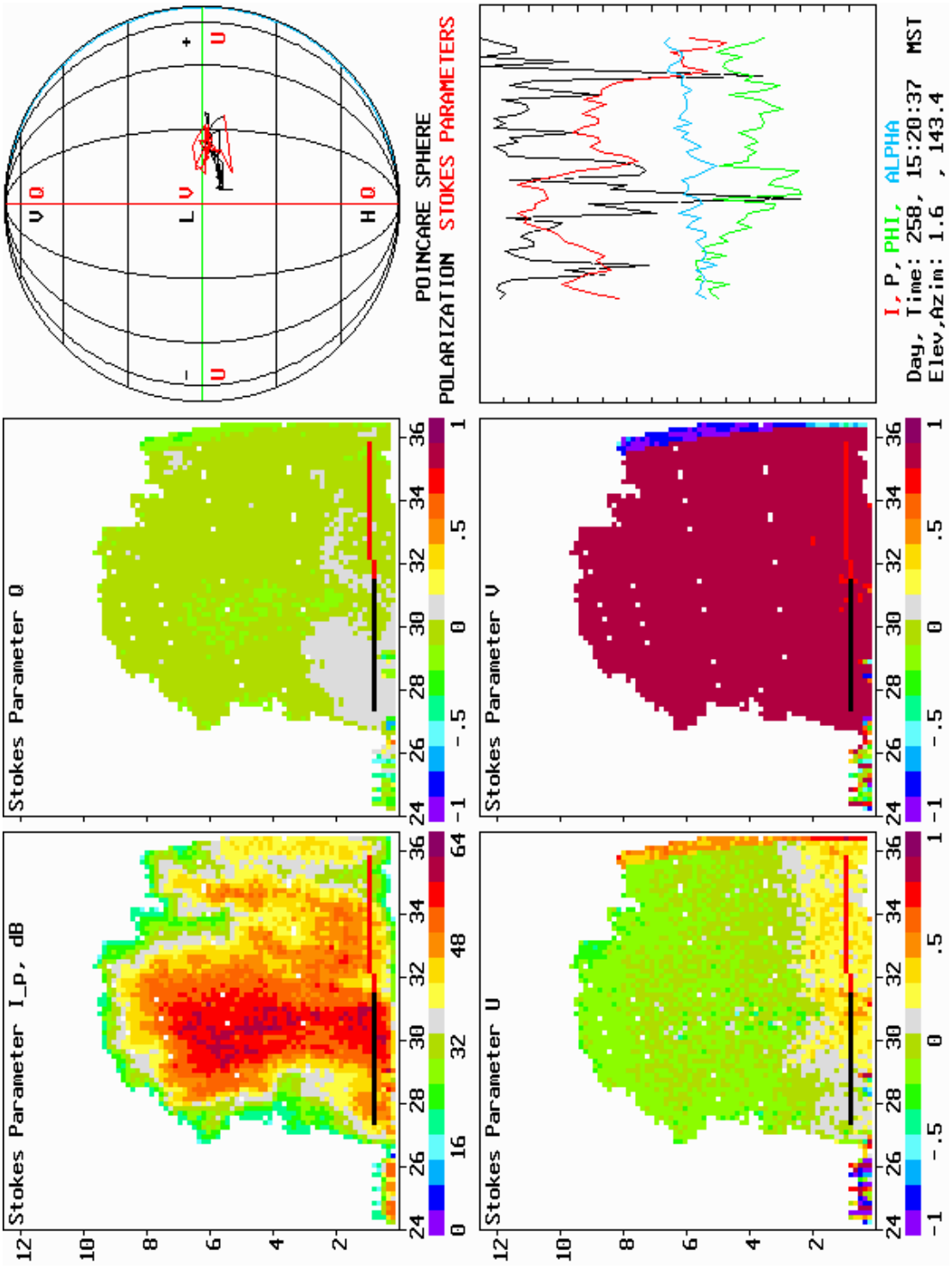

Figure 5.4: The Stokes parameter, I, and the normalized Stokes parameters s_1, s_2, and s_3 and the noisy depolarization path on the Poincaré sphere.

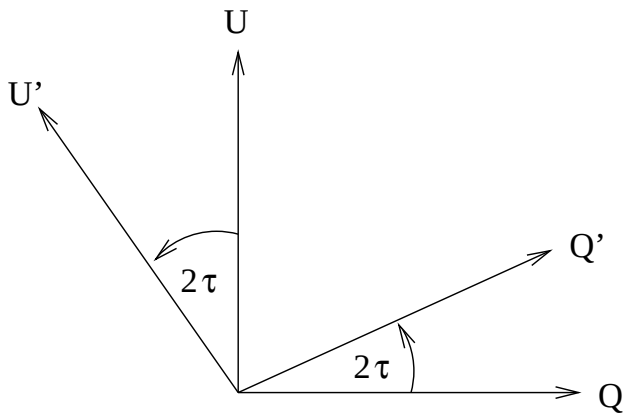

$$Q = Q' \cos 2\tau + U' \sin 2\tau$$
$$U = U' \cos 2\tau - Q' \sin 2\tau$$

Figure 5.5: The measurement basis in a system with a tilted OMT is Q'-U'. Q-U is the true H-V basis. The rotation from horizontal of the OMT is $\tau = 9.5\,^{\circ}$.

The Stokes parameter, I and the normalized Stokes parameters s_1, s_2, and s_3 are shown in panels one, two, four, and five of Figure 5.4. Panels three (Poincaré sphere) and six (range plots) are identical to Figure 5.3. The values of the polarization state on the Poincaré sphere correspond to the normalized Q, U, and V values along the ray cursor of panels two, four and five. The near uniform red color of panel five indicates a different color palette may provide more visual detail.

The Stokes parameters (s_1, s_2, s_3), the total polarized power, I_p, and the degree of polarization p, were further averaged. The averaging up to this point consisted only of the averaging of 32 beams in the DSPs. The additional averaging involved a five gate running average (5×150 meters $= 750$ meters) and a running average over five rays. The spatial resolution of the ray to ray averaging is dependent on the scan rate of the antenna. When the antenna is stationary, the ray to ray averaging is a time average. At the fastest scan rate used in the acquisition of this data, estimated to be about $8^{\circ}\ s^{-1}$, the ray to ray averaging corresponded to about 700 meters. Each data point is a result of 800 ($32 \times 5 \times 5$) independent samples. This method averaged the data in the cartesian (Q,U,V) space.

The OMT of the radar was inadvertently rotated from true H and V when the radar was originally constructed. Through calibration the tilt of the OMT was de-

termined to be about 9.5°, in a CCW direction when viewed from behind the dish in the direction of the transmitted pulse. Since the Stokes parameters are known, it is simple to correct for the feedhorn tilt. The correction is a rotation about the V axis (i.e., in the τ or Q-U plane, see Figure A.2). We will assume the Stokes parameters Q and U in (5.13) are primed quantities. We can determine Q and U in a true H-V basis using a simple rotation,

$$\begin{aligned} Q &= Q' \cos(2\tau_{tilt}) + U' \sin(2\tau_{tilt}) \\ U &= U' \cos(2\tau_{tilt}) - Q' \sin(2\tau_{tilt}) \ , \end{aligned} \tag{5.14}$$

where τ_{tilt} is the tilt of the feedhorn from horizontal or vertical. Q and U are the Q' and U' values corrected for the tilt of the OMT (see Figure 5.5).

Figure 5.6 shows the data of Figure 5.4 after the additional averaging. The path the polarization state takes from gate to gate is now much clearer on the Poincaré sphere of panel three. The rotation to correct for the feedhorn tilt can be seen when panel three of Figures 5.4 and 5.6 are compared. The averaging has reduced the variance and this is seen in the range plots of panel six. The interpretation of the gate to gate path on the Poincaré sphere is considered later.

The color palette of panels two, four and five has been changed to a "zebra palette". The zebra palette is described in *Hooker* et al. (1995). The zebra palette as developed by *Hooker* et al. (1995) has 256 distinct colors. As used in this study the zebra palette was limited to 128 colors due to size limitations in the color palette of the 800x600x256 video display mode. The zebra palette is useful since small changes in data values show up as large contrast differences in the data display.

Finally, the averaged Stokes parameters are used to recalculate the spherical angles, α and ϕ, of the Poincaré sphere,

$$\begin{aligned} \tan 2\alpha &= \frac{\sqrt{U^2 + V^2}}{Q} \\ \tan \phi &= \frac{V}{U} \ . \end{aligned} \tag{5.15}$$

The α and ϕ angles now represent the polarization state in a true H-V basis.

Figure 5.7 shows the same data of Figure 5.3 after the averaging operation that was performed on the Stokes parameters. Panels four and five show the (α, ϕ) angles of the polarization state of the radar return displayed using a zebra color palette. The range of the 2α values in panel four is 0 to π radians which corresponds to about 1.4 degrees per color. The color sensitivity range is $-\pi$ to π for the ϕ values, corresponding to about 2.8 degrees per color.

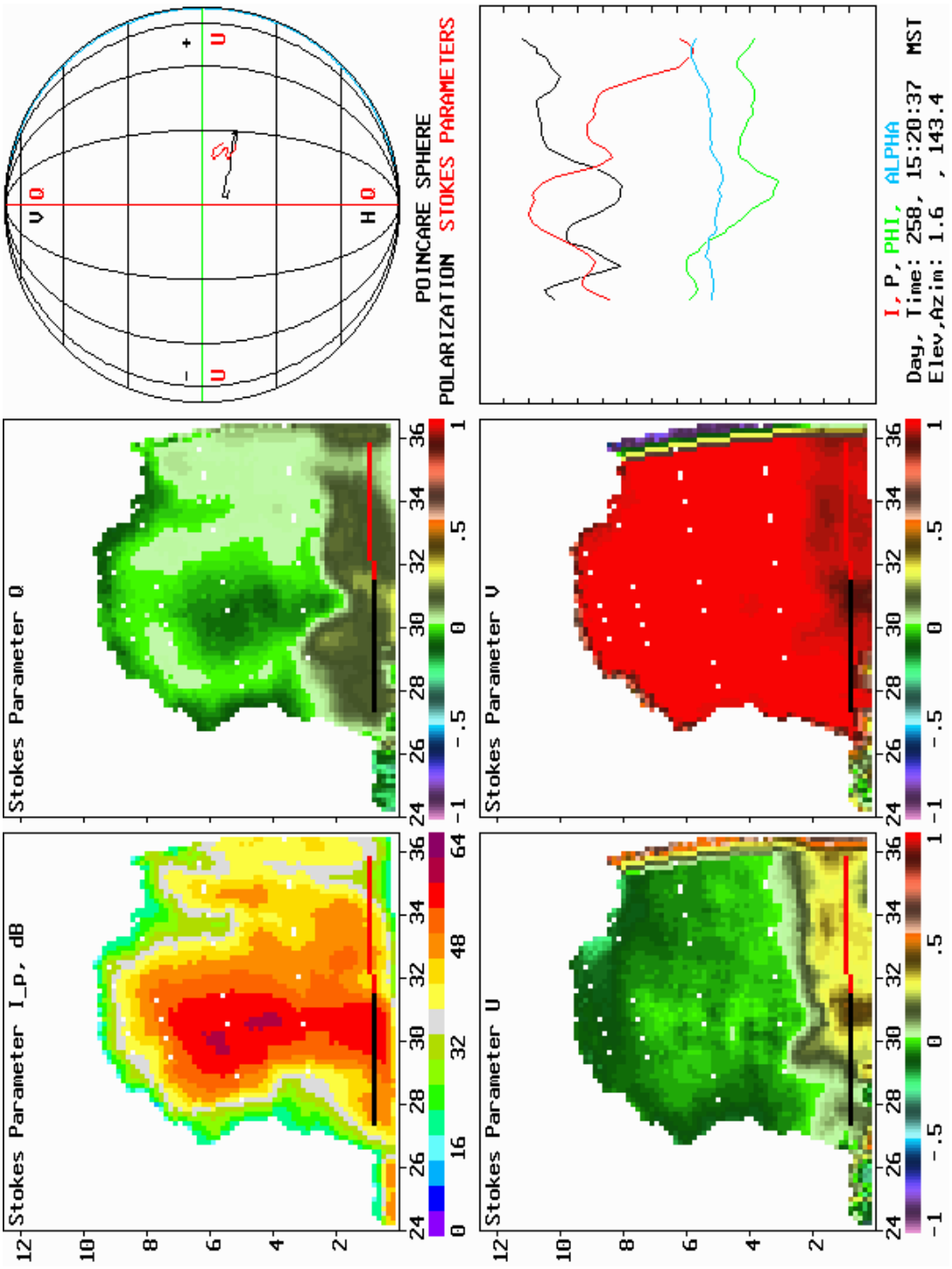

Figure 5.6: Same data as Figure 5.2 showing Stokes parameter, I, degree of polarization , p, the Poincaré sphere, and the angles, α and ϕ after averaging with a five gate running average and a five ray running average.

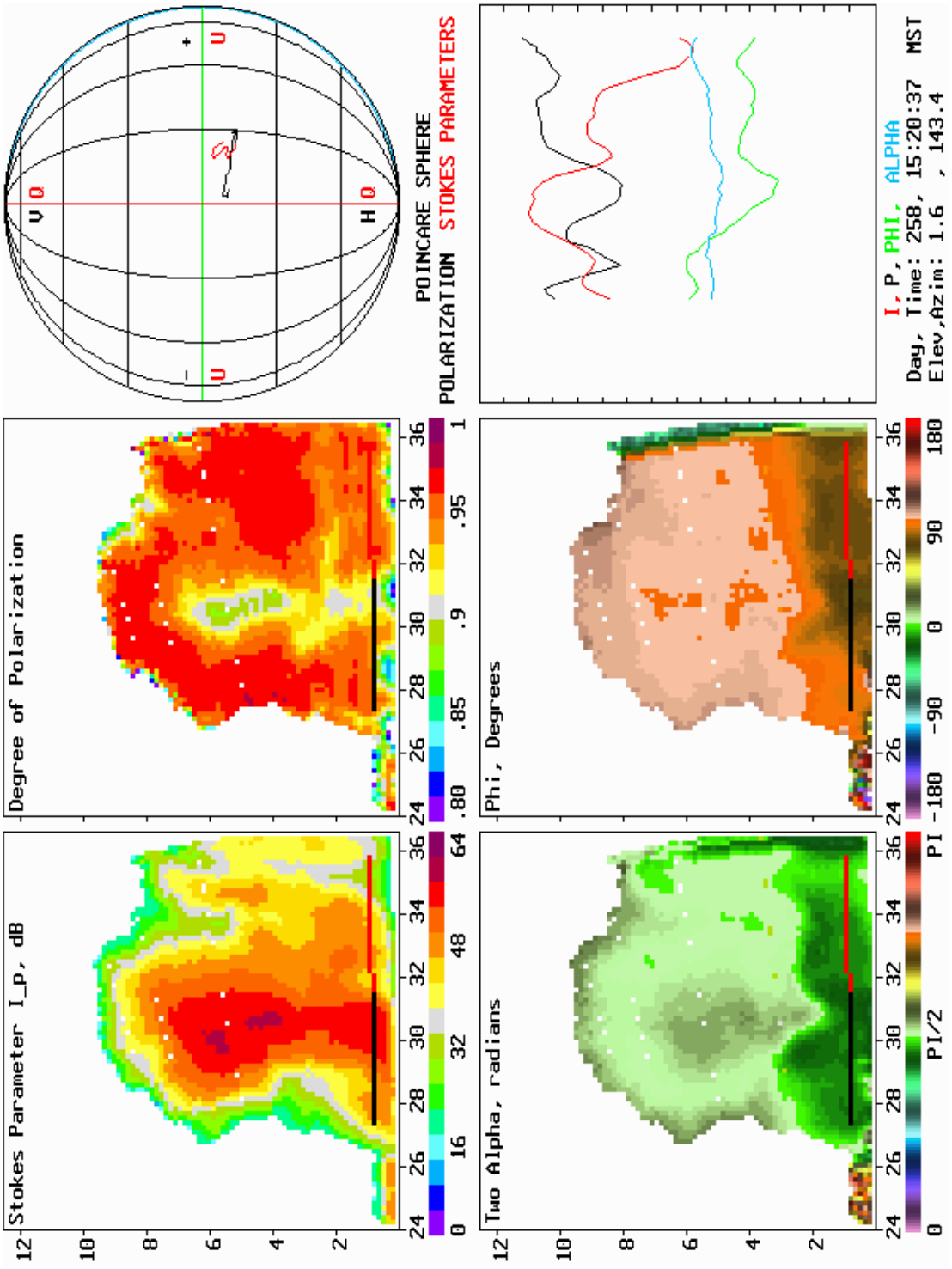

Figure 5.7: Same data as Figure 5.3 after averaging with a five gate running average and a five ray running average.

As was pointed out previously, the α and ϕ angles could be and were determined directly from the measurements. By performing the additional step of calculating the Stokes parameters, the additional averaging was be performed in a Cartesian space and any problems associated with averaging angles was avoided. Determination of the Stokes parameters also offers a convenient way to correct for the tilt of the feedhorn.

The α angle and degree of polarization calculation are seen from (5.11) and (5.12) to depend only on LPR which is a power ratio and ρ_{HV}. Only the difference (in dB) of the power in the two receiver channels and ρ_{HV} are needed to determine the polarization state and the degree of polarization.

Meteorological Quantities

The spherical angles on the Poincaré sphere can be related to meteorological quantities. The change in the angle β is related to the logarithmic difference between the differential reflectivity and the differential attenuation. The ϕ angle is related to the combined effects of differential phase shift upon backscatter and differential propagation phase.

The combined effects of differential reflectivity, ZDR, and differential attenuation, A_V/A_H, are determined from (3.11). Using the definition $\tan\beta = \sqrt{W_V/W_H}$ we find,

$$\tan\beta^s = \frac{1}{\sqrt{ZDR}}\sqrt{\frac{A_V}{A_H}}\tan\beta^i \ . \tag{5.16}$$

where A_V/A_H is the two way differential attenuation and the superscripts t and r represent the transmitted and received quantities. Converting (5.16) to logarithmic units,

$$20\log(\tan\beta^s) = \Delta A_{dB} - ZDR_{dB} + 20\log(\tan\beta^i) \ , \tag{5.17}$$

where $\Delta A_{dB} = 10\log(A_V/A_H)$ is the two way differential attenuation and $ZDR_{dB} = 10\log(ZDR)$ is the differential reflectivity, both in dB. We can solve for the quantity, $ZDR_{dB} - \Delta A_{dB} = 20\log(\tan\beta^i) - 20\log(\tan\beta^s)$. The difference of the differential reflectivity and the differential attenuation is related to the transmitted and backscattered spherical angles, β^i and β^s.

We want to use the averaged Stokes parameters to determine the combined effects of differential reflectivity and differential attenuation. From Table 2.1 we have

$$W_V/W_H = (I-Q)/(I+Q) = \tan^2\beta \ . \tag{5.18}$$

And, since $\cos 2\alpha = Q/(pI)$ from figure A.11 we also get,

$$W_V/W_H = (1 - p\cos 2\alpha)/(1 + p\cos 2\alpha) = \tan^2 \beta \ . \tag{5.19}$$

We can use Equation 5.18 to find β in terms of the averaged Stokes parameters or Equation 5.19 to find β in terms of p, and α.

Figure 5.8 shows a display of the total polarized power, I_p, the degree of polarization , p, the quantity differential reflectivity minus differential attenuation, in dB, and the specific differential phase, K_{DP}. The specific differential phase, K_{DP}, is the range derivative of ϕ, in degrees per kilometer. The depolarization path on the Poincaré sphere and range plots are also shown.

Panel one shows the Stokes parameter, I_p, or the total polarized power in dBZ. Panel two shows the degree of polarization , p. Panel four shows the difference of the differential reflectivity and the differential attenuation in dB. Panel five shows the specific differential phase, K_{DP}, in degrees per kilometer.

In panel four we see that the $ZDR - \Delta A$ over most of the storm was on the order of about 1.5 dB. At the range of about 34.5 kilometers from the radar, the ray cursor (black and red line) enters a region of lower reflectivity in panel five. The ZDR value in panel four dropped to about 0.75 dB beyond 34.5 kilometer range. There appears to be little differential attenuation along the ray.

The data in panel five indicates three regions of positive specific differential phase at 28, 31.5 and 34.5 kilometers along the ray cursor. Positive specific differential phase is an indication that the radar beam is leaving regions of large (non-Rayleigh, $\delta_\ell \neq 0$) scatterers.

The Poincaré sphere display in panel three of Figure 5.6 was used as a guide in the interpretation of the data of panels four and five of Figure 5.8.

5.3 Determining Electrical Alignment Directions

Electric fields in thunderstorms can align ice crystals or needles along the electric field lines in the upper parts of the storm where ice crystals are present. We can use analysis of the coherent depolarization path on the Poincaré sphere to determine the electrical alignment direction.

There is one assumption necessary for determining alignment direction: the coherent depolarization is dominated by differential propagation phase shift (i.e., attenuation and differential attenuation is negligible). This is a good assumption when

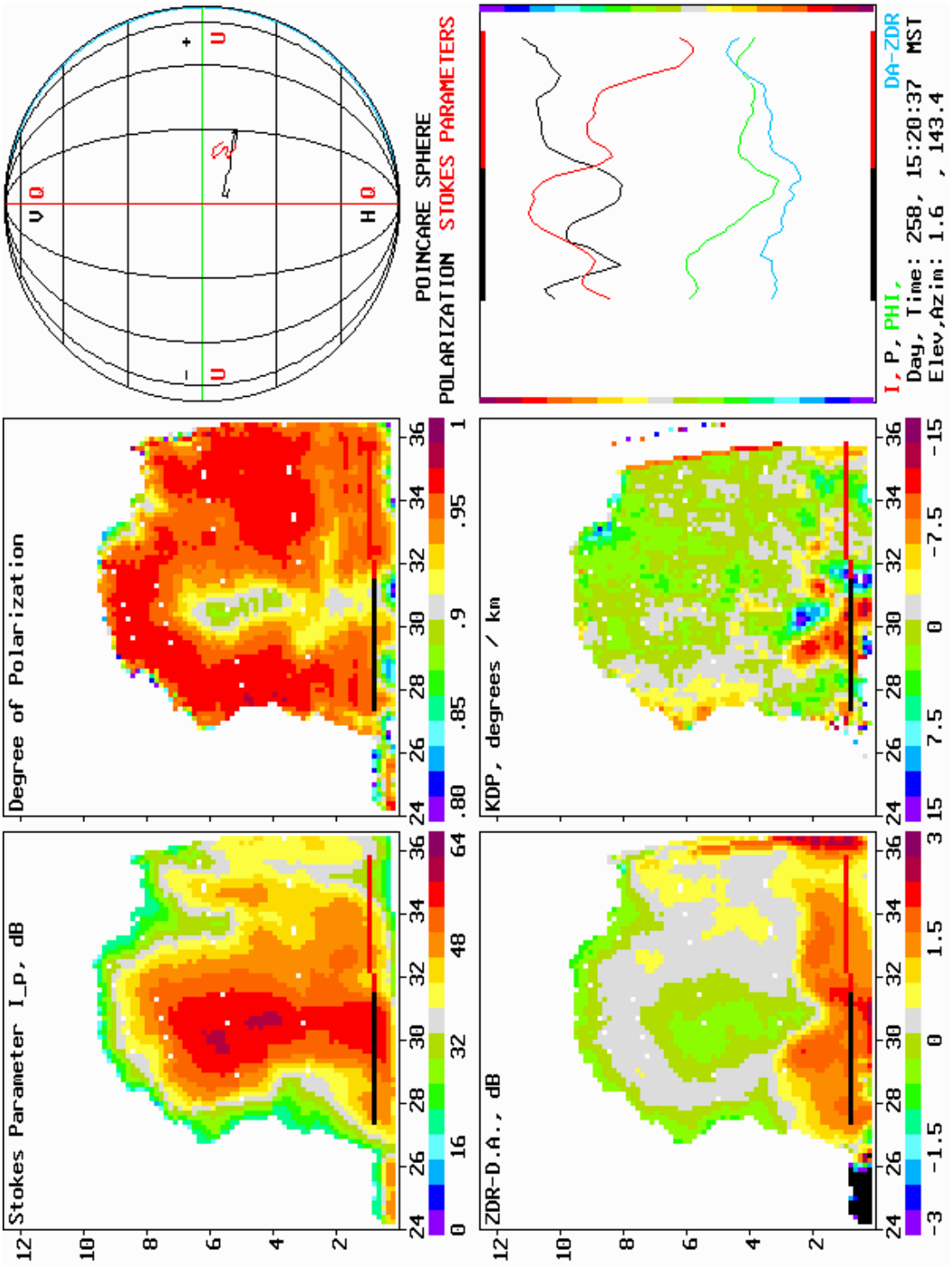

Figure 5.8: The Stokes parameter, I, degree of polarization, P, and meteorological quantities, $ZDR - DA$, and K_{DP}.

there are no large hail or graupel particles in the region of interest. Otherwise, the determined alignment directions are in error. *McCormick* and *Hendry* (1975) refer to such alignment directions as "apparent" alignment directions.

Previously, we have considered the case where the characteristic polarizations are H and V. When a characteristic polarization is incident upon a region, the backscattered polarization state from that region is the same as the incident polarization state. The characteristic polarization state is not cohrently depolarized upon backscatter. For example, ice crystals or needles that are aligned either horizontally or vertically have H and V characteristic polarizations.

When we determine intermediate alignment directions, the characteristic polarizations are the alignment angle τ and $\tau+\pi/2$ ($\delta = 0$). If the transmitted polarization state is linear, and the particles happen to be aligned at the same angle as the transmitted polarization then the radar is blind to the differential propagation effects. This is the fundamental reason why it is advantageous to transmit circular polarization and not a linear polarization state.

We have already seen that propagation through a region with a differential propagation phase shift moves the polarization state in a plane that is perpendicular to the line connecting the characteristic polarization states. In particular, the polarization state moves along the intersection of the plane with the Poincaré sphere (a circle).

If the coherent depolarization is dominated by differential propagation phase, then there is one plane that contains the polarization states at consecutive range gates and that is parallel to the V axis of the Poincaré sphere. The normal to this plane, defined in the proper way, points at an angle τ off the Q axis. The alignment direction is τ.

The τ plane is the Q-U plane. Suppose that we have at range gate n the polarization state defined by the Stokes parameters, $P_n = (Q_n, U_n, V_n)$. At range gate $n+1$ the polarization state is $P_{n+1} = (Q_{n+1}, U_{n+1}, V_{n+1})$ (see Figure 5.9). There is a plane that is defined by the two polarization states and is parallel to the V axis. We can also define this plane by two vectors $V_n\hat{v}$ and $(Q_{n+1}-Q_n)\hat{q}+(U_{n+1}-U_n)\hat{u}+V_{n+1}\hat{v}$, where $\hat{q}$, $\hat{u}$ and $\hat{v}$ are unit vectors along Q, U, and V, respectively. $V_n\hat{v}$ defines a family of planes parallel to V while $(Q_{n+1}-Q_n)\hat{q}+(U_{n+1}-U_n)\hat{u}+V_{n+1}\hat{v}$ is a particular plane of the family.

To find the direction of the normal to the plane, we will use the vector cross

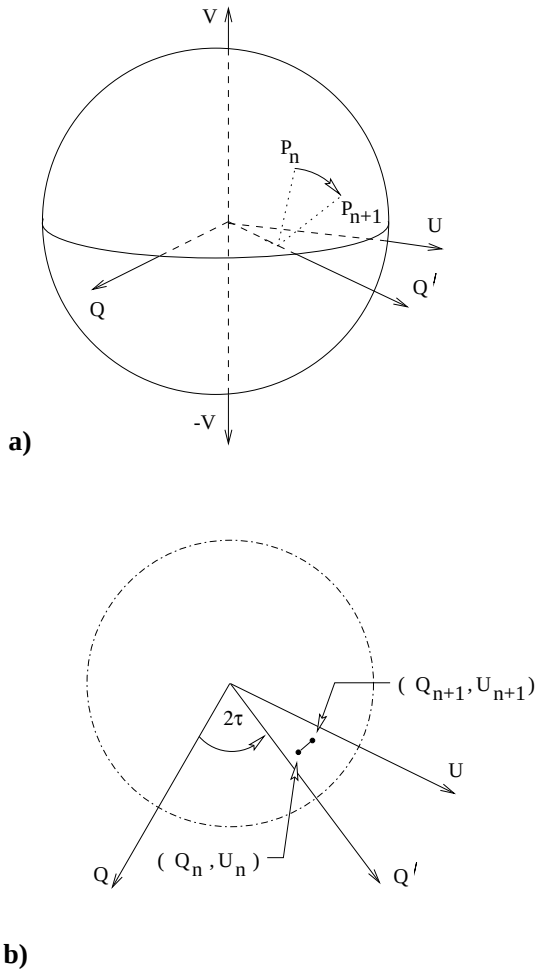

Figure 5.9: Depolarization process dominated by differential propagation phase shift a) on the Poincaré sphere and b) in the Q-U plane. The characteristic polarization is $(Q', 0, 0)$ corresponding to an alignment direction, τ of the medium.

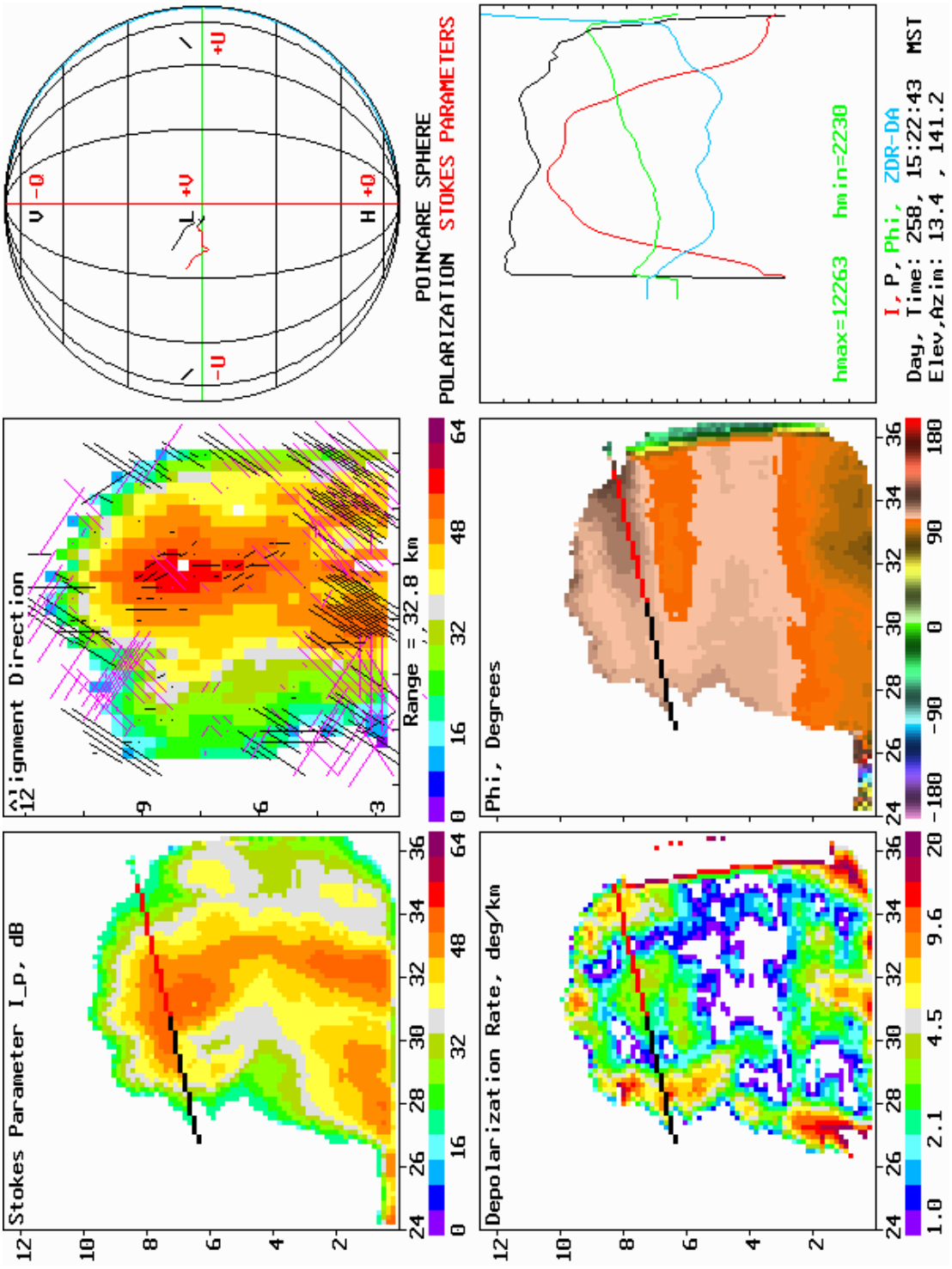

Figure 5.10: The Stokes parameter, I, degree of polarization, alignment directions, coherent depolarization rate, Γ, and ϕ.

product. Crossing the second vector into the first vector,

$$\det \begin{vmatrix} \hat{q} & \hat{u} & \hat{v} \\ Q_{n+1} - Q_n & U_{n+1} - U_n & V_{n+1} \\ 0 & 0 & V_n \end{vmatrix} = V_n(U_{n+1} - U_n)\hat{q} - V_n(Q_{n+1} - Q_n)\hat{u} \ . \quad (5.20)$$

To find the angle τ, we have from (A.59,

$$\tan 2\tau = \frac{U}{Q} = \frac{y\hat{u}}{x\hat{q}} = \frac{-V_n(Q_{n+1} - Q_n)}{V_n(U_{n+1} - U_n)} \ . \quad (5.21)$$

The sign of the V term is important since we find τ using a four quadrant arctangent look up table. When V is negative the determined alignment direction will be off by $\pi/2$ if the sign of this term is neglected.

When the incident polarization state is one of the characteristic polarizations, then (5.21) becomes,

$$\tan 2\tau = \frac{-V_n(Q_{n+1} - Q_n)}{V_n \cdot (U_{n+1} - U_n)} = \frac{-0 \cdot 0}{0 \cdot 0} \ , \quad (5.22)$$

and the alignment direction is indeterminant.

Hidden in the above analysis is the fact that we are taking the lefthanded cross product. We need to use the lefthanded rule instead of the righthanded rule because $\phi_{dp}$is by definition, positive when propagation is through a rain region. The rain is horizontally aligned. Positive ϕ_{dp} actually moves in the $-\phi$ direction on the Poincaré sphere. To determine alignment direction properly we have to use the lefthand rule.

Figure 5.10 shows the total polarized power, I_p, an electric field map perpendicular to the scan plane, the coherent depolarization path on the Poincaré sphere, the net coherent depolarization rate on the Poincaré sphere, the correlation phase, ϕ, and range plots. The ray cursor (black/red line) is through the upper part of the storm.

Panel one show the total polarized power, I_p in dBZ.

The plane of polarization of an electro-magnetic wave is always perpendicular to the direction of propagation. The display of electrical alignment directions like all the other displays in the previous figures are in the plane of the beam meaning the alignment directions can only be displayed as colors.

If we change the display plane to be perpendicular to the radar beam, we can display the alignment directions using vectors. The view of the display is electrical alignment as seen when viewed in the direction of the transmitted beam. In other words, the display plane is now the same as the plane of polarization. The direction

of the vectors will show the apparent alignment direction. The length of the vectors are scaled to the net coherent depolarization rate. The background of the alignment maps is the Stokes parameter, I_p.

Panel two shows an example the apparent alignment direction maps. For clarity vectors that are close to vertical (within $\pm 22°$) are black. Vectors that are not close to vertical are magenta. Depolarization rates in the upper part of the storm can be as high as 4 deg/km. The alignment vectors are scaled to 2 deg/km. Very small dots are regions with net coherent depolarization rates close to 2 deg/km. Vectors approaching the reflectivity box sizes apparent in the figure have close to 3 deg/km coherent depolarization rate. Vectors with a coherent depolarization rate higher than 10 deg/km are truncated to 10 deg/km for display purposes. These higher net coherent depolarization rates only occur below the melting level.

Panel three shows the coherent depolarization path on the Poincaré sphere. At about the range where the ray cursor changes color (from black to red) the polarization state is close to the equator of the Poincaré sphere. Beyond this range the polarization state shows steadily increasing ϕ values(towards -U) and with $2\alpha \approx constant$. This is an indication of vertically aligned ice crystals with no attenuation and only differential propagation phase shift.

Panel four shows the value of the net coherent depolarization rate across the surface of the Poincaré sphere. Since we know the value of 2α and ϕ at every gate, we can find $\Delta(2\alpha)$ and $\Delta\phi$ from gate-to-gate. We can then use spherical trigonometry to calculate a coherent depolarization rate. If we denote the net angular change of the polarization state from one range gate to the next as $\Delta\gamma$, then $\cos\Delta\gamma = \cos\Delta(2\alpha)\cos\Delta\phi$. The value of $\Delta\gamma$ determined in this way is in units of degrees per gate. Since the gate spacing is 150 meters we can convert this coherent depolarization rate into degrees per kilometer. In regions of aligned ice crystals, when attenuation is negligible, the only coherent depolarization effect is due to differential propagation phase shift, ϕ_{dp}.

Panel five shows the correlation phase, ϕ. Regions of vertically aligned ice crystals will show increasing ϕ with range. The ranges with the largest net coherent depolarization contain the region with the largest and/or highest concentration of ice crystals.

5.4 Summary

In this chapter we examined some of the performance capabilities of the radar. The processing of the data was examined from the four measured quantities, W_H, W_V, $|\rho_{HV}|^2$, and ϕ_{HV} to derived parameters, the spherical angles α and ϕ and the degree of polarization , the Stokes parameters, Q, U, V, and the meteorological parameters, differential reflectivity minus differential attenuation, $ZDR_{dB} - \Delta A_{dB}$, and the specific differential phase, K_{dp}. Further averaging to reduce the variance of the data was performed in the cartesian space, (Q, U, V).

Chapter 6

Discussion and Summary

6.1 Discussion

The Poincaré sphere is an extremely useful tool for understanding polarization techniques in dual-polarization radars. The set of all possible polarization states is a compact set which allows them to be described by points on a sphere. Polarization states have a definite geometrical relationship to one another. For example, orthogonal polarization states are always diametrically opposed on the Poincaré sphere. The geometrical description allows an understanding of the relationships between the various polarization techniques that have been and are currently being used by various radar meteorologists around the world. The geometrical description also allows us to answer the questions originally posed in the Introduction.

The first question posed in the Introduction was: When is a single transmitted polarization adequate for determining the meteorological quantities? A single transmitted polarization is adequate for determining the meteorological quantities for the case of horizontally aligned particles. A single transmitted polarization is adequate for determining the meteorological quantities for the case of spherical and randomly oriented particles. For many meteorological studies, aligned particles are assumed to be horizontally aligned.

The next two questions posed in the Introduction can be grouped together: What other transmitted polarization state, if any, will provide additional meteorological information? And, what conditions necessitate the transmission of orthogonal polarization pairs? For the case of horizontally aligned particles, there is no other transmitted polarization state that will provide any further information. To test the horizontal alignment assumption, alternate orthogonal polarizations must be trans-

mitted as shown in Section 3.5. When there is a mix of aligned and randomly oriented particles, alternate transmission of non-orthogonal polarizations may provide enough additional information to sort out the two particles types. This is left as an area for further research.

The last question in the introduction was concerned with the optimal transmitted polarization and receiver basis for meteorological studies. The answers to this question are enumerated below:

1. Assuming that rain is horizontally aligned, receive the backscattered signals in an H-V basis. Matching the receiver polarization basis to the characteristic polarizations of the medium results in the conceptually clear coherent depolarization trajectories on the Poincaré sphere.

2. To avoid low signal-to-noise ratios in either receiver, transmit an equal amount of H and V polarized power.

3. To maximize the change in the degree of polarization due to backscatter from randomly oriented particles, transmit circular polarization.

4. To minimize the change in the spherical angle 2δ, transmit circular polarization. The change in the 2δ angle is minimized because changes in 2δ due to backscatter from randomly oriented particles is indistinguishable from differential phase shift upon backscatter from large (non-rayleigh) horizontally aligned scatterers.

5. If there is a need to determine ice crystal alignment in the upper part of thunderstorms, do not transmit any linear polarization since the linear polarization will not be depolarized by ice crystals aligned along or perpendicular to the transmitted linear polarization.

The introduction of the spherical angle β resulted in a simplification for the case of horizontally aligned particles. The spherical angle α is defined in terms of the polarized component of the wave. The angle β is a partially polarized analog of the α angle. The relationship between the parameter $\rho_{HV}(0)$, the correlation between co-polar returns when H and V are alternately transmitted, and the degree of polarization, p, has never been clearly established before. Although, it has been stated previously that they are somehow related. The β angle provides a geometrical relationship between the degree of polarization , p and the correlation coefficient, ρ_{HV}.

Transmission and reception of alternate H and V polarizations always requires that two polarizations be transmitted to achieve the complete polarization response

(*Torlaschi* and *Holt*, 1998). We have seen that transmission of a single circular polarization will provide all the depolarization information if the liquid precipitation is assumed be aligned horizontally. Alternate transmission of orthogonally polarized waves is necessary to justify the horizontally aligned assumption and is left as an area for further study.

The use of the Mueller Matrix by many researchers (*Yamaguchi* et al., 1992; *Jin* and *Cloude*, 1994; *Cloude* and *Pottier*, 1996; *Guissard*, 1994; *Ho* and *Allen*, 1994) has not been examined here. The Mueller Matrix approach deals with the cartesian coordinates of the Stokes sub-space. It is easy to see that the coherent depolarization effects examined previously using angles on the Poincaré sphere yields relatively simple results since the polarization states are constrained to the surface of the (normalized) sphere. The changes in the cartesian coordinates due to coherent depolarization appear to change in a much more complicated fashion and are therefore difficult to interpret.

In fact, *Baylis* et al. (1993) is worth quoting in this regard.

> "Although many attractive features of coherency or density matrices have been demonstrated, it seems generally felt that transformations of such matrices are limited, as is the Jones calculus, to nondepolarizing transformations and that depolarization can only be treated with the Mueller matrices while coherent superpositions of waves require the Jones calculus. As a result, and perhaps dues as well to some inertia from those who have mastered the Mueller-matrix method and the inconvenience of competing 2×2 matrix representations, rather little attention has been paid to coherency or density matrices in modern texts, whose treatments of the action of optical elements on polarization are largely limited to Jones matrices for fully polarized waves and to the Mueller-matrix methods for partially polarized waves."

Another possible technique that is evident through an examination of the equations in the text but never explicitly discussed is that the transmission of an unpolarized wave can result in a polarized component in one of the radar receiver channels if the scatterers have a preferred direction of alignment. In this case, only one element on the main diagonal of the polarized portion of the coherency matrix is non-zero. All other elements are zero and therefore there is very little information about the scatterers contained in the backscattered wave (since there is no phase information

available that usually appears in the cross correlation term). The details are not included here since the solution is quite trivial. But, it should be noted that this method would in theory be insensitive to randomly oriented particles and could provide some information on the degree of alignment.

6.2 Summary of New Results

Poincaré's geometrical interpretation of the Stokes parameters (i.e., the Poincaré sphere) was used as a basis to examine some basic questions of radar meteorology, including: what are the best polarizations to transmit and receive? Examination of these questions within a geometrical framework provided new results that are summarized below.

1. The change in the polarization state on the Poincaré sphere, including the effects of incoherent depolarization (reduction in the degree of polarization) was determined by analysis for scattering from different classes of particles (horizontally and non-horizontally aligned, randomly oriented, and spherical).

2. It was determined from the results of the analyses it is best to transmit circular polarization and to receive in an H-V basis for the following reasons:

   (a) Transmission and reception in different polarization bases minimizes low signal-to-noise ratios (SNR's). Radar meteorologists typically employ co-polar/cross-polar techniques (transmit and receive in the same polarization basis) where the cross-polar channel usually exhibits low SNR.

   (b) Incident linear and circular polarizations are incoherently depolarized and not coherently depolarized by randomly oriented particles.

   (c) The quantities, differential reflectivity, ZDR, differential propagation phase shift, ϕ_{dp}, and the correlation between the signals in the two receiver channels, ρ_{HV} can be determined from a single transmitted polarization.

   (d) The change in the polarization state due to horizontally aligned particles is maximized when the power in the H and V components of the incident (transmitted) polarization are equal.

   (e) All possible electric alignment directions of ice crystals in the upper part of thunderstorms can be measured when the incident wave is circularly polarized. This is not true for incident linear polarizations.

3. The cross covariance amplitude ratio, W/W_2, (*McCormick* and *Hendry*, 1975) was shown to be a stereographic projection of the polarization state on the Poincaré sphere onto the complex plane.

4. A geometrical relationship between the correlation between the signals in H and V receivers, ρ_{HV}, and the degree of polarization , p was determined.

Appendix A

Descriptions of Wave Polarization

A.1 Introduction

In this appendix we will examine various ways to describe the polarization state of an electromagnetic wave. The first description of polarization state is based upon the rotating electric field vector of the electromagnetic wave. The polarization ratio description is based upon the ratio of orthogonal linear or circular components of the electric field vector. The polarization state can also be described through the Stokes parameters. Finally, Poincaré 's geometrical interpretation of the Stokes parameters is examined. All the descriptions of polarization state are equivalent for any given polarization state, except the polarization ratios contain no information about the degree of polarization.

A.2 Simple Plane Waves

The equation for an electromagnetic wave propagating in the z-direction must satisfy the one-dimensional wave equation,

$$\frac{\partial^2 \mathcal{E}(t,z)}{\partial t^2} = \nu^2 \frac{\partial^2 \mathcal{E}(t,z)}{\partial z^2} \ , \tag{A.1}$$

where ν is the velocity of light in the medium.

The solution of (A.1) is of the form,

$$\mathcal{E}(t,z) = E_0 \cdot e^{j(\omega t \pm kz)} \ , \tag{A.2}$$

where $k = 2\pi/\lambda$ is the wavenumber, λ is the wavelength, ω is the frequency of the wave in rad$\cdot$s^{-1}i, and E_0 is the magnitude of the electric field. The plus (minus) sign

is a solution for a wave propagating in the minus (plus) z direction. We can verify that (A.2) is a solution to (A.1) by direct substitution of (A.2) into (A.1) and by noting that $\nu k = \omega$.

The solution (A.2) is in complex exponential form. To find the instantaneous value of the field we must take the real or imaginary part of the complex solution. We will choose to take the real part to find the instantaneous value of the field.

Furthermore, we can decompose the solution into spatial and temporal components. The instantaneous value of the electric field is then given by

$$\mathcal{E}(t,z) = \mathcal{E}(t)\mathcal{E}(z) = E_0 e^{j\omega t} e^{\pm jkz} \ . \tag{A.3}$$

A common convention is to suppress the temporal component of the solution ($e^{j\omega t}$). When the temporal component is suppressed it is an implicit part of the solution.

The direction of the electric field in (A.2) is not specified. But, there cannot be a component along the direction of propagation since that would violate the wave equation. For example, assume a solution of the form

$$\mathcal{E}(t,z) = E(z) \cdot e^{j(\omega t \pm jkz)} \ , \tag{A.4}$$

where the magnitude of the electric field is some unspecified function of z. Upon direct substitution into (A.1) the result is

$$\pm jkz \frac{\partial E(z)}{\partial z} + \frac{\partial^2 E(z)}{\partial z^2} = 0 \ . \tag{A.5}$$

The solution is found by equating the real and imaginary parts of both sides of the equation. The result is

$$\begin{aligned} \frac{\partial E(z)}{\partial z} &= 0 \\ \frac{\partial^2 E(z)}{\partial z^2} &= 0 \ . \end{aligned} \tag{A.6}$$

The magnitude of the electric field has to be independent of z. The electric field of the solution to the wave equation has to lie in a plane perpendicular to the direction of propagation. The plane perpendicular to the direction of propagation is known as the plane of polarization. Within the plane of polarization, we can choose a direction for the electric field of the solution, for example the x-direction. The electric field of the propagating wave of this example will always be directed along x. The wave is said to be linearly polarized in the x direction.

A.3 The Polarization Ellipse

In the previous section we found a solution to the wave equation which describes a propagating electromagnetic wave. The most general propagating wave is elliptically polarized. Circular and linearly polarized waves are degenerate cases of the elliptically polarized case. In this section we demonstrate how an elliptically polarized wave can be decomposed into orthogonal linear components (i.e., horizontal and vertical) or into orthogonal circular components (i.e., left and right hand circular). Finally, we show how the polarization ellipse can be defined by either of two sets of angles that are related to the polarization ellipse.

Since free space and the atmosphere are a linear media, the principle of superposition applies. Any number of linearly polarized waves may be added to obtain a general elliptically polarized (GEP) wave. In fact, we will show the sum of two linearly polarized waves are elliptically polarized in general. The following derivations follow those of *Mott* (1986); *Kraus* and *Carver* (1973), and *Collin* (1991).

First, we will define horizontal and vertical directions in a plane perpendicular to the propagation direction (the polarization plane). When the propagation path is horizontal, the horizontal and vertical in the polarization plane are true horizontal and vertical. When the propagation path is vertical, horizontal and vertical are defined even though the polarization plane is horizontal. In other words, the definition of horizontal and vertical directions in the polarization plane is independent of the propagation direction. We can now define two waves, one polarized horizontally and one polarized vertically, propagating in the positive z direction with the same frequency. The instantaneous values of these waves are then given by

$$\begin{aligned} \mathcal{E}_H &= Re[E_H e^{j(-kz+\phi_H)}] = E_H \cos(-kz+\phi_H) \\ \mathcal{E}_V &= Re[E_V e^{j(-kz+\phi_V)}] = E_V \cos(-kz+\phi_V) \ . \end{aligned} \tag{A.7}$$

E_H and E_V are the wave amplitudes and ϕ_H and ϕ_V are the phase of the waves when $t = 0$ and $z = 0$. The direction of propagation is defined by $\hat{h} \times \hat{v}$. where $\hat{h}$ and $\hat{v}$ are unit vectors in the direction of H and V, respectively.

We are interested in the form of the solution when we sum these two components ($\mathcal{E} = \mathcal{E}_H\hat{h} + \mathcal{E}_V\hat{v}$). Specifically, we want to show that this wave is elliptically polarized. To this end we rewrite the above equations as

$$\frac{\mathcal{E}_H}{E_H} = \cos\phi_H \cos(kz) + \sin\phi_H \sin(kz)$$

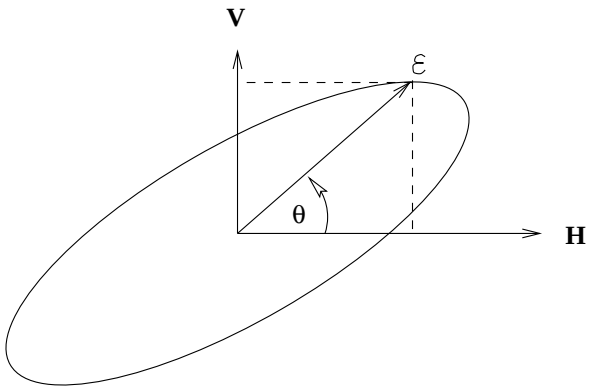

Figure A.1: A polarization ellipse described by a rotating electric field vector

$$\frac{\mathcal{E}_V}{E_V} = \cos\phi_V \cos(kz) + \sin\phi_V \sin(kz) \ . \tag{A.8}$$

If we multiply the first equation in (A.8) by $\sin\phi_V$ and the second equation by $\sin\phi_H$ and subtract the two we obtain the result,

$$\frac{\mathcal{E}_H}{E_H}\sin\phi_V - \frac{\mathcal{E}_V}{E_V}\sin\phi_H = \cos(kz)\sin(\phi_V - \phi_H) \ . \tag{A.9}$$

We now multiply the first equation in (A.8) by $\cos\phi_V$ and the second equation by $\cos\phi_H$ and subtract the two,

$$\frac{\mathcal{E}_H}{E_H}\cos\phi_V - \frac{\mathcal{E}_V}{E_V}\cos\phi_H = \sin(kz)\sin(\phi_H - \phi_V) \ . \tag{A.10}$$

Squaring (A.9) and (A.10) and adding the result,

$$\begin{aligned} \left(\frac{\mathcal{E}_H}{E_H}\right)^2 - 2\frac{\mathcal{E}_V\mathcal{E}_H}{E_V E_H}\cos(\phi_H - \phi_V) + \left(\frac{\mathcal{E}_V}{E_V}\right)^2 &= \sin^2(\phi_H - \phi_V) \\ \left(\frac{\mathcal{E}_H}{E_H}\right)^2 - 2\frac{\mathcal{E}_V\mathcal{E}_H}{E_V E_H}\cos\phi + \left(\frac{\mathcal{E}_V}{E_V}\right)^2 &= \sin^2\phi \ , \end{aligned} \tag{A.11}$$

where in the second equation we have defined $\phi \equiv \phi_H - \phi_V$.

Equation A.11 is the equation of a rotated ellipse. The general form of a rotated ellipse is given by $Ax^2 + Bxy + Cy^2 + Dx + Ey + F = 0$ (*Eves*, 1973), where $x = \mathcal{E}_H$ and $y = \mathcal{E}_V$. For the case in which the ellipse is centered at the origin the ellipse is of the form $Ax^2 + Bxy + Cy^2 + F = 0$. Thus we have shown the sum of two linearly polarized waves is an ellipse. When $\phi = \pm\pi/2$, Equation A.11 can be written as

$$\left(\frac{\mathcal{E}_H}{E_H}\right)^2 + \left(\frac{\mathcal{E}_V}{E_V}\right)^2 = 1 \ . \tag{A.12}$$

When $E_V = E_H$, Equation A.12 is the equation of a circle. Figure A.1 shows the rotated ellipse of (A.11) that is traced out by the time varying instantaneous values of the electric field vector, $\mathcal{E} = \sqrt{\mathcal{E}_H^2 + \mathcal{E}_V^2}$.

A.3.1 The Polarization Ellipse in terms of δ and τ

Continuing the investigation of Equation (A.11), we note that at a particular instant in time shown in Figure A.1 that the H and V components of $\mathcal{E}$ are

$$\begin{aligned} \mathcal{E}_H &= \mathcal{E}\cos\theta \\ \mathcal{E}_V &= \mathcal{E}\sin\theta\ , \end{aligned} \tag{A.13}$$

where θ is the time varying angle from the H axis to $\mathcal{E}$. We can substitute these values in for the instantaneous components into Equation (A.11); the result is

$$\begin{aligned} \sin^2\phi &= \left(\frac{\mathcal{E}\cos\theta}{E_H}\right)^2 + \left(\frac{\mathcal{E}\sin\theta}{E_V}\right)^2 - \frac{\mathcal{E}^2 2\sin\theta\cos\theta}{E_H E_V}\cos\phi \\ \sin^2\phi &= \mathcal{E}^2\frac{E_V^2\cos^2\theta + E_H^2\sin^2\theta - 2\sin\theta\cos\theta E_H E_V\cos\phi}{E_H^2 E_V^2}\ . \end{aligned} \tag{A.14}$$

Solving for $\mathcal{E}$,

$$\mathcal{E}^2 = \frac{(E_H E_V\sin\phi)^2}{(E_V\cos\theta)^2 + (E_H\sin\theta)^2 - 2\sin\theta\cos\theta E_V E_H\cos\phi}\ . \tag{A.15}$$

Or,

$$\mathcal{E} = \frac{E_H E_V\sin\phi}{[(E_V\cos\theta)^2 + (E_H\sin\theta)^2 - \sin 2\theta E_V E_H\cos\phi]^{\frac{1}{2}}}\ . \tag{A.16}$$

The magnitude of the electric field vector will be a maximum for some value of θ. To find this angle, we can differentiate Equation (A.16) with respect to θ and set it equal to zero. The value of θ that maximizes $\mathcal{E}$ is designated τ and is shown in Figure A.2a. The resulting expression for τ is:

$$\tan 2\tau = \frac{2\cos\phi}{(\frac{E_H}{E_V} - \frac{E_V}{E_H})}\ . \tag{A.17}$$

The angle τ is seen to explicitly depend on the magnitudes of the H and V components and on the phase difference between them. τ is called the ellipse tilt angle or the orientation angle.

The angle δ in Figure A.2a provides a measure of the ratio of the radii of the circles that inscribe and circumscribe the ellipse. Figure A.2b shows the polarization

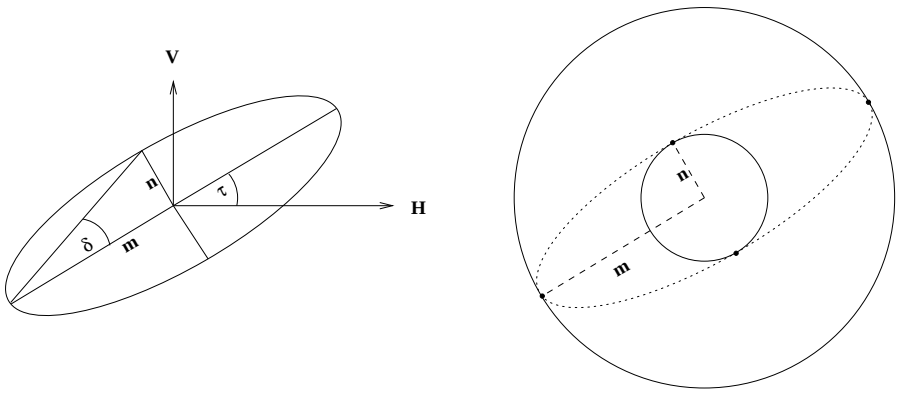

Figure A.2: Polarization ellipse and a) the definition of angles τ and δ and the semi-major and semi-minor axes (m and n), b) inscribed and circumscribed circles.

ellipse with the inscribed and circumscribed circles. The derivation of the equation for δ in terms of the H and V components of the wave is more involved than the derivation for τ, even though the result appears to be as simple. The derivation in (*Mott*, 1986, pages 58-62) is recommended for the interested reader. The result is

$$\sin 2\delta = \frac{2\sin\phi}{\frac{E_H}{E_V} + \frac{E_V}{E_H}} \; . \tag{A.18}$$

From Figure A.2a we can see $\tan\delta = n/m$, where n is the length of the minor semi-axis and m is the length of the major semi-axis of the ellipse. Since (A.18) is in terms of 2δ we would like to find $\sin 2\delta$ in terms of n and m. Using a trigonometric identity and the definition of $\tan\delta$, we can find

$$\begin{aligned} \sin 2\delta &= \frac{2\tan\delta}{1+\tan^2\delta} \\ &= \frac{2(n/m)}{1+(n/m)^2} \\ \sin 2\delta &= \frac{2nm}{m^2+n^2} \; . \end{aligned} \tag{A.19}$$

We can write A.19 in the same form as A.18 and equate the two,

$$\frac{2\sin\phi}{\frac{E_H}{E_V} + \frac{E_V}{E_H}} = \frac{2}{\frac{n}{m} + \frac{m}{n}} \; . \tag{A.20}$$

This equation relates the ratio of the major and minor semi-axes (m and n) to the magnitude and phase difference of the H and V components of the polarization ellipse.

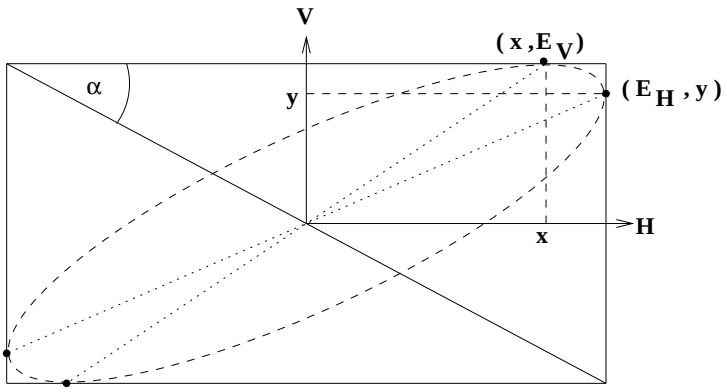

Figure A.3: Polarization ellipse described by a circumscribed rectangle (with aspect ratio α) and its intersection with the polarization ellipse.

The polarization ellipse is defined in terms of the magnitude of the H and V electric field components. The ellipse can also be defined in terms of the shape, through the angle, δ, and the orientation of the ellipse through the angle, τ.

A.3.2 The Polarization Ellipse in terms of α and ϕ

There is an alternate way to visualize Equation (A.11). The rotating E-field vector of Figure A.1 will always fit in a rectangle with sides $2E_H$ and $2E_V$ (see Figure A.3). Equation A.11 holds in general. When $\mathcal{E}_V = \pm E_V$, (A.11) simplifies to

$$\begin{aligned} \left(\frac{\mathcal{E}_H}{E_H}\right)^2 \mp 2\frac{\mathcal{E}_H}{E_H}\cos\phi + 1 - \sin^2\phi &= 0 \\ \left(\frac{\mathcal{E}_H}{E_H}\right)^2 \mp 2\frac{\mathcal{E}_H}{E_H}\cos\phi + \cos^2\phi &= 0 \\ \left(\frac{\mathcal{E}_H}{E_H} \mp \cos\phi\right)^2 &= 0\ . \end{aligned} \tag{A.21}$$

This equation shows that the intersection of the ellipse and the horizontal sides of the bounding rectangle depends only on the phase difference, ϕ, between the H and V components. One of the intersection points is shown in Figure A.3 as

$$y = \mathcal{E}_H = E_H \cos\phi\ . \tag{A.22}$$

Similarly the intersection of the ellipse and the vertical sides of the bounding rectangle in Figure A.3) can be found to be

$$x = \mathcal{E}_V = E_V \cos\phi\ . \tag{A.23}$$

We can look at some special cases to learn more about the above relationships. For example, if the H and V components are in phase ($\phi = 0$) or out of phase ($\phi = \pi$) the polarization ellipse degenerates into a line drawn between opposite corners of the bounding rectangle. This corresponds to a linear polarization rotated at the angle τ. If $\phi = \pm\pi/2$, the polarization ellipse intersects the bounding rectangle where the H and V axes intersect the rectangle which is an ellipse rotated at the angle $\tau = 0$ or $\tau = \pi/2$.

We could have investigated where the polarization ellipse intersects the V axis and we would have found that the relationships are similar to the above except the $\cos\phi$ term is replaced by $\sin\phi$ ($\mathcal{E}_V/E_V = \pm\sin\phi$). This relationship will look familiar to anyone familiar with Lissajous figures and phase measurements made using an oscilloscope.

The angle α in Figure A.3 is defined as the arctangent of the ratio of the sides of the bounding rectangle,

$$\tan\alpha = \frac{E_V}{E_H} \; . \tag{A.24}$$

The tangent of α depends on the magnitudes of the H and V components of the wave. For example, when $E_V = 0$, $\alpha = 0$ and the polarization state is linear at an angle $\tau = 0$ which corresponds to a horizontally polarized wave. When $E_H = E_V$, $\alpha = \pi/4$ and the polarization ellipse is bounded by a square. The phase angle between the H and V components determines the intersection of the bounding square and the polarization ellipse from (A.22) and (A.23).

In Figure A.2 we see the (δ, τ) description of the polarization ellipse involves the ratio of the radii of circumscribed and inscribed circles can the tilt angle of the ellipse, τ. The description of the polarization ellipse through the angles δ and τ can be thought of as a circular description.

On the other hand, Figure A.3 shows that the polarization ellipse can be described by the size and aspect ratio of a bounding rectangle. The aspect ratio of the sides of the rectangle is related to the angle α. The orientation of the polarization ellipse inside the bounding rectangle is determined by the phase difference (ϕ) between the H and V components of the wave. The description of the polarization ellipse by the angles α and ϕ can be thought of as a rectangular description.

We can see the polarization state may be described in terms of two sets of angles, δ and τ or α and ϕ. We refer to these as two sets of angles as the (δ, τ) or (α, ϕ) description of polarization state. Since the (δ, τ) and (α, ϕ) descriptions refer to

the same polarization ellipse, the two descriptions are related. The relationships between the two descriptions will be determined after two geometrical descriptions of polarization state are developed.

A.4 Polarization Ratios

In the previous section we presented a description of the polarization state of an electro-magnetic wave in terms of the magnitude and the phase of the component electric field vectors. The rotating electric field vector shown in Figure A.1 appears as it would at a fixed point along the propagation path if electric fields could be visualized. In this section the description of polarization state moves into the realm of mathematical abstraction. The polarization state is described as a point in the extended complex plane through the use of polarization ratios. This description of polarization state is a planar description. The mathematical abstraction is extended in subsequent sections where any polarization state will be described as a point on a sphere.

A.4.1 Linear Polarization Ratios

As we have seen in Section 2.2, the polarization state can be described in terms of the magnitude and phase of electric field components in two orthogonal bases (e.g., H and V). In a linear *H-V* polarization basis, a complex polarization ratio can be defined as:

$$\begin{aligned} P &\equiv \frac{E_V e^{j\phi_V}}{E_H e^{j\phi_H}} \\ \tan\alpha &= \frac{E_V}{E_H} \\ P &= (\tan\alpha)\, e^{-j\phi} \ . \end{aligned} \tag{A.25}$$

P is termed the linear polarization ratio (LPR). The domain of P is the complex plane. The magnitude of P varies between zero and infinity. The extremal values occur when $E_V = 0$ and when $E_H = 0$. The polarization state when $E_V = 0$ corresponds to the origin in the complex plane and is termed polarization *base*. The range of α is $0 \leq \alpha \leq \frac{\pi}{2}$ since $0 \leq E_V/E_H \leq \infty$. The range of ϕ is $-\pi \leq \phi < \pi$.

Figure A.4 shows the complex plane and the location of specific polarizations states in terms of the linear polarization ratio, P. Specific polarization states in terms

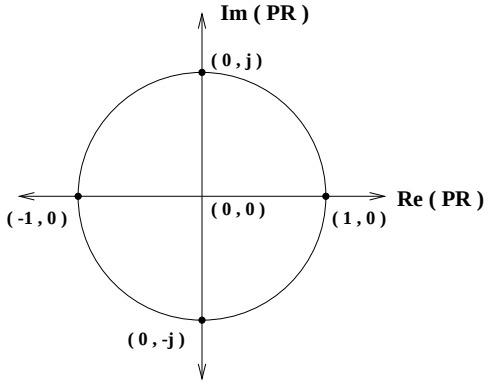

Linear Polarization Ratios	
H	0
V	inf.
+45	1
LHC	j
-45	-1
RHC	-j

Circular Polarization Ratios	
LHC	0
RHC	inf.
H	1
+45	j
V	-1
-45	-j

Slant Polarization Ratios	
+45	0
-45	inf.
LHC	1
H	j
RHC	-1
V	-j

Figure A.4: Generic polarization ratio in the complex plane. The polarization base corresponds to the origin and the polarization orthogonal to the base is at infinity. Other special polarization ratios lie on the unit circle.

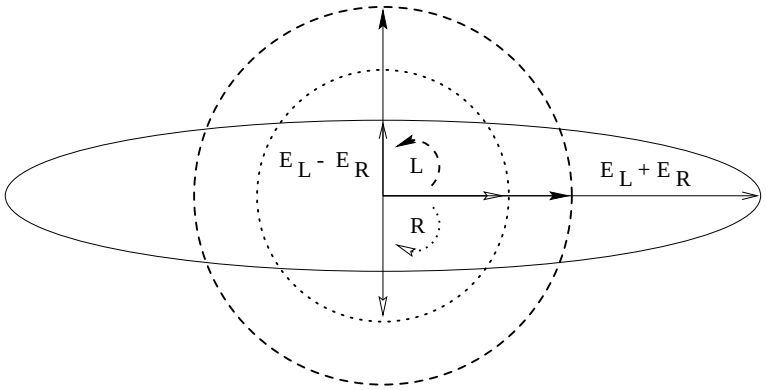

Figure A.5: polarization ellipse in terms of the τ angle and n and m.

of other polarization ratios are also shown and will be discussed later. P can be written in the complex form $P = \tan\alpha(\cos\phi + j\sin\phi)$. Thus, any polarization state can be expressed as a complex number; a point in the complex plane. A point in the complex plane can also be defined through the angles $\tan\alpha = E_V/E_H$, the ratio of the magnitude of the H and V components and the phase difference between the H and V components, $\phi \equiv \phi_H - \phi_V$.

When $|P| = 1$, the H and V components of the wave are equal, $\tan\alpha = E_V/E_H$. When $E_V < E_H$, $\tan\alpha < 1$. Polarizations states that lie within the unit circle in the complex plane have H components that are larger than V components ($E_H > E_V$). Polarization states that lie outside the unit circle in the complex plane have larger V components than H components ($E_V > E_H$). Polarization states that lie on the unit circle have equal H and V components ($E_V = E_H$).

A.4.2 Circular Polarization Ratios

In the previous sections we showed that two linear polarized waves (H and V) can be used as a basis to generate an elliptically polarized wave. In this section we will show how two left and right hand circularly polarized waves may also be used as a basis to generate an elliptically polarized wave.

A general elliptically polarized wave can be constructed by adding left hand circular (L) and right hand circular (R) waves. We define the magnitude of the waves as E_L for the L component and E_R for the R component. E_L and E_R are nonnegative real quantities.

When the counter rotating waves electric field vectors align they will add con-

structively so that $m = E_L + E_R$ (See Figure A.5). The angle where this occurs is τ. The τ of Figure A.5 is zero. When the counter rotating waves are anti-parallel at $tau \pm \pi/2$ they will add destructively to give $\pm n = E_L - E_R$. The $\pm$ is needed since n is a nonnegative length. The negative sign is used when $E_R > E_L$ and the positive sign is used when $E_R < E_L$. We can use these two relationships to determine E_L and E_R in terms of n and m,

$$\begin{aligned} E_L &= \frac{m \pm n}{2} \\ E_R &= \frac{m \mp n}{2} \ . \end{aligned} \tag{A.26}$$

When $n = m$ either $E_L = 0$ or $E_R = 0$ and the wave is circularly polarized. When $n = 0$ then $E_L = E_R$ and the wave is linearly polarized. m is never zero since it is by definition the major semi-axis of the ellipse ($0 \leq n \leq m$ and $m > 0$).

The circular polarization ratio (CPR) is defined as,

$$q = \frac{E_R}{E_L} e^{j2\tau} \ , \tag{A.27}$$

where E_L and E_R are the magnitudes of the LHC and RHC components, and τ is the angle where the two counter rotating electric field vectors align. Substituting in the m and n values from (A.26) for E_L and E_R we find

$$q = \frac{m \mp n}{m \pm n} e^{j2\tau} \ . \tag{A.28}$$

From Figure A.2, $\tan\delta = n/m$ so that the circular polarization ratio in terms of δ is,

$$\begin{aligned} q &= \frac{m \mp n}{m \pm n} e^{j2\tau} \\ &= \frac{1 \mp \frac{n}{m}}{1 \pm \frac{n}{m}} e^{j2\tau} \\ q &= \frac{1 \mp \tan\delta}{1 \pm \tan\delta} e^{j2\tau} \ . \end{aligned} \tag{A.29}$$

We can sort out the signs in the above equations by recognizing that the polarization base of the circular polarization ratio as defined here is L ($q = 0$ when $E_R = 0$). For left hand circular polarization $n = m$, $E_L = m$ and $E_R = 0$. And since $\tan\delta = m/m = 1$ the correct sign convention for the CPR with an LHC base is,

$$q = \frac{1 - \tan\delta}{1 + \tan\delta} e^{j2\tau} \ . \tag{A.30}$$

We should note here that the alternate sign convention for the CPR would result from a change in the polarization base to right hand circular polarization. The range of δ is defined so that $q = 0$ for LHC and $q = \infty$ for RHC, δ is $-\frac{\pi}{4} \leq \delta \leq \frac{\pi}{4}$. And the range of τ is $-\pi/2 \leq \tau < \pi/2$. The factor of two in the phase factor in the definition of CPR is necessary so the domain is the entire complex plane.

The linear polarization ratio, P, and the circular polarization ratio, q, can be used to describe the same polarization state. Therefore, it should be possible to map between the two polarization ratios: P and q. *Mott* (1986) has shown that the mapping from any linear polarization ratio P into the circular polarization ratio q is given by:

$$q = \frac{1 + jP}{1 - jP} \ . \tag{A.31}$$

Equation (A.31) is a bilinear fractional transform. The bilinear fractional transform is also known as a linear fractional transform or Möbius transform (*Kreyszig*, 1972). A polarization ratio in any basis can be transformed into any other basis and any polarization state can be transformed into any other polarization state using a bilinear fractional transform (*Bolinder*, 1981). The general form of a bilinear fractional transform is given by

$$w = \frac{az + b}{cz + d} \ , \tag{A.32}$$

where w, a, b, c, d and z are all complex, in general.

The bilinear fractional transform is a conformal mapping. The z-plane is mapped into the w-plane. One important aspect of the bilinear fractional transform is there are always two polarization states that are mapped into themselves. These two polarizations are invariant to the transformation. They are also referred to as the characteristic polarizations of the transformation. For example, particles aligned horizontally will backscatter a horizontally polarized wave with no vertically polarized component. The backscattered polarization state is the same as the incident polarization state. An incident H polarization state a characteristic polarization of the horizontally aligned backscatters. If circular polarization is incident upon the same horizontally aligned scatters, the backscattered polarization state would include both left and right hand circular polarization components.

Figure A.6 is identical to Figure 13 of *Slater* (1950) showing how the bilinear fractional transforms the polarization states in two ways. The first is a streaming from one characteristic polarization towards the other. The other is a rotation around the

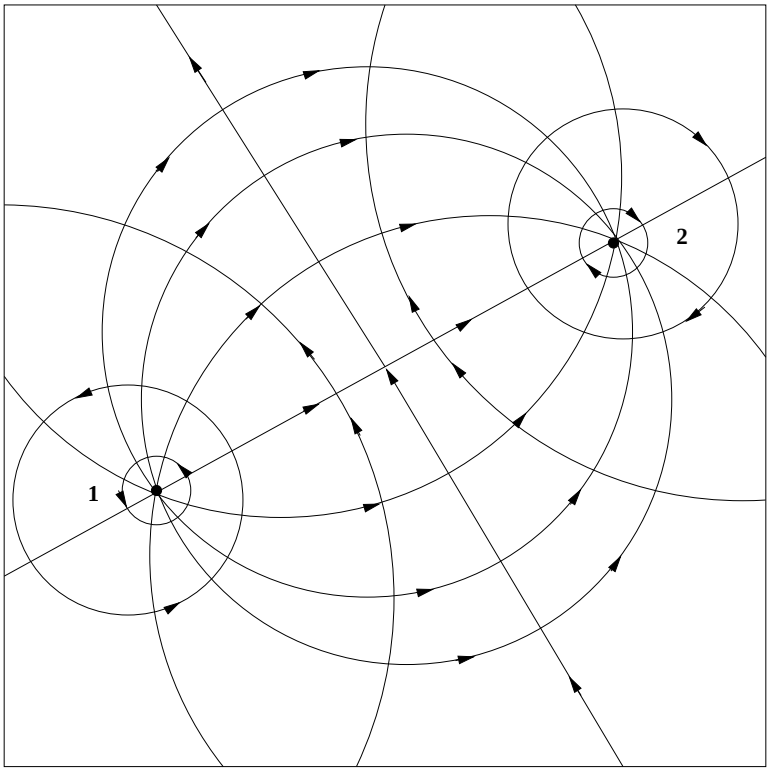

Figure A.6: The conformal mapping of the bilinear fractional transforms polarization states two ways. There is a general streaming from one characteristic polarization (1) to the other (2). And a general rotation around the characteristic polarizations.

characteristic polarization states. The characteristic polarizations of the transform of (A.31) can be found by solving

$$z = \frac{az + b}{cz + d} \,. \tag{A.33}$$

The two characteristic polarizations of the general bilinear fractional transform are,

$$z = \frac{a - d}{2c} \pm \sqrt{\left(\frac{a - d}{2c}\right)^2 + \frac{b}{c}} \,. \tag{A.34}$$

The solution of the above equation is not as important as the concept that there are *always* two polarization states that are invariant to a particular polarization transformation (or mapping).

A.4.3 Summary

Of the three "special" polarization ratios of Figure A.4: linear, circular and slant. The linear and circular are most often used to describe polarization states. The slant polarization ratio is seldom used and is generally considered to be a special case of the LPR. The polarization base is the polarization that lies at the origin in the complex plane when polarization ratios are used to describe the polarization state. The common, but not exclusive, choices of bases are Horizontal, +45°, and Left Hand Circular (*Mott*, 1986) (H,+,L). These are the assumed polarization ratio bases used in this dissertation.

Figure A.4 shows a generic polarization ratio in the complex plane. The polarization that corresponds to the polarization base lies at the origin. The orthogonal polarization is at infinity. The other "special" polarizations lie on the unit circle. Note that for the Circular Polarization Ratio case that the rotation direction (or helicity) inside and outside the unit circle have opposite senses.

A.5 The Stokes Parameters

In the middle of the nineteenth century, *Stokes* (1852) showed that the polarization state of light could be determined by measurements using a combination of polarizers and phase retarding plates. The first measurement involves measuring the total power incident on a detector from a particular source. This measurement determines the total intensity and the first Stokes parameter (I). A linear polarizer is then placed between the source and detector. The difference of the detected power when the polarizer is rotated to pass horizontally and vertically polarized light is the second Stokes parameter (Q). The third Stokes parameter (U) is similar to (Q) except that the power differences are taken with the linear polarizer set to +45° and -45° off horizontal (or vertical). The linear polarizer and a phase retarder (quarterwave plate) are then used to resolve the power into left and right hand circular components of the light. The difference between the power in LHC and RHC polarized components determines the fourth and final Stokes parameter (V).

The Stokes parameters as defined by the measurements can be related to the components of the polarized wave as,

$$\begin{aligned} I &= E_H^2 + E_V^2 = E_+^2 + E_-^2 = E_L^2 + E_R^2 \\ Q &= E_H^2 - E_V^2 \end{aligned}$$

$$\begin{aligned} U &= E_+^2 - E_-^2 \\ V &= E_L^2 - E_R^2 \ , \end{aligned} \tag{A.35}$$

where E_H^2 is the power in the horizontal, E_V^2 is the power in the vertical, E_+^2 is the power in the $+45°$, E_-^2 is the power in the $-45°$, E_L^2 is the power in the left hand circular, and E_R^2 is the power in the right hand circular power component of the polarized wave. Each Stokes parameter in (A.35), except I, is positive only when the polarization base is the predominant wave component. Since the Stokes parameters represent differences in power in two orthogonal polarizations, Q, U, and V can be positive, negative or zero. The first Stokes parameter I is always positive since it represents total power. The first equation in (A.35) shows that the total power is independent of the measurement basis.

The measurements are not all independent. For completely polarized light (or other electromagnetic waves) the validity of the measurements can be verified from the fact that:

$$I^2 = Q^2 + U^2 + V^2 \ . \tag{A.36}$$

In general, though, there will be a portion of the wave that is not polarized. When there is an unpolarized component the wave is said to be partially polarized and Equation (A.36) is modified to

$$I^2 \geq Q^2 + U^2 + V^2 \ . \tag{A.37}$$

The equality holds only when the wave is completely polarized. The degree of polarization (p) is defined as the ratio of the polarized power to the total power and can be written as:

$$p \equiv \frac{\sqrt{Q^2 + U^2 + V^2}}{I} \ . \tag{A.38}$$

The degree of polarization lies between zero (unpolarized) and unity (fully polarized). Table A.1 shows examples of the Stokes parameters for various completely polarized waves.

Sometimes it is desirable to work with the normalized Stokes parameters. The normalized Stokes parameters are obtained by dividing each Stokes parameter by the intensity of the polarized component ($I_p = pI$).

$$s_0 = \frac{I}{I_p}$$

Stokes Parameters	Polarization (H)	(V)	(+)	(-)	(L)	(R)	(LEP)	(REP)
I	2	2	2	2	2	2	3	3
Q	2	-2	0	0	0	0	1	2
U	0	0	2	-2	0	0	2	2
V	0	0	0	0	2	-2	2	-1

Table A.1: Example Stokes parameters for various completely polarized waves

$$\begin{aligned} s_1 &= \frac{Q}{I_p} \\ s_2 &= \frac{U}{I_p} \\ s_3 &= \frac{V}{I_p} \ . \end{aligned} \tag{A.39}$$

The notation for the normalized Stokes parameters in (A.39) differs from the notation for the unnormalized Stokes parameters so it is obvious when the Stokes parameters are normalized.

The originally posed Stokes parameters provided a systematic method of determining the polarization state of light. More importantly the Stokes parameters have become a convenient way of characterizing the polarization state.

A.6 The Poincaré Sphere

Poincaré (1892) showed that the Stokes parameters could be interpreted geometrically. The triplet (Q, U, V) can be considered to represent the three cartesian coordinates. For the case of a completely polarized wave the Stokes parameter I represents the radius of a sphere, centered at the origin, that passes through the point (Q, U, V). In the case of a partially polarized wave, the radius of the sphere that passes through the point (Q, U, V) is pI. This sphere is commonly referred to as the Poincaré sphere. The angle pairs (α, ϕ) and (δ, τ) were previously defined in terms of orthogonal wave components of the rotating electric field vector of the polarization ellipse. In this section, (α, ϕ) and (δ, τ) are related to the Stokes parameters using Poincaré's geometrical interpretation of the Stokes parameters.

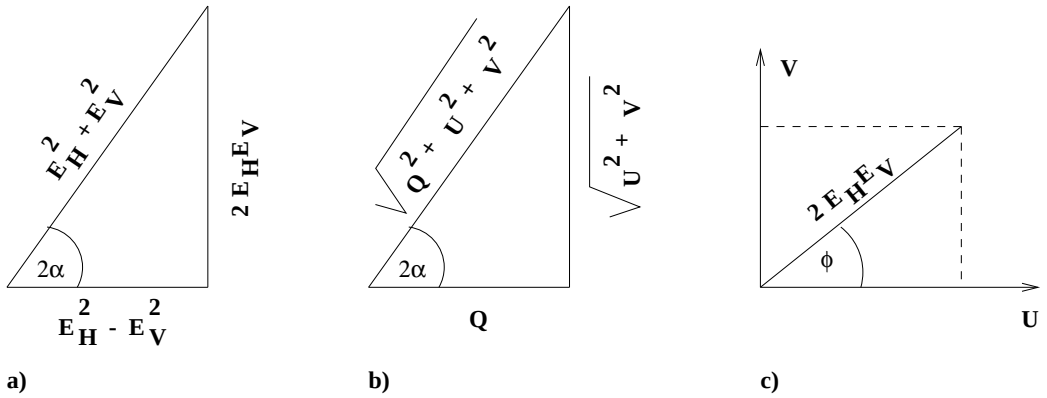

Figure A.7: Definition the α and ϕ angles on the Poincaré sphere a) 2α in terms of the H and V component values, b) 2α in terms of the Stokes parameters and c) ϕ in terms of H and V components in the U-V plane.

A.6.1 Spherical (α, ϕ) Angles in terms of the Stokes Parameters

In this section we show how the spherical angles, (α, ϕ), on the Poincaré sphere is related to the Stokes parameters. In the description of the polarization state based on the polarization ellipse, we showed that,

$$\tan\alpha = \frac{E_V}{E_H} \; . \tag{A.40}$$

Using the trigonometric identity

$$\tan 2\alpha = \frac{2\tan\alpha}{1-\tan^2\alpha} \; , \tag{A.41}$$

we find that

$$\begin{aligned} \tan 2\alpha &= \frac{2\frac{E_V}{E_H}}{1-\left(\frac{E_V}{E_H}\right)^2} \\ \tan 2\alpha &= \frac{2E_V E_H}{E_H^2 - E_V^2} \; . \end{aligned} \tag{A.42}$$

We recognize The denominator is the Stokes parameter Q in Equation A.35. In Figure A.7a, we have constructed a right triangle using (A.42). Using the Pythagorean theorem we can find the hypotenuse of the triangle is $E_H^2 + E_V^2$ which we recognize as I from (A.36), $I = \sqrt{Q^2+U^2+V^2}$. Figure A.7b shows 2α in terms of the Stokes

parameters. From Figure A.7a and b, we see that $2E_V E_H = \sqrt{U^2 + V^2}$. The result is the spherical angle, 2α, in terms of Stokes parameters is given by,

$$\tan 2\alpha = \frac{\sqrt{U^2 + V^2}}{Q} \ . \tag{A.43}$$

The angle 2α is the angle from the positive Q axis in the (Q, U, V) coordinate system.

To determine how the spherical angle, ϕ, is related to the Stokes parameters, we let $Q = 0$ and $U = 0$ in Equation A.35. When $Q = U = 0$, $E_H = E_V$, $E_+ = E_-$, and $I = V$ and the wave is left hand circularly polarized. From the linear polarization ratio,

$$P = \frac{E_V}{E_H} e^{-j\phi} = e^{-j\phi} \ , \tag{A.44}$$

where we have used $E_H = E_V$. From Figure A.4, the linear polarization ratio, $P = j$, for left hand circular polarization. Therefore, $\phi = \pi/2$. We can find the relationship between the Stokes parameters and the H and V components and the phase difference between them,

$$\begin{aligned} I &= E_H^2 + E_V^2 \\ Q &= E_H^2 - E_V^2 \\ U &= 2E_H E_V \cos\phi \\ V &= 2E_H E_V \sin\phi \ . \end{aligned} \tag{A.45}$$

And the spherical angles, $|phi$, is related to the Stokes parameters through the equation,

$$\tan\phi = \frac{V}{U} \ . \tag{A.46}$$

ϕ represents the angle in the $U - V$ plane from the U axis (see Figure A.7c). 2α is the polar angle from Q.

A.6.2 Spherical (δ, τ) Angles in terms of the Stokes Parameters

In this section we show how the spherical angles, (δ, τ), on the Poincaré sphere is related to the Stokes parameters. The angle δ was previously defined in terms of the polarization ellipse,

$$\tan\delta = \frac{n}{m} \ , \tag{A.47}$$

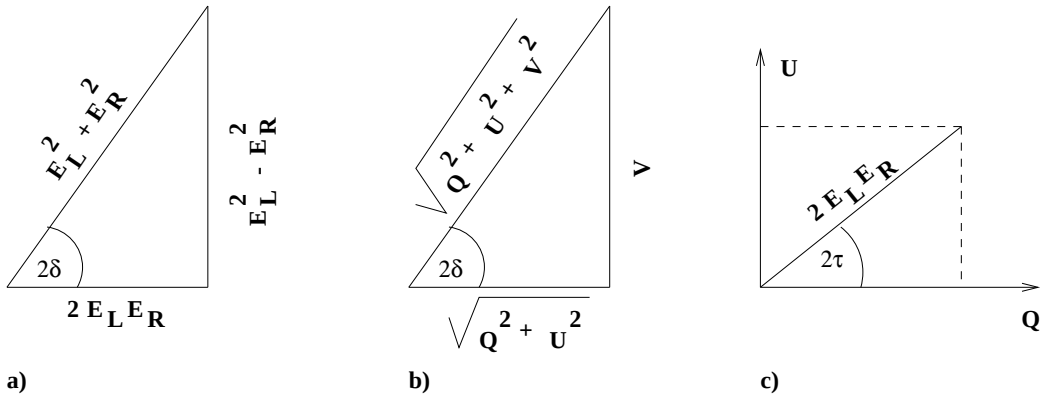

Figure A.8: Definition the δ angle of the Poincaré sphere a) 2δ in terms of the L and R component values, b) 2δ in terms of the Stokes parameters and c) 2τ in terms of L and R components in the Q-U plane.

where n and m are the lengths of the minor and major semi-axes of the polarization ellipse. Using the trigonometric identity of (A.41),

$$\tan 2\delta = \frac{2nm}{m^2 - n^2} \ . \tag{A.48}$$

We can determine the magnitude of the L and R components (E_L and E_R) of the wave in terms of n and m,

$$\begin{aligned} n &= \frac{E_L - E_R}{2} \\ m &= \frac{E_L + E_R}{2} \\ 2nm &= \frac{E_L^2 - E_R^2}{2} \\ m^2 - n^2 &= \frac{E_L E_R}{2} \ . \end{aligned} \tag{A.49}$$

We can find 2δ in terms of E_L and E_R circular components of the polarized wave,

$$\tan 2\delta = \frac{E_L^2 - E_R^2}{2E_R E_L} \ . \tag{A.50}$$

We recognize the numerator as the Stokes parameter, V from Equation A.35. In Figure A.8a, we construct a right triangle using (A.50). Using the Pythagorean theorem we can find the hypotenuse of the triangle is $E_L^2 + E_R^2$ which we recognize from (A.36) as the Stokes parameter, $I = \sqrt{Q^2 + U^2 + V^2}$. Figure A.8b shows 2δ in terms

of the Stokes parameters. From Figure A.8a and b, we see that $2E_LE_R = \sqrt{Q^2+U^2}$. The result is the spherical angle, 2δ, is related to the Stokes parameters as,

$$\tan 2\delta = \frac{V}{\sqrt{Q^2+U^2}} \ . \tag{A.51}$$

The angle 2δ is the angle from the $Q-U$ plane in the (Q,U,V) coordinate system.

To determine how the spherical angle, 2τ is related to the Stokes parameters, we let $U=0$ and $V=0$ in (A.35). When $U=V=0$, $E_R=E_L$, $E_+=E_-$, and $I=Q$ and the wave is horizontally polarized. From the circular polarization ratio,

$$q = \frac{1-\tan\delta}{1+\tan\delta}\, e^{j2\tau} \ . \tag{A.52}$$

Since the wave is horizontally polarized $n=0$, $\tan\delta = 0$ and,

$$q = e^{j2\tau} = \cos 2\tau + j \sin 2\tau \ . \tag{A.53}$$

From Figure A.4 for horizontal linear polarization $q=1$ and therefore, $\tau = 0$. The Stokes parameters are related to the L and R components and the angle 2τ,

$$\begin{aligned} I &= E_L^2 + E_R^2 \\ Q &= 2E_LE_R\cos 2\tau \\ U &= 2E_LE_R\sin 2\tau \\ V &= E_L^2 - E_R^2 \ . \end{aligned} \tag{A.54}$$

The spherical angle, 2τ is related to the Stokes parameters through the equation

$$\tan 2\tau = \frac{U}{Q} \ . \tag{A.55}$$

The spherical angle, 2τ, represents the angle in the $Q-U$ plane from the Q axis (see figure A.8c) and the spherical angle, 2δ, is the angle up or down from $Q-U$ plane.

Figure A.9 is a three dimensional depiction of the two dimensional views in Figures A.7 and A.8. This geometrical interpretation of the Stokes parameters yields another way to depict polarization states. Any polarization state can be depicted as a point on the Poincaré sphere. Any point on a sphere can be represented by two angles, a polar angle and an azimuthal angle. There is an arbitrary choice of which of the three axes (Q, U, or V) to chose as the polar axis. For two of the choices for the polar axis, the (δ,τ) and (α,ϕ) descriptions of polarization state are obtained. A

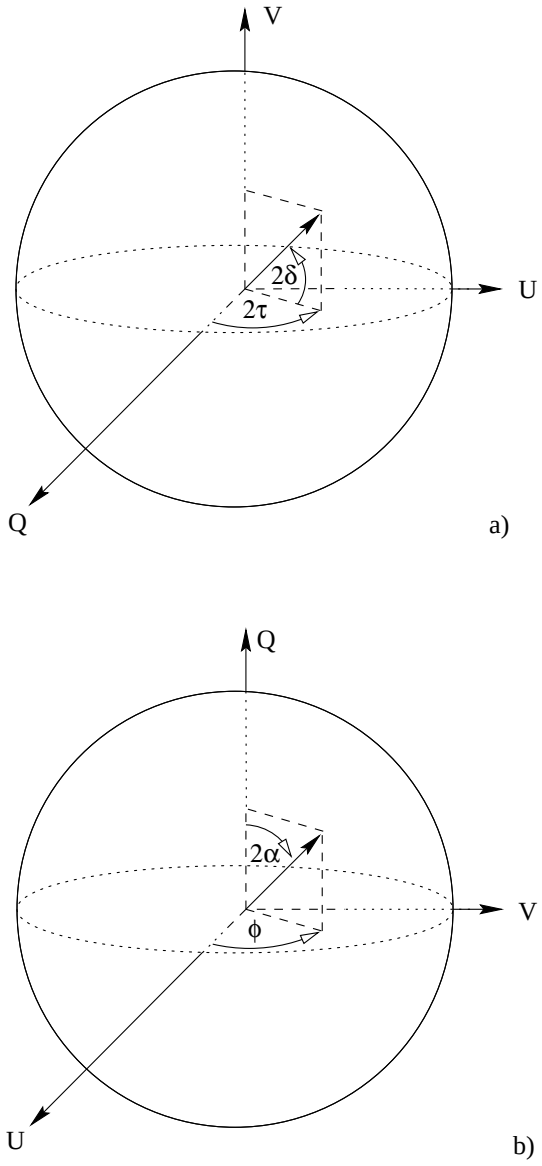

Figure A.9: Definition the angles of the Poincaré sphere a) (δ, τ) and b) (α, ϕ) description.

third choice for the polar axis yields a polarization description based upon the slant linear polarizations as the basis.

The Poincaré sphere is a powerful tool for polarization analysis because of the geometrical nature of the description. It may be more correct when using the Poincaré sphere description of polarization state to refer to the two descriptions of polarization state as $(2\alpha, \phi)$ and $(2\delta, 2\tau)$ since the physical angles of the polarization ellipse description are doubled in the Poincaré sphere description. This doubling of the physical angles of the polarization ellipse makes the cartesian space of the Stokes parameters a sub-space.

From Figures A.9a and b we can determine the relationship between the (δ, τ) and the (α, ϕ) angles and the Stokes parameters using simple trigonometry,

$$\begin{aligned} s_1 &= \tfrac{Q}{I_p} &&= \cos 2\delta \cos 2\tau = \cos 2\alpha \\ s_2 &= \tfrac{U}{I_p} &&= \cos 2\delta \sin 2\tau = \sin 2\alpha \cos \phi \\ s_3 &= \tfrac{V}{I_p} &&= \sin 2\delta = \sin 2\alpha \sin \phi \ . \end{aligned} \tag{A.56}$$

From Equation (A.56) we can solve for δ and τ in terms of α and ϕ,

$$\begin{aligned} \sin 2\delta &= \sin 2\alpha \sin \phi \\ \tan 2\tau &= \tan 2\alpha \cos \phi \ . \end{aligned} \tag{A.57}$$

Alternately, we can solve for α and ϕ in terms of δ and τ.

$$\begin{aligned} \cos 2\alpha &= \cos 2\delta \cos 2\tau \\ \tan \phi &= \tan 2\delta \csc 2\tau \ . \end{aligned} \tag{A.58}$$

These equations allow us to go back and forth between the two angular descriptions of polarization state, without using bilinear fractional transformations. Using Equation (A.56) we can determine the (δ, τ) and (α, ϕ) angles in terms of the Stokes parameters.

$$\begin{aligned} \tan 2\tau &= \frac{U}{Q} \\ \tan 2\delta &= \frac{V}{\sqrt{Q^2 + U^2}} \\ \tan \phi &= \frac{V}{U} \\ \tan 2\alpha &= \frac{\sqrt{U^2 + V^2}}{Q} \ . \end{aligned} \tag{A.59}$$

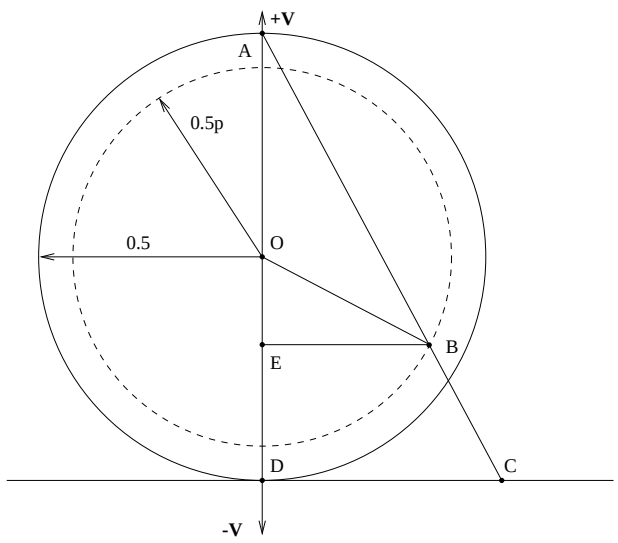

$$OE = \frac{W_L - W_R}{2(W_L + W_R)}$$

$$AO + OE = \frac{W_L}{W_L + W_R}$$

$$BE = \frac{|W|}{W_L + W_R}$$

Triangle ABE is similar to ACD
Therefore, BE : AE = CD : AD
Or, $|W| / W_L = CD$

Figure A.10: Cross sectional view of the stereographic projection of the polarization point (B) onto the complex circular polarization ratio plane. The plane of the view is in the plane through point (B) and the V-axis. The plane of the projection is tangent to the point $V = 1/2$ and perpendicular to the V-axis.

A.7 Relationship Between the Poincaré Sphere and W/W_2

Mott (1986) shows that the polarization ratios (the polarization description in the complex plane) are the stereographic projections of points on the Poincaré sphere onto a plane tangent to the Poincaré sphere when the sphere is normalized to unity diameter. Each type of polarization ratio is due to a stereographic projection from a different reference point on the sphere onto a different tangent plane. When there is partial polarization, we normalize the diameter of the total power sphere to unity.

An example of a stereographic projection shows that the magnitude of the $\frac{W}{W_2}$ parameter of *McCormick* and *Hendry* (1979) is the stereographic projection of Figure A.10. Figure A.10 shows a cross sectional view of the stereographic projection. Point

(B) on the Poincaré Sphere is the polarization state. The polarization base for the projection is LHC polarization since when $W_R = 0$ the point in the complex plane is at the origin ($AO + OE = 1$, see Table 2.1). In the $|W|/W_2$ description due to McCormick and Hendry, W_2 corresponds to the co-polar power (which in this example is LHC) (*Chen*, 1994).

A.8 Summary

This appendix covered the different descriptions of polarization state: polarization ellipse, polarization ratios, Stokes parameters, and the Poincaré sphere. It is important to realize that all these descriptions of polarization state are equivalent for any given polarization state except that the polarization ratios contain no information about the degree of polarization. Each description is important because depending on the circumstances one will yield the simplest mathematical and conceptual formulation.

A common thread running through all the polarization descriptions is the (δ, τ) and (α, ϕ) angular characterization. Figure A.11 is a convenient reference showing the polarization angles (α, ϕ) and (δ, τ) and their relationship to the Stokes parameters for *H-V* and *L-R* receiver bases. The requirement that $I_p^2 = Q^2 + U^2 + V^2$ ensures that the figures in A.11 can be folded into tetrahedrons with four right angles. A similar tetrahedron can be constructed using the total power I. In this case, the angles opposite the total power edge are no longer right angles. And, the δ and α angles are reduced from their actual values. Polarization tetrahedrons constructed using total power are therefore not as useful the completely polarized polarization tetrahedrons and are therefore not shown. The relationship between the polarization tetrahedron and the Poincaré sphere is shown in Figure A.12. The polarization tetrahedron is an original result of this work.

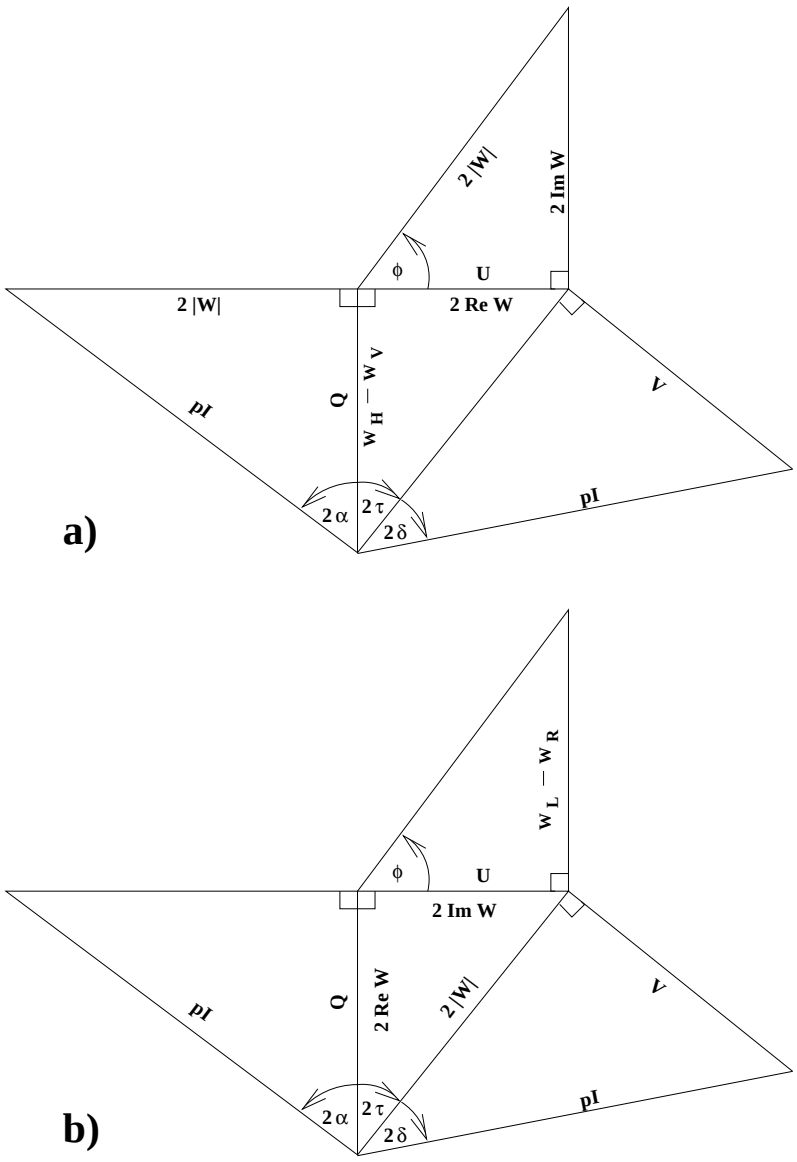

Figure A.11: Relationship between the Stokes Parameters and the radar measurables for: a) *H-V* and b) *L-R* receiver basis. The figures when folded form polarization tetrahedrons.

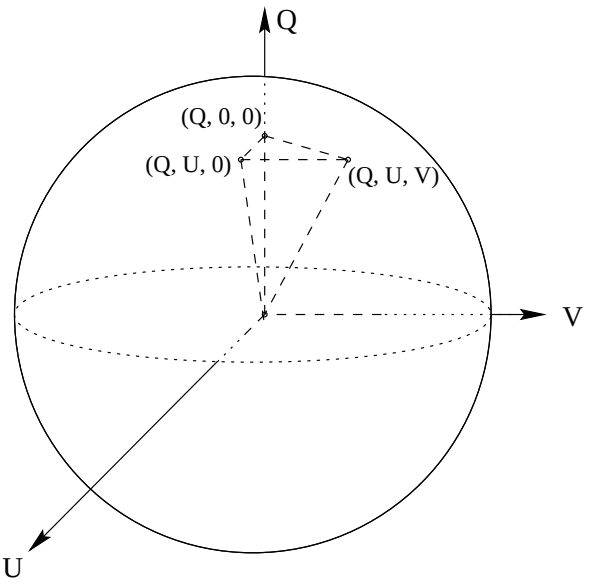

Figure A.12: Relationship between the polarization tetrahedron (see Figure A.11) and the Poincaré sphere. The polarization state represented is (Q, U, V).

Appendix B

Conversion of Radar Parameters Between Different Receiver Bases

One of the best features of this technique is the ability to convert from one receiver basis to the any other. This makes the familiar radar parameters of various other techniques available for inspection.

For example, a common radar parameter in a L-R receiver basis is the circular depolarization ratio ($CDR \equiv W_L/W_R$). It is possible to find the CDR in terms of measurements in an H-V basis.

Equations for determining two of the more familiar parameters CDR and W/W_2 in terms of an H-V receiver basis will be examined in this appendix.

In the case of an L-R receiver basis, one might wish to determine the parameters in an H-V basis, $\rho_{HV}(0)$ and ZDR. These relationships are also derived here.

B.1 Circular Depolarization Ratio

The Circular Depolarization Ratio (CDR) is defined as

$$CDR \equiv \frac{W_L}{W_R} \,, \tag{B.1}$$

depending on the transmitted polarization state. In this case, LHC is the assumed transmitted polarization and therefore RHC is the co-polar return.

From Table 2.1 we see that in terms of Stokes parameters this can be written as

$$\begin{aligned} CDR &= \left(\frac{I+V}{2}\right) / \left(\frac{I-V}{2}\right) \\ &= \frac{I+V}{I-V} \,. \end{aligned} \tag{B.2}$$

In terms of the (δ, τ) description of polarization state we can also write this as

$$CDR = \frac{1 + \sin 2\delta}{1 - \sin 2\delta} \ . \tag{B.3}$$

CDR is seen to depend only on δ and not τ.

In terms of an *H-V* receiver basis we can find CDR using table 2.1,

$$CDR = \frac{I + 2\mathrm{ImW_{HV}}}{I - 2\mathrm{ImW_{HV}}} \ . \tag{B.4}$$

In terms of H and V components, CDR depends only on the total power I and the imaginary part of W_{HV}.

B.2 $\mathbf{W/W_2}$

In the W/W_2 description of *McCormick* and *Hendry* (1979), W is the (un-normalized) receiver cross-correlation and W_2 is the co-polar power. Again we will assume that we are transmitting LHC so that the co-polar power is RHC.

From Table 2.1 and for a *L-R* receiver basis, we find,

$$|W| = \sqrt{Q^2 + U^2}/2 \ , \tag{B.5}$$

and since RHC is the co-polar return,

$$W_2 = W_R = (I - V)/2 \ . \tag{B.6}$$

In terms of a linear *H-V* receiver basis we then can find that

$$|W|/W_2 = \frac{\sqrt{(W_H - W_V)^2 + (2\mathrm{ReW_{HV}})^2}}{I - 2\mathrm{ImW_{HV}}} \ . \tag{B.7}$$

The phase of W/W_2 can be found as

$$\begin{aligned} \phi_{LR} &\equiv \tan^{-1}\left[\frac{\mathrm{ImW_{LR}}}{\mathrm{ReW_{LR}}}\right] \\ &= \tan^{-1}\left[\frac{U}{Q}\right] \\ &= \tan^{-1}\left[\frac{2\mathrm{ReW_{HV}}}{W_H - W_V}\right] \ . \end{aligned} \tag{B.8}$$

B.3 $\rho_{\mathbf{HV}}(\mathbf{0})$ from a *L-R* Receiver Basis

The parameter $\rho_{HV}(0)$ that is usually measured in and *H-V* receiver basis can also be found from *L-R* receiver basis data.

In terms of the Stokes parameters, $|\rho_{HV}(0)|$ is defined as

$$\begin{aligned} |\rho_{HV}(0)| &\equiv \frac{|W_{HV}|}{\sqrt{W_H W_V}} \\ &= \sqrt{\frac{U^2+V^2}{(I+Q)(I-Q)}} \ . \end{aligned} \tag{B.9}$$

From table 2.1 we can find ρ_{HV} in terms of measurements in an *L-R* receiver basis,

$$\begin{aligned} |\rho_{HV}(0)| &= \sqrt{\frac{(2\mathrm{ImW_{LR}})^2+(\mathrm{W_L}-\mathrm{W_R})^2}{[(W_L+W_R)+2\mathrm{ReW_{LR}}][((\mathrm{W_L}+\mathrm{W_R})-2\mathrm{ReW_{LR}}]}} \\ &= \sqrt{\frac{(2\mathrm{ImW_{LR}})^2+(\mathrm{W_L}-\mathrm{W_R})^2}{(W_L+W_R)^2-(2\mathrm{ReW_{LR}})^2}} \ . \end{aligned} \tag{B.10}$$

The phase angle of $\rho_{HV}(0)$ is defined through the Stokes parameters as

$$\phi \equiv \tan^{-1}\left[\frac{V}{U}\right] \ . \tag{B.11}$$

In terms of *L-R* receiver basis measurements,

$$\phi = \tan^{-1}\left[\frac{W_L-W_R}{2\mathrm{ImW_{LR}}}\right] \ . \tag{B.12}$$

The phase of the $\rho_{HV}(0)$ is due to ϕ_{dp} and δ_ℓ. This equation is the same as derived by *Holt* (1988) who derived his result from integrals over the drop size distribution and assumed that $\delta_\ell = 0$.

B.4 ZDR from a *L-R* Receiver Basis

The Differential Reflectivity (ZDR) is defined in a linear *H-V* basis as,

$$\begin{aligned} ZDR &\equiv \left[\frac{W_H}{W_V}\right] \\ &= \left[\frac{I+Q}{I-Q}\right] \ . \end{aligned} \tag{B.13}$$

In terms of *L-R* receiver basis data

$$ZDR = \frac{(W_L + W_R) + 2\mathrm{ReW_{LR}}}{(W_L + W_R) - 2\mathrm{ReW_{LR}}} \; . \tag{B.14}$$

Here, we have neglected the propagation effects to and from the scattering volume. And, we are again assuming that the transmitted polarization is RHC.

The results from *Holt* (1988) are essentially the same except for sign changes since he is assuming that RHC was transmitted. His result shows a correction to ZDR due to propagation effects (at S-Band).

Appendix C

System Calibration Technique

C.1 Introduction

The calibration of a dual-polarized radar system is important because of the possibility of gain and phase differences in the two receiver chains. It is easy to see that gain differences in the receiver chain will bias the measured α angles towards the H or V polarization with the higher gain (just like ZDR). On the other hand, phase differences in the receiver chains will bias the measured ϕ values.

Other sources of data contamination are possible from small differences in the linearity of the log-amplifiers and differences in the limiting of the constant-phase limiters.

Errors resulting from differences in the log-amp and constant-phase limiters cannot be corrected unless the role of the receivers is swapped from pulse to pulse. (*Sachidananda* and *Zrnić*, 1985, Figure 16b) shows just such a technique that is also self correcting for gain and phase differences (the gain and phase differences average to zero). It is highly recommended that the New Mexico Tech dual-polarization radar be modified to utilize this technique in the future to improve data quality.

C.2 Poincaré Sphere as a Calibration Aid

A standard pyramidal gain horn was mounted to a rotary joint that was mounted to a tripod. The horn was equipped with two bubble balances for accurate determination of horizontal and vertical alignment of the horn. The rotary joint had an attached protractor for determining the angle position.

The radar was then operated in a passive mode (no transmitted power). The

horn was driven with an RF test generator. The sync pulse of the radar was used synchronize the test generator. Delay after the sync pulse was dialed in to obtain a mid range response in the radar real-time display.

The radar was configured to receive in an *H-V* basis. The test horn was about 30 meters from the radar antenna and pointed directly at the antenna. The test horn was positioned to transmit approximately slant 45 polarization and the power of the test generator was adjusted so that the power in the two receivers was well above the receiver noise and approximately equal in the two channels. The power levels of the two channels as indicated on the radar's analog scope was used to position the radar antenna so that the test signal was received in the center of the main lobe of the antenna. Finally, the frequency of the test generator was adjusted to peak the power in the receivers.

C.3 Radar Phase Calibration

As long as the transmitted polarization from the test horn is not near H or V polarizations, the phase difference of the H and V component are well determined as the phase of the cross correlation of the signals in the H and V receiver channels. And, at slant 45 polarizations that phase difference should be zero. At slant -45 polarization the phase difference should be $\pm\pi$. Phase offset values in the host computer software were then adjusted to correct for the receiver channel phase differences.

$$\begin{aligned} \hat{\phi} &= \phi_H - \phi_V + \epsilon \\ \hat{\phi} &= \phi + \epsilon \\ \phi &= \hat{\phi} - \epsilon \ , \end{aligned}$$

where $\hat{\phi}$ is the measured phase value and ϵ is the difference in the phase length of the two receiver paths. ϵ was found to be 53 degrees.

The frequency of the signal generator was re-peaked several times to make ensure that the phase calibration was repeatable.

C.4 Radar Gain Calibration

At this point it is important to clarify the way the angles are defined since there are many possible ways that this may be done. For example, *Guissard* (1994) refers to two such possible conventions as the forward scattering alignment (FSA) or the

back scattering alignment (BSA). *Torlaschi* and *Holt* (1998) have chosen to define Left Handed and Right Handed rotation when viewed from the radar regardless of whether the wave is propagating towards or away from the radar. In the field of optics, LHC and RHC are defined in terms of the beam of light propagating toward the viewer. While traditionally, radar meteorologists have defined LHC and RHC in terms of looking in the direction of propagation (opposite of the optics convention)(*Bringi* and *Hendry*, 1990).

This is a very subtle point but one that can change the interpretation of the data if care is not taken. Because of the way we have defined the axes of the Poincaré sphere, we will chose a FSA convention, that is looking from the radar. The angle, $\tau = 0$, is defined as H polarization. And a positive τ is measured in a CCW direction from the horizontal when view from the radar. Of course from the test horn the convention would then be BSA and the angles would be measured in a CW direction.

Figure A.9 is repeated here for reference. i The orientation angle of the polarization ellipse is τ. The orientation angle of the polarization ellipse rotates as the test horn is rotated. Comparing Figures A.9a and b, we can see that if the transmitted polarization state of the test horn is linear, the polarization state on the Poincaré sphere must be in the Q-U plane ($\delta = 0$). The angle ϕ can only take on values of zero and $\pm\pi$ for any polarization in the Q-U plane.

The phi angle should change abruptly when 2τ passes through zero and π (see Figure C.1). In fact, for $\delta = 0$ and $\tau = 0$ or $\pm\pi$ the ϕ angle is not even defined. Fortunately, there was a small V component even when the horn was aligned horizontally (or a small amount of circular polarization). As the horn was rotated through zero degrees for example, the phase changed rapidly from zero to π. These rapid phase changes were used along with the protractor readings off the rotary joint to determine the precise setting of the horn to produce H and V polarizations. The settings of the slant polarizations then occur half way between the two protractor readings.

The test horn was then aligned to +45 slant linear polarization. Slant +45 corresponds to equal power in the H and V polarizations. The gain difference between the two receiver channels was then adjusted to zero. The test was repeated for -45 slant linear and the gain difference was again adjusted to zero. The entire test was also repeated to check for consistency.

Note that when there are small differences for the gain offset values for the two slant polarizations, the value halfway between the two should be used as the actual calibration value.

The actual offset in gain for +45 slant linear polarization was a count of one in the realtime display program which corresponds to about 0.25 dB. For -45 slant linear polarization the correction was a count of zero. The correction of the gain differences involves integer arithmetic in the host program. A correction value for the gain differences of the two receiver chains was chosen to be zero.

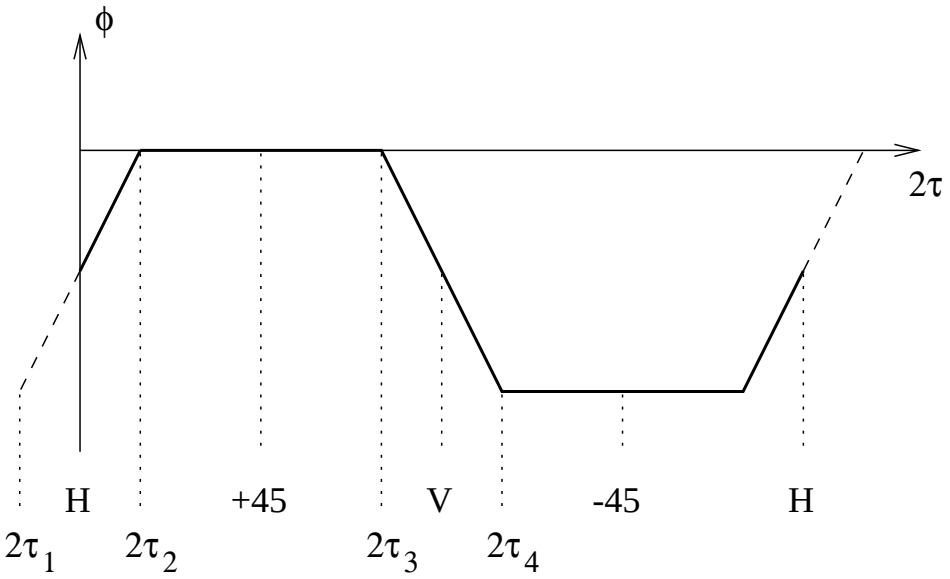

Figure C.1: The ϕ angle changes abruptly as the antenna rotation angle, 2τ passes through zero and π radians. The jump would be discontinuous if there were no residual circularly polarized component in the transmitted polarization state.

Bibliography

Atlas, D., ed. (1990), *Radar in Meteorology*, American Meteorological Society, Boston.

Balakrishnan, N. and D. Zrnić (1990), Use of polarization to characterize precipitation and discriminate large hail, *J. Atmos. Sci.*, **47**, 13, 1525–1540.

Baylis, W. E., J. Bonenfant, J. Derbyshire, and J. Huschilt (1993), Light polarization: A geometrical approach, *Am. J. Phys.*, **61**, 6, 534–545.

Bolinder, E. F. (1981), Geometric network theory, *Proc 1981 European Conf on Circuit Theory and Design*, The Hague, The Netherlands.

Born, M. and E. Wolf (1975), *Principles of Optics*, 5th edn., Pergamon Press, New York.

Bringi, V. N. and A. Hendry (1990), Technology of polarization diversity radars for meteorology, *Radar Meteorology*, Atlas, D., ed., chap. 19a, American Meteorological Society, Boston, 153–190.

Chen, T. (1994), *Radar Detection of Electrically Aligned Particles in Thunderstorms*, Phd thesis, New Mexico Institute of Mining and Technology.

Cloude, S. R. and E. Pottier (1996), A review of target decomposition theorems in radar polarimetry, *IEEE Trans. Geosci. Rem. Sens.*, **34**, 2, 498–518.

Collin, R. E. (1991), *Field Theory of Guided Waves*, 2nd edn., IEEE Press.

Doviak, R. J. and D. S. Zrnić (1993), *Doppler Radar and Weather Observations*, 2nd edn., Academic Press.

Eves, H. (1973), Analytic geometry, *Standard Mathematical Tables*, Shelby, S. M., ed., 21st edn., The Chemical Rubber Company, Cleveland, Ohio.

Guissard, A. (1994), Mueller and Kennaugh matrices in radar polarimetry, *IEEE Trans. Geosci. Rem. Sens.*, **32**, 3, 590–597.

Ho, K. C. and F. S. Allen (1994), An approach to the inverse obstacle problem from the scattering Mueller matrix, *Inverse Problems*, **10**, 2, 387–400.

Holt, A. R. (1988), Extraction of differential propagation phase from data from S-band circularly polarised radars, *Electronic Letters*, **24**, 19, 1241–1242.

Hooker, S. B., J. W. Brown, and J. A. D. Kirwan (1995), Detecting "dipole ring" separatrices with zebra palettes, *GRSS*, **33**, 6, 1306–1312.

Hubbert, J., V. Chandrasekar, V. Bringi, and P. Meischner (1993), Processing and interpretation of coherent dual-polarized radar measurements, *J. Atmos. Oceanic Tech.*, **10**, 155–164.

Jin, Y.-Q. and S. R. Cloude (1994), Numerical eigenanalysis of the coherency matrix for a layer of random nonspherical scatterers, *IEEE Trans. Geosci. Rem. Sens.*, **32**, 6, 1179–1185.

Kostinski, A. (1992), Depolarization criterion for incoherent scattering, *Applied Optics*, **31**, 18, 3506–3508.

Kraus, J. D. and K. R. Carver (1973), *Electromagnetics*, 2nd edn., McGraw Hill Book Co.

Krehbiel, P., T. Chen, S. McCrary, W. Rison, G. Gray, and M. Brook (1996), The use of dual channel circular-polarization radar observations for remotely sensing storm electrification, *Meteor. Atmos. Phys.*, **58**, 1, 65–82.

Kreyszig, E. (1972), *Advanced Engineering Mathematics*, 3rd edn., John Wiley and Sons, Inc., New York.

McCormick, C. G. and A. Hendry (1975), Principles for the radar determination of the polarization properties of precipitation, *Radio Science*, **10**, 421–434.

McCormick, G. and A. Hendry (1979), Radar measurement of precipitation-related depolarization in thunderstorms, *IEEE Trans. Geosci. Elec.*, **GE-17**, 4, 142–150.

Mott, H. (1986), *Polarization in Antennas and Radar*, John Wiley and Sons, New York.

Oguchi, T. (1983), Electromagnetic wave propagation and scattering in rain and other hydrometeors, *Proc. IEEE*, **71**, 9, 1029–1078.

Poincaré, H. (1892), *Théorie mathematique de la lumière*, G. Carré, Paris.

Pruppacher, H. R. and K. V. Beard (1970), A wind tunnel investigation of the internal circulation and shape of water drops falling at terminal velocity in air, *Quart. J R. Met. Soc.*, **96**, 247–256.

Sachidananda, M. and D. Zrnić (1985), ZDR measurement considerations for a fast scan capability radar, *Radio Science*, **20**, 4, 907–922.

Slater, J. C. (1950), *Microwave Electronics*, D. Van Nostrand Co., Inc.

Stokes, G. G. (1852), On the composition resolution of streams of polarized light from different sources, *Trans. Camb. Phil. Soc.*, **9**, 3, 399–416.

Torlaschi, E. and A. Holt (1998), A comparison of different polarization schemes for the radar sensing of precipitation, *Radio Sci.*, **33**, 2, 1335–1352.

Torlaschi, E. and B. Pettigrew (1990), Propagation effects on reflectivity for circularly polarized S-band radars, *J. Atmos. Oceanic Tech.*, **7**, 114–117.

Yamaguchi, Y., W. Boerner, H. Eom, M. Sengoku, S. Motooka, and T. Abe (1992), On charateristic polarization states in the cross-polarized radar channel, *IEEE Trans. Geosci. Rem. Sens.*, **30**, 5, 1078–1080.